Genetic analysis of *Vprbp* in mice

Sarah C. Jackson

A dissertation submitted to the faculty of the University of North Carolina at Chapel Hill in partial fulfillment of the requirements for the degree of Doctor of Philosophy in the Department of Biochemistry and Biophysics.

Chapel Hill
2011

Approved by:

Yue Xiong, Ph.D.

Jeanette Gowen Cook, Ph.D.

William F. Marzluff, Ph.D.

Robert J. Duronio, Ph.D.

Norman E. Sharpless, M.D.

ABSTRACT

SARAH C. JACKSON: Genetic analysis of *Vprbp* in mice
(Under the direction of Dr. Yue Xiong)

Ubiquitin-mediated protein degradation is a critical mechanism for regulating many cellular functions. Substrate proteins are specified through the activity of an E3 ubiquitin ligase. Cullin proteins serve as scaffolds to assemble hundreds of distinct multi-subunit E3 ubiquitin ligase complexes. My research focused on CUL4-based complexes, which use linker protein DDB1 to bind one of approximately 100 putative substrate recruiting proteins. Specifically, I investigated HIV1 viral protein R binding protein (VprBP), a WD40 repeat-containing protein which binds to CUL4-DDB1 and is predicted to function as a substrate recognition subunit. Functional studies of VprBP remain limited; there are currently no known substrates for CUL4-DDB1-VprBP and *Vprbp* knockout mice are early embryonic lethal. In my work, I first tested a hypothesis that VprBP functions in epigenetic modification of histones and intriguingly observed a possible role in histone H4 ubiquitylation. My subsequent work focused on understanding the function and mechanism of *Vprbp* by analyzing conditional mouse embryonic fibroblasts (MEFs) and mice. I discovered that VprBP is required for MEF proliferation and paradoxically that high levels of VprBP protein are associated with quiescent cells. Finally, by crossing conditional *Vprbp* mice with transgenic *Ubiquitin C* promoter driven *Cre-ERT2*$^{+}$ mice, I was able to temporally control *Vprbp* disruption in an unbiased manner to explore phenotypes beyond embryonic lethality This work uncovered a role for *Vprbp* in the proliferation and survival of lymphocytes in mice.

ACKNOWLEDGEMENTS

I would like to thank Yue, members of the Xiong lab, my committee members and my family for providing me with support and inspiration during my journey

TABLE OF CONTENTS

LIST OF TABLES

LIST OF FIGURES

LIST OF ABBREVIATIONS

Abbreviation	Full name
4OHT	4-hydroxytamoxifen
53BP1	p53 binding protein 1
7AAD	7-Aminoactinomycin D
AAA	ATPase Associated with diverse cellular Activities
ABI5	Abscisic acid-insensitive 5
ADP	Adenosine Diphosphate
AhR	Aryl hydrocarbon receptor
APC	Anaphase promoting complex
APC-AF750	Allophycocyanin-Alexa Fluor 750
APC-conjugated	Allophycocyanin-conjugated
ATP	Adenosine Triphosphate
ATPase	Enzymes that catalyze conversion of ATP to ADP
ATR	Ataxia Telangiectasia Mutated and Rad3-related
AUX/IAA	Auxin-responsive protein/ indole-acetic acid responsive
B220	Protein tyrosine phosphatase, receptor type, C
BBAP	B-lymphoma and BAL-associated protein
BC-box	Domain for binding Elongins B and C
Bcl2	B-cell leukemia/lymphoma 2
BRCA1	Breast Cancer Associated 1
BrdU	5'-bromo-2'-deoxyuridine
BTB	Domain homologous to Bric-a-brac, Tramtrack, and Broad-complex
β-TRCP	Beta-transducin repeat containing protein

C57BL/6	C57 black 6 inbred mouse strain
CAND1	Cullin-associated NEDD8-associated 1
CD	Cluster of differentiation
Cdc	Genes required for cell division cycle
cDNA	Complementary DNA
CDT1	Cdc10-dependent transcript 1, chromatin licensing and DNA replication factor
CDT2	Cdc10-dependent transcript 2
CDW	CUL4–DDB1–associated WDR
cFlip	Cellular FLICE-like inhibitory protein
CFSE	Carboxyfluorescein diacetate succinimidyl ester
CHK1	Checkpoint kinase 1
c-Kit	Cellular homolog of the feline sarcoma viral oncogene v-kit
Clr4	*S. pombe* histone H3 methyltransferase
COP	Constituative Photomorphogenic
Cre	Type I topoisomerase from P1 bacteriophage
Cre-ERT2	Cre fused with modified estrogen receptor which binds tamoxifen
CRL	Cullin-ROC E3 ubiquitin ligase
CSA	Cockayne Syndrome Gene A
CSB	Cockayne Syndrome Gene B
CSN	COP9 signalosome subunit
CUL	Cullin
DCAF	DDB1–CUL4 associated factors
DCN1	Defective in cullin neddylation 1
DDB	Damage DNA Binding

DET1	De-etiolated 1
DIAP-1	*Drosophila* inhibitor of apoptosis
DMEM	Dulbecco's Minimum Essential Medium
DN	Double negative
DNA	Deoxyribonucleic acid
DP	Double positive
DTT	Dithiothreitol
DWA	DWD protein hypersensitive to abscisic acid
DWD	DDB1-binding WD40
DYRK2	Dual-specificity tyrosine-(Y)-phosphorylation regulated kinase 2
E1	Ubiquitin activating enzyme
E2	Ubiquitin conjugating enzyme
E3	Ubiquitin ligase
E6AP	Human papillomavirus protein E6 associated protein
EDD	E3 identified by differential display
EDTA	Ethylenediaminetetraacetic acid
EDVP	EDD-DYRK2-DDB1-VprBP complex
EGF	Epidermal growth factor
EGFR	EGF receptor
EIIA	Adenovirus EIIa promoter
Epe1	Jmjc domain chromatin associated protein
ERK	Extracellular regulated Mitogen Activated Protein kinase
ER-α	Estrogen receptor α
FACS	Fluorescence activated cell sorting
F-box	Domain homologous to cyclin F

FBS	Fetal bovine serum
FBW	F-box WD40 domain-containing
FERM	Domain homologous to 4.1 protein (F), ezrin (E), radixin (R) and moesin (M), involved in localizing proteins to the plasma membrane
FITC	Fluorescein isothiocyanate
FLICE	Caspase 8, apoptosis-related cysteine peptidase
FLK2	Fetal liver tyrosine kinase 2
FLP	Flippase
FRT	Flippase Recognition Target
G1	Cell cycle gap phase 1
G2	Cell cycle gap phase 1
GAPDH	Gyceraldehyde-3-phosphate dehydrogenase
GFP	Green Fluorescent Protein
Gr-1	Granulocyte differentiation antigen 1
H1	Histone 1
H2A	Histone H2A
H2AX	Histone 2A variant X
H2B	Histone H2B
H3	Histone H3
H4	Histone H4
HA	Hemagglutinin
HECT	Homologous to the E6AP Carboxyl Terminus
HIV	Human Immunodeficiency Virus
HOXA9	Homeobox A9
HSC	Hematopoietic stem cells

IgD	Immunoglobulin heavy constant delta
IgM	Immunoglobulin heavy constant mu
IL2	Interleukin 2
IκB	Inhibitor of kappa B
LATS	Large tumor suppressor, Warts homolog
Lgl	Lethal giant larvae
LisH	Domain homologous to Alpha-helical motif in Lis1. Often associated with dimerization
Lkb1	Liver kinase B1, serine threonine kinase
LoxP	Locus of Crossover in P1
Mac1	Integrin, alpha M (complement component 3 receptor 3 subunit), expressed mainly on myeloid cells and NK-cells
MBK-2	MiniBrain Kinase homolog
MEF	Mouse embryonic fibroblast
MEI-1	Defective MEIosis
MLL1	Mixed-lineage leukemia complex-1
M-phase	Cell cycle mitotic phase
MST	Mammalian STE20-like serine/threonine kinase
MYC	Myelocytomatosis viral related oncogene
NAE1	NEDD8 activating enzyme E1 subunit 1
NEDD8	Neural precursor cell expressed, developmentally downregulated 8
Nf2	Neurofibromatosis type 2
p21	21 kDa, cyclin dependent kinase inhibitor
p53	53 kDa, tumor supressor
PAGE	Polyacrylamide gel electrophoresis

PALS1	Membrane protein, palmitoylated 5
PARP	Poly-(ADP-ribose) polymerase
PATJ	Pals1-associated tight junction protein
PBS	Phosphate-buffered saline
PCI	Domain homologous to Proteasome, COP9, eukaryotic translation initiation factor
Pcid2	PCI domain containing 2
PCNA	Proliferating cell nuclear antigen
PCR	Polymerase chain reaction
Pcu	*Pombe* cullin
PDCD4	Programmed cell death protein 4
PDK1	3- phosphoinositide-dependent protein kinase 1
PE	Phycoerythrin
PI	Propidium iodide
Pol η	DNA polymerase pol-eta
PRC1	Polycomb repressive complex 1
PVDF	Polyvinylidene Fluoride
qPCR	Quantitative PCR
RAC	Ras (rat sarcoma homolog)-related protein, small GTPase
Rad	Genes required for Radiation-induced checkpoint
RASSF1A	Ras association (RalGDS/AF-6) domain family member 1
RB	Retinoblastoma protein
RBX	RING Box
RICH1	RhoGAP interacting with CIP4 homolog 1
RING	Really interesting new gene, conserved domain in E3 ubiquitin ligase

RNA	Ribonucleic acid
RNAi	RNA interfernece
RNF	RING finger protein
ROC	RING of Cullins
RPMI	Roswell Park Memorial Institute medium
RPMI-10	RPMI with 10% FBS
RT-PCR	Reverse transcriptase-PCR
Sca-1	Stem cell antigen 1
SCF	SKP1-CUL1-F-box
SDS	Sodium dodecyl sulfate
SET8	SET domain containing (lysine methyltransferase) 8
shRNA	Small hairpin RNA
siRNA	Small interfering RNA
SKN-1	SKiNhead
SKP1	S-phase kinase-associated protein 1
SOCS	Suppressor of cytokine signaling
Sox9	SRY-box containing gene 9
SP	Single positive
Spd1	Ribonucleotide reductase (RNR) inhibitor
S-phase	DNA synthesis phase of cell cycle
SRY	Sex determining region of Chr Y
STAT	Signal transducer and activator of transcription
SUMO	Small Ubiquitin-like modifier
SV5	Simian Virus 5
Tam	Tamoxifen

TAP	Tandem Affinity Purification
TCR	T-cell receptor
TRPC4AP	Transient receptor potential cation channel, subfamily C, member 4 associated protein
TSC2	Tuberous sclerosis complex gene 2
Ub	Ubiquitin
UBA3	Ubiquitin-like modifier activating enzyme 3
UBC12	NEDD8-conjugating enzyme Ubc12
UNG2	Uracil nucleotide glycosylase 2
UV	Ultraviolet
V(D)J	Variable, Diversity, Joining genes
VHL	Von Hippel-Lindau
Vpr	HIV1 viral protein R
VprBP	Vpr-binding protein
WD40	Tryptophan-aspartic acid domain - 40 residues
WDR	WD40 Repeat Protein
WEE1	Dual specificity protein kinase, CDK1 inhibitor
WW45	Salvador homolog 1
XPC	Xeroderma Pigmentosum group C protein
YAP1	Yes-associated protein 1, Yorkie homolog
YFP	Yellow Fluorescent protein

Chapter I

INTRODUCTION

(including modified portions from Jackson S and Xiong Y. 2009. Trends Biochem Sci. 34(11):562-70.)

Ubiquitin-mediated protein degradation

Appropriate degradation of specific proteins is crucial for a number of cellular functions including cell cycle progression, induction of apoptosis, and DNA damage response. Most proteins regulated by degradation are targeted by the ubiquitin-proteasome system. Ubiquitin is a small protein which can be covalently linked to a substrate protein or to another ubiquitin through the enzymatic cascade known as ubiquitylation (Pickart, 2001). Ubiquitylation proceeds through an E1 (ubiquitin-activating enzyme), an E2 (ubiquitin-conjugating enzyme) and an E3 ubiquitin ligase (substrate targeting protein). The C-terminal glycine of ubiquitin (Ub_1) is bound to a lysine residue on the substrate. Subsequently, an additional ubiquitin (Ub_2) can be ligated to a lysine on Ub_1 to form a polyubiqutin chain. Substrates with lysine 48 linked polyubiquitin chains are rapidly detected and degraded by the 26S proteasome. In addition, some substrates are mono-ubiquitylated or polyubiquitylated through chains linked by other lysine residues in ubiqutin (K6R, K11R, K27R, K29R, K33R, or K63R). In these cases, ubiquitylation may not direct proteolysis, but rather appears to function like other post-translational modifications, regulating protein conformation, localization or binding partners.

Eukaryotes typically have one E1 ubiquitin activating enzyme, and a limited number of E2 ubiquitin conjugating enzymes (13 in *S. cerevisiae*, 22 in *C. elegans*, 30 in humans) (Kipreos, 2005). In contrast, a large number of E3 ubiquitin ligases are found, and substrate binding by the ubiquitin ligase is critical for conferring specificity to proteolysis. There are two major families of E3 ligases distinguished by their active domains: the HECT family ('homologous to the E6-AP carboxy terminus') and the RING family (containing a cross-braced structure characterized by cysteine and histidine residues that bind to zinc atoms and first recognized in the human 'really interesting new gene product') (Freemont, 2000; Huibregtse et al., 1995; Lovering et al., 1993). The

HECT domain mediates interaction with the cognate E2 and, through an evolutionarily conserved cysteine residue, forms a thioester linkage with ubiquitin. Human cells contain as many as 28 HECT proteins and most, if not all, are believed to function as E3 ligases. Unlike the HECT domain, the RING domain promotes a direct transfer of ubiquitin from the E2 to the substrate without forming an intermediate with ubiquitin. Human cells express more than 450 RING proteins, and E3 ligase activity has been experimentally demonstrated for many of them. A ubiquitin ligase can be a single protein with an intrinsic RING finger domain or a multi-subunit complex which contains a RING finger protein.

Cullin Family Ubiquitin Ligases

Although not containing a RING domain themselves, members of the evolutionarily conserved cullins constitute a large family of cullin-RING E3 ligases (CRLs). The highly conserved C-terminal domain of the cullin binds with a RING finger protein, ROC1 (RING of cullins; also known as Rbx1 or Hrt1) or ROC2, and facilitates transfer of ubiquitin from E2. There are three cullins in yeast, six in *Caenorhabditis elegans* and *Drosophila melanogaster* (CUL1-6), up to nine in *Arabidopsis thaliana*, and six canonical cullins in humans (CUL1, 2, 3, 4A, 4B and 5). In addition, three other proteins, CUL7 and CUL9 (also known as PARC) in mammals and APC2 (anaphase promoting complex subunit 2) in all eukaryotes, contain significant sequence homology to cullins over a ~180 residue region and bind ROC or a homologous small RING finger protein, APC11. Cullins do not bind substrates directly, but rather rely on substrate recruiting receptors that are joined to the cullin complex by a linker protein (Figure 1.1). Cullins serve as bona fide scaffold proteins, assembling substrate targeting and RING finger proteins into a single complex. Remarkably, each cullin can associate with a

Figure 1.1

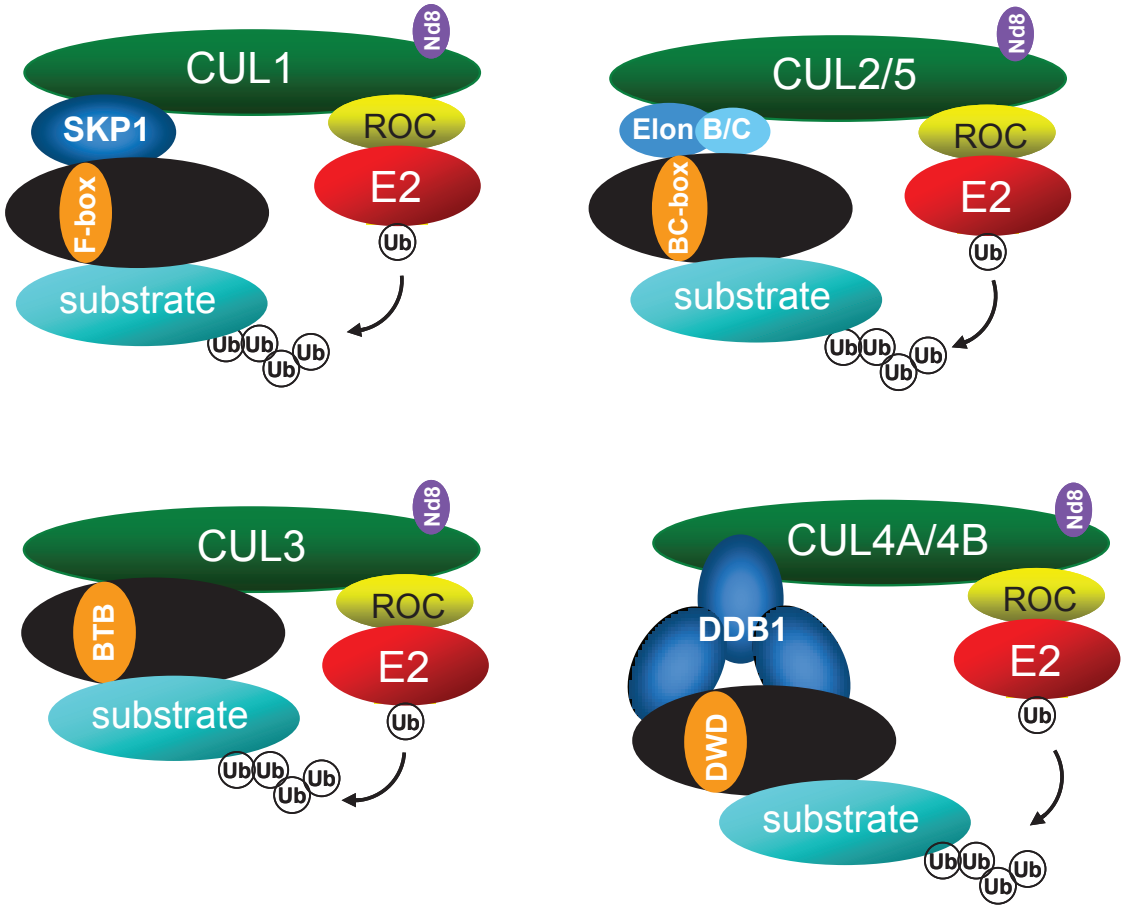

Figure 1.1. Cullin-RING ubiquitin ligases (CRLs).

Each cullin uses modular assembly to recruit different substrates to a common catalytic core by varying its substrate receptor. Cullin family members (green) from different organisms share similar mechanisms for assembling a multi-subunit complex to ubiquitylate specific substrate protein (light blue). An N-terminal domain interacts either directly with a protein motif (orange) present in substrate receptors (black) or via a linker (blue). Separately, a C-terminal domain binds with a small RING protein (ROC1 or ROC2, yellow) which recruits and allosterically activates an E2 enzyme (red) that transfers ubiquitin to the substrate. Cullins are activated by the covalent conjugation with the ubiquitin-like modifier, NEDD8 (Nd8; purple).

different family of substrate receptors, leading to the assembly of as many as 400 distinct CRLs. A recent estimate suggests that 20% of all proteins subject to proteasomal degradation are targeted by CRLs (Soucy et al., 2009).

The founding cullin gene, Cul1(also called Cdc53 in budding yeast), was first identified in *Saccharomyces cerevisiae* where its mutation blocked the G1-to-S transition (Mathias et al., 1996) and led to an accumulation of G1 cyclin (Willems et al., 1996), and was separately identified in *C. elegans* where loss of Cul1 function caused hyperplasia of multiple tissues (Kipreos et al., 1996). These diverse or even seemingly irreconcilable phenotypes were subsequently explained by the discovery that CUL1 can assemble into distinct E3 complexes and thereby ubiquitylate multiple substrates. CUL1 binds a small protein, SKP1 (S-phase kinase-associated protein 1), which in turn binds a conserved protein motif, the F-box, which is present in many different proteins (Bai et al., 1996). Through additional protein–protein interaction modules, individual F-box proteins can then recruit different substrates to the CUL1–ROC1–E2 catalytic core (Zheng et al., 2002b). In this modular SKP1–CUL1–F-box (SCF) assembly, CUL1 indeed acts as a scaffold, SKP1 as a linker and F-box proteins as substrate receptors (Figure 1.1). By only varying the substrate targeting receptor, many different substrates can be ubiquitylated by a shared catalytic core.

Each cullin interacts with a distinct family of substrate targeting receptors through the divergent N-terminal domain of the cullin. To bring specific substrates to CUL2- and CUL5-based ligases, a heterodimeric linker complex containing Elongins B and C binds to an analogous N-terminal domain in CUL2 and CUL5 and to two similar protein motifs, the VHL-box and SOCS box. VHL and SOCS proteins, via their additional protein–protein interaction modules, target various substrates differentially to the CUL2–ROC1–E2 or CUL5–ROC2–E2 catalytic cores, respectively (Kamura et al., 2004). Omitting a

linker, CUL3 utilizes its N-terminal domain to bind to a conserved 100-residue protein motif known as a BTB domain, which then target substrates to the CUL3–ROC1–E2 catalytic core (Furukawa et al., 2003; Geyer et al., 2003; Pintard et al., 2003b; Xu et al., 2003) (Figure 1.1). CUL4-based E3 ubiquitin ligases use DDB1 as a linker protein and a subset of WD40 proteins, known as DWD proteins, serve as the substrate receptor (discussed in detail below). Cullins control the ubiquitylation of a wide variety of substrates, and form the largest known family of ubiquitin ligase complexes -- mammals express approximately 70 F-box proteins, 30 BC-box proteins, 200 BTB proteins, and 100 DWD proteins. My thesis research focused on a specific DWD protein, VprBP, which functions as part of a CUL4-based complex.

Regulation of CRL Complexes

Assembly and activation of cullin complexes must be carefully regulated. CUL1, and CUL3 complexes have been noted to form dimers in vivo, and, in the case of CUL1, dimerization was required for elongation of ubiquitin chains (Chew et al., 2007; Tang et al., 2007). All cullins require post-translational modification by NEDD8, a ubiquitin-like proteins, to form an active ubiquitin ligase complex. Cullin-bound NEDD8 can directly bind E2, promoting E2 recruitment and possibly facilitating the processivity of polyubiquitylation (Sakata et al., 2007; Kawakami et al., 2001; Saha and Deshaies, 2008). Like modification by ubiquitin, modification with NEDD8 requires an enzymatic cascade consisting of an E1 (heterodimeric NAE1/UBA3), E2 (UBC12) and E3 (consisting of the scaffold protein DCN1 and ROC1) (Liakopoulos et al., 1998; Gong and Yeh, 1999; Kurz et al., 2008; Kurz et al., 2005; Morimoto et al., 2003). A recently developed cullin inhibitor, MLN4924, functions by blocking the activity of the NEDD8 E1, further underscoring the requirement for neddylation for cullin function (Soucy et al., 2009).

There are three primary ways to negatively regulate cullin activity: auto-ubiquitylation of substrate targeting receptors, binding to a negative regulator (CAND1), and removal of NEDD8 modification. In the absence of substrate binding, cullins have been frequently shown to ubiquitylate their own substrate targeting receptors, thereby inactivating the complex (Galan and Peter, 1999; Wirbelauer et al., 2000; Li et al., 2004; Chen et al., 2001; Zhou and Howley, 1998). CAND1 (cullin-associated and neddylation dissociated) binds to N-terminal and C-terminal regions of cullins, masking sites in the cullin N-terminus required for the binding with linker proteins (Liu et al., 2002; Zheng et al., 2002a; Goldenberg et al., 2004). Finally, removing NEDD8 from a cullin (known as deneddylation) inactivates the catalytic core. Deneddylation requires the COP9 signalosome (CSN), an eight subunit complex that shares homology with the proteasome lid (Cope and Deshaies, 2003).

While biochemical studies of CSN and CAND1 have shown evident negative regulation of CRL complexes, genetic analysis of CSN genes and CAND1 has revealed more complicated interactions. In *Arabidopsis*, loss of genes encoding CSN subunits led to an accumulation of neddylated cullins but paradoxically did not lead to a depletion of SCF substrates such as AUX/IAA (Schwechheimer et al., 2001). Likewise, loss of CSN reduced activity of CRL3 complexes in *C. elegans* despite elevated levels of neddylated CRL3 (Pintard et al., 2003a). These results suggested a model that cycles of neddylation and deneddylation are required for cullin ubiquitin ligase activity and potentially functions to prevent autoubiquitylation of substrate recruiting receptors (Cope and Deshaies, 2006; He et al., 2005; Wu et al., 2005). In the case of CAND1, while biochemical studies indicate CAND1 is a general CRL inhibitor, genetic studies suggest a more nuanced role. Studies in *Arabidopsis*, *S. pombe*, and *C. elegans* show that CAND1 is required for the function of at least a subset of CRL complexes, but does not appear to globally regulate levels of neddylated cullins (Zhang et al., 2008; Schmidt et

al., 2009; Bosu et al., 2010). A current model suggests that CAND1 may function to facilitate the formation of rare CRL complexes, even in the presence of more abundant substrate recruiting receptors (Schmidt et al., 2009), but additional studies will be required to clarify the precise in vivo function of CAND1. Nevertheless, it's clear cells rely on multiple levels of regulation to precisely control the assembly of the appropriate cullin family ubiquitin ligase complexes.

CRL4 complexes

Following the discoveries that CUL1, CUL2 and CUL3 each interacts with multiple substrate receptors and that CUL4 performs pleiotropic functions, it was anticipated that CUL4 very likely would also interact with a protein motif present in multiple proteins. Taking different approaches -- proteomic, bioinformatic and structural analyses -- four independent studies collectively identified and experimentally demonstrated 52 different DDB1 binding WD40 proteins, referred to variously as DWD (DDB1-binding WD40), DCAF (DDB1–CUL4 associated factors) or CDW (CUL4–DDB1–associated WDR) proteins (He et al., 2006; Higa et al., 2006b; Angers et al., 2006; Jin et al., 2006; and reviewed in Lee and Zhou, 2007). It was also clear that only a subset of, but not all WD40 proteins, interact with DDB1 and CUL4. DDB1-binding proteins contain a common motif, variably defined as the "double DxR box" with two DxR motifs located at the end of two consecutive WD40 repeats (Angers et al., 2006), the "DWD box", a 16-residue stretch that correspond to the second half of a WD40 repeat and an Arg residue at position 16 following the WD dipeptide (He et al., 2006), the "DXXXR/KXWDXR/K" motif as the subdomain of WD40 repeats (Higa et al., 2006b), or simply as the "WDXR" motif to emphasize the Arg residue following the WD dipeptide (Jin et al., 2006). Some DWD proteins contain one, most contain two and a few contain three such motifs.

Mutational analysis and conservation of the WDXR motif in all DWD proteins initially suggested that this motif directly mediated binding with DDB1. However, a co-crystal structure of human DDB1 and zebrafish DDB2 unexpectedly revealed that the corresponding Arg residue in zebrafish DDB2 (Arg309) did not contact DDB1 (Scrima et al., 2008), though mutation of the WDXR motif in DDB2 disrupted binding to DDB1 (Rapic-Otrin et al., 2003). In addition, WDTC1 (Li et al., 2010a) and WDR21 (Fukumoto et al., 2008) were also shown to bind to DDB1 independently of their WDXR motifs. An alpha-helical region in these proteins termed the H-box, which has structural similarity with DDB1-binding viral protein SV5 (Li et al., 2010a), but is clearly distinct from the WDXR motif, was required for binding. The H-box was identified by sequence homology in seven DWD proteins, though the vast majority of DWD proteins lacked an H-box, at least as determined by primary sequence homology (Li et al., 2010a). It remains possible that divergent primary sequence might converge to a similar alpha-helical structure, though this has yet to be demonstrated. Although a consensus sequence for residues that contact DDB1 is not yet precisely defined for most DWD proteins, the current definition of the DWD motif is highly predictive of and likely structurally important for DDB1 binding proteins. Future studies will be needed to further understand why the DWD motif is so critically important in CRL4 substrate receptors.

How many DWD proteins are there? The human genome encodes about 320 unique WD40 proteins. Database searches using the DWD box predicted that 78 unique DWD proteins could bind to DDB1; 25 of these proteins were experimentally validated in the 2006 papers which established DDB1-WD40 protein binding (He et al., 2006; Higa et al., 2006b; Angers et al., 2006; Jin et al., 2006; my unpublished analysis of the dataset). An additional 27 proteins, which contain the smaller WDXR or WDXK consensus sequence, have been experimentally demonstrated to bind DDB1, suggesting DDB1 binds as many as 105 different WD40 proteins (He et al., 2006; Higa et al., 2006b;

Angers et al., 2006; Jin et al., 2006). Similar searches of the DWD motif predicted 33 DWD proteins in fission yeast, 36 in *C.elegans*, 75 in *Drosophila*, 78 in rice and 85 in *Arabidopsis* (He et al., 2006; Lee et al., 2008). When 11 predicted *Arabidopsis* DWD proteins were tested for their direct interaction with DDB1 by yeast two-hybrid assay, all were found to be positive (Lee et al., 2008), suggesting that most of these predicted DWD proteins indeed bind to DDB1.

Genetic analysis of CUL4 and DDB1

A single *CUL4* gene exists in *Schizosaccharomyces pombe*, *C. clegans*, *Drosophila*, and *Arabidopsis* whereas mammalian cells express two closely related paralogues, *CUL4A* and *CUL4B*. Two closely related CUL4 genes are also present in zebrafish and frog, but not in sea urchin, suggesting that the *CUL4* gene duplication is unique to vertebrates. Characterization of null mutations or reduced expression of *CUL4* in these organisms has revealed a wide range of cellular and organismal defects, including many associated with deregulated chromatin.

S. pombe Cul4 mutations cause multiple chromatin defects

Cul4 (also known as *pcu4*) deletion in fission yeast results in extremely elongated cells with a severely reduced growth rate and decondensed chromosomes (Osaka et al., 2000). The defect in chromosome condensation can be attributed in part to a role for Cul4 in maintaining the heterochromatin formation through its interaction with Rik1, a protein that is distantly related to mammalian DDB1. Cul4, using Rik1 as linker protein, binds with Clr4 histone H3K9 methyltransferase and is required for Clr4 localization to heterochromatin (Horn et al., 2005; Jia et al., 2005; Thon et al., 2005). Further, this complex was shown to require ubiquitin ligase activity, as a expression of a Cul4 mutant lacking the Nedd8 modification site could not compensate for *cul4Δ* (Jia et al., 2005).

C.elegans cul-4 mutations cause CDT1 accumulation and DNA re-replication

Inactivation of *cul-4* in *C.elegans* by RNA interference (RNAi) resulted in a developmental arrest at the L2 larval stage and caused massive DNA re-replication (Zhong et al., 2003). In *cul-4* RNAi animals, there was sustained accumulation of the DNA replication-licensing factor, CDT-1 (chromatin licensing and DNA replication factor 1), after S-phase completion whereas wild-type cells expressed undetectable CDT-1 (Zhong et al., 2003). Additionally, nuclear export of the other replication licensing factor, Cdc6, was inhibited indirectly due to a failure to ubiquitylate the p21 homolog, CKI-1, thus contributing to the dramatic re-replication phenotype (Kim et al., 2007). Removal of one genomic copy of *cdt-1* suppressed the *cul-4* re-replication phenotype (Zhong et al., 2003). These results demonstrated a function for CUL-4 in maintaining genome stability in part by facilitating CDT-1 degradation during the cell cycle and preventing aberrant licensing of DNA replication.

Arabidopsis CUL4 mutations impair development

Arabidopsis CUL4 is expressed abundantly and broadly in almost all tissues examined. *Arabidopsis* expresses two different CUL4 isoforms from a single gene, with one (CUL4-L) containing an additional 50 amino acid sequence at the N-terminus absent in the other (CUL4-S). Reduced CUL4 expression in *Arabidopsis* by transgene-mediated co-suppression or RNAi results in pleiotropic cop-like (constitutive photomorphogenesis) phenotypes and widespread developmental defects in lateral roots, abnormal vascular tissue, and stomatal development (Chen et al., 2006; Bernhardt et al., 2006), providing genetic evidence supporting the notion that CUL4 can assemble multiple distinct CRL4 complexes and regulate many different substrates.

Figure 1.2

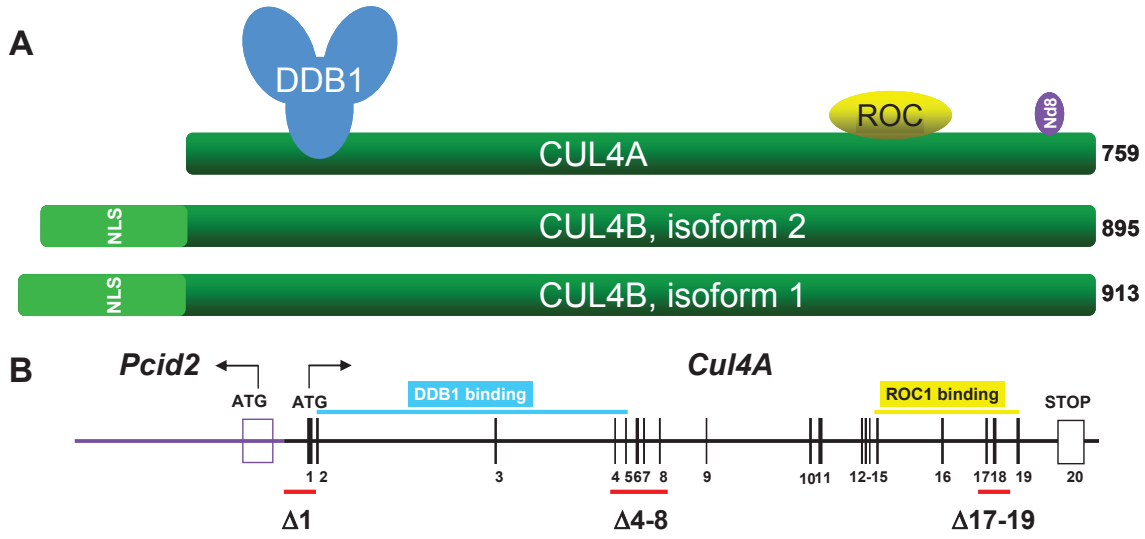

Figure 1.2 Schematic comparison of CUL4 proteins and mouse Cul4A mutants.

(A) Human cells contain two *CUL4* genes encoding CUL4A (NP_001008895) and two isoforms of CUL4B (NP_001073341 and NP_003579.3) proteins which differ by only 22 amino acids at the N-terminus. The extended N-terminus of CUL4B contains a nuclear localization signal (NLS).

(B) Wild type mouse *Cul4A* gene and comparison of three targeted *Cul4A* mutants. Filled and open boxes denote coding and non-coding exons, respectively. Exons encoding the DDB1 and ROC 1 binding regions in CUL4A have been noted. Three mouse models targeting *Cul4A* have been generated to date, deleting exon 1, exons 4-8, and exons 17-19, respectively. Discrepancies in reported phenotypes might be due to unintentional disruption of a nearby neighboring gene, *Pcid2*.

Mammalian CUL4A and CUL4B are not entirely redundant

In mammals, genetic analysis of *CUL4* function is complicated by the existence of two closely related genes, *CUL4A* and *CUL4B*, which encode proteins sharing 80% identity (Figure 1.2A). CUL4B contains additional N-terminal residues and a nuclear localization signal (Zou et al., 2009). A *Cul4A* mutant mouse created by deleting exon 1 ($Cul4A^{\Delta 1/\Delta 1}$, Figure 1.2B) was reported to cause early embryonic lethality (Li et al., 2002) and widespread defects in hematopoeisis when conditionally deleted (Li et al., 2007). This phenotype led to the early impression that the two CUL4 genes in mammals are functionally distinct. Recently, a different *Cul4A* mutant mouse strain, targeting exons 17-19 ($Cul4A^{\Delta 17\text{-}19/\Delta 17\text{-}19}$) which encode the ROC binding region and Nedd8 modification site, unexpectedly showed no apparent phenotype (Liu et al., 2009). This significant discrepancy was explained by the inadvertent disruption in the $Cul4A^{\Delta 1/\Delta 1}$ mutant strain of a very close neighboring gene, *Pcid2*, which encodes an uncharacterized protein with homology to essential proteasome subunits (Liu et al., 2009). Supporting this explanation, deletion of exons 4-8 ($Cul4A^{\Delta 4\text{-}8/\Delta 4\text{-}8}$), which encode for a portion of the DDB1 binding domain, resulted in only a mild decrease in the proliferation in mouse embryonic fibroblasts (MEFs) and viable mice with male infertility (Kopanja et al., 2011; Kopanja et al., 2009).

Despite their high degree of sequence homology, wide expression and apparent compensation for *Cul4A* loss by *Cul4B* in the mouse, the two *Cul4* genes are not entirely functionally redundant. Deletion of exons 17-19 of *Cul4* resulted in an increase in stability of several CRL4 substrates (discussed in detail below), including DNA repair factors DDB2 and xeroderma pigmentosum complementation group c (XPC) as well as CDK inhibitor p21. Furthermore, DDB2-dependent global genomic repair activity was enhanced and $Cul4A^{\Delta 17\text{-}19/\Delta 17\text{-}19}$ mice had increased resistance to UV-induced skin

cancer (Liu et al., 2009). These findings, which are consistent with the enhanced resistance to UV-induced carcinogenesis in DDB2 transgenic mice (Alekseev et al., 2005), point to a role for CUL4A in restricting the activity of DNA damage responsive proteins by promoting DDB2 degradation, a function that is apparently not fully compensated by CUL4B.

Using a screen to inactivate genes on the X-chromosome in mice by gene-trap, *Cul4b* was recently shown to be required for mouse embryonic development; *Cul4b* disruption resulted in incomplete embryo turning, as well as defective neural and cardiac development (Cox et al., 2010). These genetic results demonstrate that while CUL4B can compensate for loss of *Cul4a*, CUL4A is unable to compensate for loss of *Cul4b*. In humans, several familial mutations in *CUL4B* have been identified in association with X-linked mental retardation (XLMR); the majority of mutations result in frame-shift and truncation, indicating that loss-of-function of CUL4B contributes to XLMR (Tarpey et al., 2007; Zou et al., 2007). It is not entirely clear why loss of *Cul4b* leads to embryonic lethality in mice while in humans *CUL4B* mutation leads to XLMR.

Supporting a distinct genetic function of *CUL4B* gene, the N-terminus of CUL4B, but not CUL4A, has been shown to uniquely bind to the dioxin receptor (AhR), assembling a CUL4B specific ubiquitin ligase complex that targets estrogen receptor α (ER-α) for degradation (Ohtake et al., 2007). DDB1, the linker that is commonly used by both CUL4A and CUL4B for interacting with different substrate receptors, was identified, along with CUL4B in the AhR-immouncomplex, but its function in promoting CUL4B-mediated substrate degradation remains unclear as it was not apparently required for substrate recruitment. In addition, the Xiong lab recently discovered that CUL4B, but not CUL4A, promotes the ubiquitylation of WDR5, a core component of the trimeric MLL1 histone H3K4 methyltransferase complex (Nakagawa and Xiong, 2011, in press). The specificity of CUL4B for WDR5 is due primarily to a nuclear localization signal in the N-

terminus of CUL4B which is required for co-localization with WDR5. Thus biochemical and genetic data support the conclusion that CUL4B has unique functions for which CUL4A cannot compensate in vivo.

The Ddb1 gene is required for development and DNA repair

Like CUL4, DDB1 is essential for development in multiple organisms. Knockdown of DDB1 in *Drosophila* caused lethality early in development (Takata et al., 2004). *Ddb1* is allelic to a previously defined locus termed *piccolo* (*pic*) (Hu et al., 2008). Semi-lethal *piccolo* mutants were originally characterized based on shared irregularities in bristle, wing, and body segment growth (Clark and Chovnick, 1986). *Ddb1* mutants growth arrest at the second instar stage, thus failing to develop completely (Hu et al., 2008). In addition, knockdown of DDB1 in wing imaginal disks caused increased sensitivity to methyl-methanesulfonate (MMS)-induced DNA damage (Shimanouchi et al., 2006).

Unlike other model organisms, *Arabidopsis* contains two *DDB1* genes, *AtDDB1A* and *AtDDB1B*, complicating the assessment of the functional dependency of CUL4 on DDB1. *AtDDB1B* disruption is lethal whereas the only effect of homozygous loss of *AtDDB1A* is decreased UV tolerance for a short period of time immediately following UV irradiation (Al Khateeb and Schroeder, 2009; Schroeder et al., 2002). The inability of *AtDDB1A* to complement *AtDDB1B* is puzzling given that *AtDDB1A* is 91% identical to *AtDDB1B* over the entire 1088 residues, also binds to AtCUL4 (Bernhardt et al., 2006), and is widely and concurrently expressed in many tissues; however *AtDDB1B* is often expressed at higher levels (Al Khateeb and Schroeder, 2007).

Ddb1 knockout in mouse resulted in lethality prior to embryonic day 12.5, and conditional deletion in brain and lens tissue using Nestin-Cre resulted in accumulation of CDT1, accumulation of DNA damage, and apoptosis of proliferating neuronal progenitor

cells (Cang et al., 2006). Crossing these mice to mice lacking the tumor suppressor gene encoding p53 (*TP53*) partially rescued the apoptotic defect, but surviving cells showed irregularly shaped nuclei and high frequency of mitotic division (Cang et al., 2006). The *Nestin-Cre; Ddb1*$^{F/F}$ mice and the *Nestin-Cre; Ddb1*$^{F/F}$*; TP53*$^{-/-}$ mice died at day one post-birth (Cang et al., 2006).

Deletion of *ddb1* in fission yeast resulted in cells that are viable, but are hypersensitive to various DNA damage agents, delayed in DNA replication progression, accumulate DNA damage, and show elongated phenotypes, abnormal nuclei and retarded growth (Holmberg et al., 2005; Zolezzi et al., 2002). Many of these phenotypes are similar to those observed in *cul4Δ* cells (Osaka et al., 2000), Notably, *S. pombe* contains an additional protein, Rik1 that shares 21% identity with DDB1 and also assembles into E3 ligases with Cul4. However, the use of multiple adaptor proteins in CRL4 ligases is not evolutionarily conserved as metazoans do not contain a Rik1 homolog.

Cullin 4 ubiquitin ligase complexes in DNA replication & repair

CUL4-DDB1 complexes have frequently been reported in regulating DNA damage response. DDB2 and CSA encode two related WD40 proteins which control two different pathways of nucleotide excision repair, global genome repair and transcription-coupled repair, and when mutated they lead to two distinct hereditary diseases, xeroderma pigmentosum and Cockayne syndrome, respectively. In a search for the molecular basis underlying the function of DDB2 and CSA in DNA repair, it was, at the time, surprising to find that they assemble into similar complexes that contain DDB1, CUL4A, ROC1 and all 8 subunits of COP9 signlaosome (Groisman et al., 2003). This study provided the initial basis for recognizing the importance of CRL4 complexes in DNA repair (discussed further below and in Chapter 2). In addition, multiple lines of

genetic and biochemical research established DDB1 as an essential component for CDT1 ubiquitylation by the CUL4A–ROC1–E2 catalytic core (Hu et al., 2004; Cang et al., 2006). These studies, as well as cul-4 studies by the Kipreos lab and work by the Walter lab in *Xenopus* extracts, firmly established the role of CRL4 in regulating DNA replication through targeted ubiquitylation of the DNA licensing factor CDT1 (Jin et al., 2006; Zhong et al., 2003). Subsequent studies broadened the function of CRL4 complexes in DNA replication, repair and beyond.

PCNA is required for the ubiquitylation of multiple PIP box proteins by CRL4^{CDT2}

A unique feature of CRL4^{CDT2}-mediated CDT1 ubiquitylation is the requirement of proliferating cell nuclear antigen (PCNA), (Nishitani et al., 2006; Arias and Walter, 2006; Hu and Xiong, 2006; Senga et al., 2006) a cofactor of DNA polymerases that functions as a sliding clamp encircling DNA (Moldovan et al., 2007). The function of PCNA in CRL4^{CDT2}-mediated ubiquitylation remains unclear, but is not limited to CDT1 alone. Recently, additional CRL4^{CDT2} substrates, CDK inhibitor p21 (Nishitani et al, 2008; Kim et al, 2008; Abbas et al, 2008), *C. elegans* polymerase η (Kim and Michael, 2008), *Drosophila* E2f1 (Shibutani et al., 2008), PR-SET7 (Abbas et al., 2010; Centore et al. 2010, ; Jorgensen et al., 2011; Oda et al., 2010) and *S. pombe* JmjC family protein Epe1 (Braun et al., 2011), have all been reported to be degraded in a PCNA-dependent manner. All reported CRL4^{CDT2} substrates contain a conserved PCNA-interacting motif (PIP box) and bind PCNA directly. Further, this direct binding is required for their ubiquitylation. Although the human genome encodes 47 PIP box proteins, and most have chromatin-associated functions (Moldovan et al., 2007), only a subset are predicted to bind CDT2 (Havens and Walter, 2009).

Table 1.1. CRL4 Substrates

Substrate	Function	Receptor	Organism[a]	Reference
CDT1	DNA replication	CDT2	*Hs*, *Xl*, *Dm*, *Ce*, *Sp*	(Arias and Walter, 2005, 2006; Higa et al., 2006a; Higa et al., 2003; Hu et al., 2004; Hu and Xiong, 2006; Jin et al., 2006; Nishitani et al., 2006; Sansam et al., 2006; Senga et al., 2006; Zhong et al., 2003)
p21	Cell cycle inhibitor	CDT2	*Hs, Ce*	(Nishitani et al., 2008) (Kim et al., 2008)(Abbas et al., 2008)
E2F1	Cell cycle/ transcription factor	CDT2	*Dm*	(Shibutani et al., 2008)
pol η	DNA replication during damage	CDT2	*Ce*	(Kim and Michael, 2008)
Spd1	DNA replication inhibitor	Cdt2	*Sp*	(Bondar et al., 2004; Holmberg et al., 2005; Liu et al., 2005; Liu et al., 2003)
Epe1	Histone demethylase	Cdt2	*Sp*	(Braun et al., 2011)
PR-SET7/ SET8	Histone H4 methyltransferase	CDT2	*Hs*	(Abbas et al., 2010; Centore et al., ; Jorgensen et al., 2011; Oda et al., 2010)
PCNA	DNA replication/ repair	CDT2	Hs	(Terai et al., 2010)
Histones H2A, H3, H4	Chromatin formation	DDB2	*Hs*	(Kapetanaki et al., 2006; Wang et al., 2006)
XPC	DNA damage repair	DDB2	*Hs*	(Sugasawa et al., 2005)
DDB2	DNA damage repair	DDB2	*Hs*	(El-Mahdy et al., 2006; Sugasawa et al., 2005)
CSB	DNA damage repair	CSA	*Hs*	(Groisman et al., 2006)
TSC2	Cell growth	FBW5	*Hs*, *Dm*	(Hu et al., 2008)
SKN-1	Stress response and longevity	WDR23	*Ce*	(Choe et al., 2009)
ER-α[c]	Estrogen receptor	AhR[b]	*Hs*	(Ohtake et al., 2007)
WDR5[c]	Epigenetic regulation	WDR5	Hs	(Nakagawa and Xiong, 2011)
ABI5	Signal transduction	DWA1, DWA2	*At*	(Lee et al., 2010a)
Myc	Proto-oncogenic transcription factor	TRPC4AP/ TRUSS	*Hs*	(Choi et al., 2010)
c-Jun	Proto-oncogenic transcription factor	?	*Hs*	(Wertz et al., 2004)
HOXA9	Development	?	*Hs*	(Zhang et al., 2003)
CHK1	Cell cycle checkpoint	?	*Hs*	(Leung-Pineda et al., 2009)
Dacapo	Cell cycle inhibitor	?	*Dm*	(Higa et al., 2006c)
Cyclin E	Cell cycle	?	*Dm*	(Higa et al., 2006c)
β-catenin	Development	?	*Hs*, *Dm*	(Tripathi et al., 2007)
RASSF1A	Mitosis	?	*Hs*	(Jiang et al., 2011)
STAT1,2,3	Signal transduction	SV5[b,d]	*Hs*	(Andrejeva et al., 2002; Precious et al., 2005; Ulane and Horvath, 2002; Ulane et al., 2005; Ulane et al., 2003)
UNG2	DNA repair	VprBP-Vpr[d]	*Hs*	(Ahn et al., 2010; Schrofelbauer et al., 2005)

[a]Abbreviations for organisms: *Hs*, *Homo sapiens*; *Xl*, *Xenopus laevis*; *Dm*, *Drosophila melanogaster*; *Ce*: *Caenorhabditis elegans*; *Sp*: *Schizosaccharomyces pombe; At: Arabidopsis thaliana*
[b] Not a WD40 protein
[c] CUL4B specific
[d]viral protein

CRL4 ubiquitylation does not always lead to degradation

In addition to targeting substrates for proteolytic degradation, $CRL4^{CDT2}$ can promote mono-ubiquitylation on PCNA itself in undamaged cells and cooperates with RAD18 to promote translesion DNA synthesis (Terai et al., 2010). PCNA ubiquitylation seems to be constantly antagonized by the action of ubiquitin-specific protease 1 (USP1) and may function to poise cells for repair during DNA replication (Terai et al., 2010). Likewise, several studies have observed $CRL4^{DDB2}$-dependent mono-ubiquitylation of core histones (Wang et al., 2006; Guerrero-Santoro et al., 2008; Kapetanaki et al., 2006) that have been suggested to function as a signal for the binding of repair factors to damaged DNA. From a biochemical standpoint, it remains unclear how one E3 ligase apparently causes monoubiquitylation of some substrates and polyubiquitylation of others that leads to degradation. Further complicating matters, $CRL4^{DDB2}$ has been suggested to also promote non-proteolytic polyubiquitylation of XPC during DNA repair (Kapetanaki et al., 2006). It will be important to determine how different ubiquitin lysine residues are linked on different substrates, whether ROC1 can itself switch between different E2s or if additional factors that control the ROC1–E2 binding yield such a diverse set of ubiquitylated substrates.

Though not all CRL4 substrates identified to date are associated with chromatin, (as illustrated by the ubiquitylation of cytoplasmically localized TSC2 (tuberous sclerosis 2) by $CRL4A^{FBW5}$ (Hu et al., 2008) and ER-α ubiquitylation by $CRL4B^{AhR}$ (Ohtake et al., 2007)), the majority of the literature on CUL4 complexes supports essential functions in DNA repair and replication. Indeed, VprBP, the focus of my thesis research, is bound to chromatin in a cell cycle specific manner, and loss of VprBP in cultured cells causes defects in S phase progression (McCall et al., 2008). However, there is currently no clear evidence linking VprBP directly to DNA replication or repair (discussed in detail below).

Viral Hijacking of DDB1-CUL4

Many viruses are known to exploit the ubiquitylation pathway to evade innate cellular antiviral mechanisms or otherwise benefit viral propagation (Randow and Lehner, 2009). CRL4s are targeted by several viruses including members of the paramyxovirus, herpesvirus, lentivirus, and hepadnavirus families. Although these diverse viruses commonly target DDB1, they appear to disrupt CRL4s in different ways. Viruses from the paramyxovirus family including simian virus 5, mumps virus and human parainfluenza virus type 2, use CUL4–DDB1 to degrade signal transducer and activator of transcription (STAT) proteins that respond to interferon signaling and initiate cellular antiviral responses (Andrejeva et al., 2002; Ulane and Horvath, 2002). The crystal structure of simian virus 5 V (SV5-V) protein in complex with DDB1 showed that despite almost no primary sequence homology with DDB2, SV5-V protein similarly inserts a helix between β-propellers BPA and BPC (Li et al., 2006). Hepatitis B virus X protein (HBx) also binds to DDB1, which is thought to facilitate viral replication (Leupin et al., 2005; Leupin et al., 2003) by causing an extended S-phase (Martin-Lluesma et al., 2008). Binding assays show that SV5-V and HBx bind DDB1 in a mutually exclusive manner (Leupin et al., 2003). Furthermore, structural analysis revealed that HBx, as well as SV5-V contains primary sequence homology to DDB2's helix h1 that inserts into a cavity formed by BPA and BPC in DDB1 (Scrima et al., 2008). Collectively, these structural analyses suggest that HBx and SV5-V viral proteins, although lacking WD40 repeats and sharing little primary sequence homology with each other, might form a similar structural motif and bind to a region in the BPA-BPC pocket of DDB1 in a manner similar to that of DDB2. The cellular protein(s) targeted by HBx to DDB1–CUL4 ligase remains unknown, raising the possibility that HBx facilitates viral propagation by interfering with the ubiquitylation of a host protein instead of targeting a novel host protein for degradation. This could also be the case for the murine gamma herpesvirus 68 M2

protein that binds to CUL4–DDB1, impairs the DNA damage response and inhibits apoptosis through unknown cellular mechanisms (Liang et al., 2006). Most recently, several groups have established that HIV-1 Vpr and the related simian immunodeficiency virus protein Vpx bind to $CRL4^{VprBP}$ (Belzile et al., 2007; Hrecka et al., 2007; Le Rouzic et al., 2007; Tan et al., 2007; Wen et al., 2007) (discussed further below). Mechanisms for how CRL4 is exploited by so many divergent viruses remain to be shown in detail, but clearly this family of broadly expressed ubiquitin ligases is an attractive target.

HIV1 Vpr Binding Protein, VprBP

VprBP (also known as DDB1-Cullin 4 associate factor, DCAF1) was first identified as the HIV1 viral protein r binding protein (Zhang et al., 2001; Zhao et al., 1994). HIV1 viral protein r (Vpr) is an accessory protein that is not required for viral replication in vitro, but is highly conserved in HIV1, HIV2, and the related simian immunodeficiency virus. Vpr is associated with multiple functions in vivo including inducing a G2 cell cycle arrest, promoting apoptosis, and nuclear transport of preintegration complexes (Le Rouzic and Benichou, 2005). Vpr is a multifunctional protein and associates with a number of host proteins such as uracil DNA glycosylase (UNG2), CDC25, adensosine nucleotide translocator (ANT), and Vpr binding protein (VprBP). A number of long-term nonprogressor patients, individuals who are HIV positive but experience extremely slow progression to AIDS even in the absence of antiretroviral treatment, have been found to have mutations in Vpr (Rodes et al., 2004). Recently, a long-term nonprogressor patient-derived point mutant in Vpr (Q65R) was identified to abolish binding with VprBP, suggesting that this association may be important for disease progression (Jacquot et al., 2009).

Vpr has been reported to arrest infected cells in the G2 phase of the cell cycle by activating atacia telengiectasia and Rad3-related protein kinase (ATR). Vpr does not appear to trigger ATR by causing double strand breaks in DNA, but may cause stalled replication forks (Lai et al., 2005; Zimmerman et al., 2006). Vpr associates with VprBP in the context of $CRL4^{VprBP}$ (Belzile et al., 2007; Hrecka et al., 2007; Le Rouzic et al., 2007; Tan et al., 2007; Wen et al., 2007). Studies by several groups demonstrated that RNAi-mediated knockdown of *Vprbp* or *Ddb1* mRNA relieves the G2 arrest caused by Vpr overexpression (Belzile et al., 2007; DeHart et al., 2007; Hrecka et al., 2007; Le Rouzic et al., 2007; Tan et al., 2007; Wen et al., 2007), though observations from our lab suggest a caveat to these experiments is that knockdown of *Vprbp* alone can induce a partial G1 arrest.

Vpr may function to hijack the $CRL4^{VprBP}$ complex to degrade UNG2, a uracil DNA glycosylase that removes uracil from DNA as part of the base excision repair pathway (Ahn et al., 2010)(Figure 1.3B). Vpr expression was shown to increase the degradation of UNG2, and knockdown of *DDB1* or *CUL4A/B* stabilized UNG2 in the presence of Vpr (Schrofelbauer et al., 2007; Wen et al., 2007). More recently, in vitro ubiquitylation of UNG2 by CRL4 and a fragment of VprBP containing residues 987–1396 was demonstrated (Ahn et al., 2010). However, it remains unclear whether UNG2 is the sole target of $CRL4^{VprBP\text{-}Vpr}$ or if additional targets are exploited to benefit HIV propagation. Furthermore, depletion of CUL4 or DDB1 had no effect on UNG2 degradation in the absence of Vpr (Schrofelbauer et al., 2007; Wen et al., 2007; Ahn et al., 2010) indicating that $CRL4^{VprBP}$ cannot ubiquitylate UNG2 in the absence of Vpr. The normal physiological substrate(s) for $CRL4^{VprBP}$ are currently unknown.

Figure 1.3

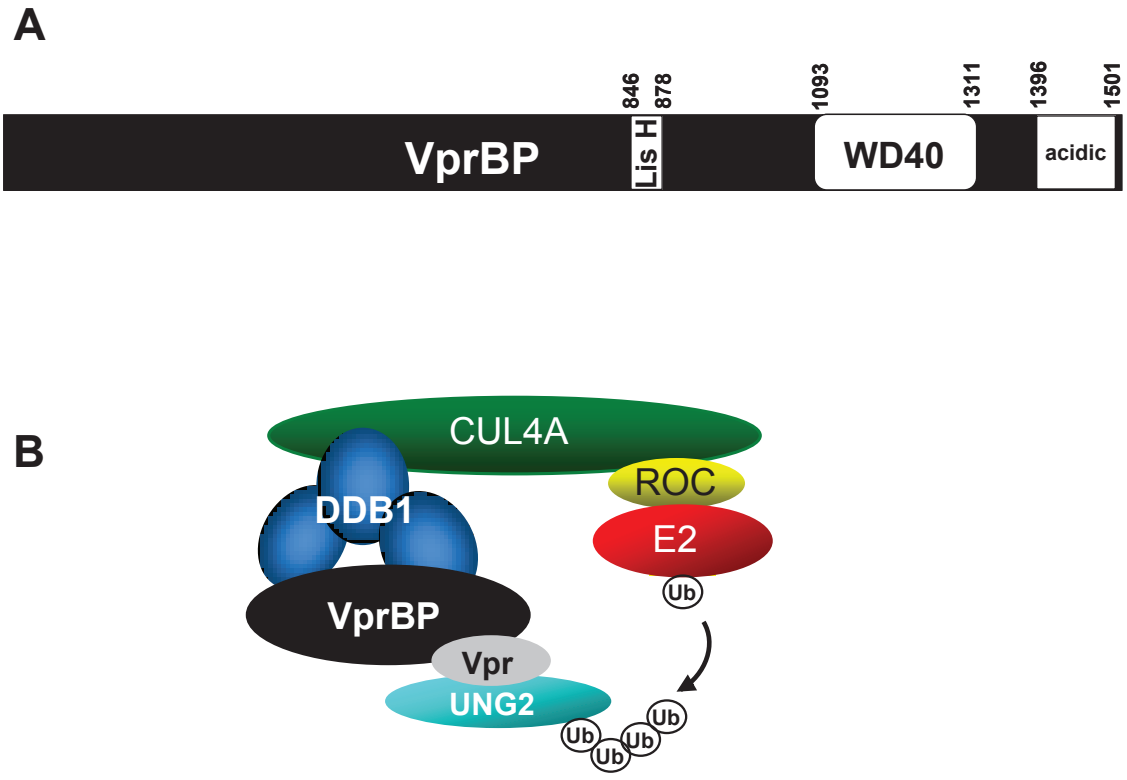

Figure 1.3. Schematic of VprBP.

(A) Schematic of VprBP protein structure. VprBP is a 1507 amino acid protein that contains an alpha-helical LisH domain, a WD40 domain containing two WDXR motifs and five additional WD40 motifs, and an acidic residue rich tail. The N-terminal portion of VprBP contains no known protein motifs

(B) VprBP is a component of a CUL4 ubiquitin ligase complex. VprBP binds to CUL4A through the adaptor protein DDB1. Though no substrate has been identified in for $CRL4^{VprBP}$ in normal cells, the uracil DNA glycosylase UNG2 has been proposed to be targeted by the complex in the presence of HIV-1 viral protein R (Vpr).

VprBP was identified in the Xiong lab by former graduate student Chad McCall (McCall et al., 2008). VprBP function as a substrate recruiting receptor for CRL4 is inferred from binding with the CUL4-DDB1-ROC1 complex and the presence of the two WDXR motifs which are shared in other experimentally demonstrated CRL4 substrate receptors. Thus far, only one candidate substrate, the neurofibromatosis type 2 (*NF2*) tumor suppressor gene product, Merlin, has been reported to be targeted by $CRL4^{VprBP}$ ligase for degradation (Huang and Chen, 2008). However, this finding has been seriously challenged by more recent data from the Giancotti lab which suggests that Merlin instead functions as an upstream regulator of VprBP (Li et al., 2010b) (discussed further in Chapters 3).

Without any known substrate, the in vivo function of $CRL4^{VprBP}$ remains obscure, but a possible function in replication has been proposed. Knocking down VprBP resulted in defective progression through S phase and inhibited proliferation (McCall et al., 2008; Hrecka et al., 2007), indicating that VprBP is required for normal cell cycle progression in cultured cells. Furthermore, genetic disruption of *Vprbp* in mice, *Drosophila* or *Arabidopsis* caused early embryonic lethality (McCall et al., 2008; Tamori et al., 2010; Zhang et al., 2008), indicating that *Vprbp* is an essential gene.

The goal of my research has been to explore the in vivo function and mechanism of VprBP through a combination of biochemical and genetic approaches. In chapter 2, I describe research testing a hypothesis that VprBP functions in epigenetic modification of histones in a manner analogous to the $CRL4^{DDB2}$ complex. Intriguingly, I observed a possible role for VprBP in histone H4 ubiquitylation. In chapter 3, I focused on analyzing conditional *Vprbp* mouse embryonic fibroblasts (MEFs) and found that VprBP is required for MEF proliferation. Unexpectedly, I also discovered that high levels of VprBP protein are associated with quiescent cells, suggesting functions beyond proliferation. In Chapter 4, I describe data (which has been submitted to the journal Molecular and

Cellular Biology for publication) examining temporally controlled disruption of conditional *Vprbp* in mice using the tamoxifen-inducible, *Ubiquitin C* promoter driven *Cre-ERT2*. This approach allowed me to probe *Vprbp* function in an unbiased manner to explore phenotypes beyond early embryonic lethality and uncovered a role for *Vprbp* in the proliferation and survival of lymphocytes. Finally, Chapter 5 provides a perspective on outstanding questions in VprBP research and discusses potential experiments to address these issues.

CHAPTER II

BIOCHEMICAL ANALYSIS OF VPRBP IN HISTONE MODIFICATION

Summary

Epigenetic modifications are critical for normal development, regulation of gene transcription, DNA replication and DNA repair. Known post-translation modifications of histones include phosphorylation, acetylation, methylation, sumolyation, and ubiquitylation. The $CUL4A^{DDB2}$ complex specifically associates with damaged DNA and ubiquitylates histones, among other substrates, to mediate the DNA damage response. In addition, the Xiong lab previously demonstrated that VprBP specifically binds to chromatin. Based on these observations, we hypothesized that VprBP may function to ubiquitylate histones. I found that loss of VprBP or DDB1 in HeLa cells decreased global levels of ubiquitylated histone H4 but not other core histones. Site-directed mutagenesis experiments failed to identify a single lysine residue in histone H4 that is ubiquitylated by VprBP, suggesting that multiple residues may be targeted. Furthermore, I found that loss of VprBP resulted in an increase in ubiquitylation of the linker histone H1.1 suggesting a cross-talk between histone modifications. These data support a role for VprBP in regulating epigenetic modification and suggest that $CRL4^{VprBP}$ may regulate a novel ubiquitylation event on histone H4.

Background

To condense the massive amount of DNA in eukaryotic genomes, DNA is organized into chromatin fibers. The fundamental unit of chromatin is the nucleosome, which consists of 147 base pairs of DNA wrapped around a histone octomer containing two copies each of H2A, H2B, H3, and H4 (Bhaumik et al., 2007). Additional linker histones, such as histone H1, are required to form higher order chromatin structures. Regulation of processes involving chromatin dynamics, such as replication, repair and transcription, rely on post-translational modifications of histones. Each core histone has a central globular domain, which contains the histone fold required for interactions between histones and histone-DNA interactions, as well as N-terminal and C-terminal tails. Post-translational modifications of histones have been observed in the tails as well as the globular domain, though the N-terminal tails have the best-characterized modifications. Histones are modified by phosphorylation, acetylation, methylation, ADP ribosylation, sumoylation, and ubiquitylation and are highly regulated by enzymes that add and remove these modifications (Kouzarides, 2007). In this chapter, I focus on the role that histone ubiquitylation plays in regulating chromatin dynamics.

In mammalian cells, ubiquitylated histone H2B is associated with active transcription, whereas ubiquitylated H2A has been well-studied in both gene repression and DNA repair (Groth et al., 2007; Minsky et al., 2008). H2B is predominately ubiquitylated at lysine 120 by BRE1/RNF20 and requires RAD6 as its E2 ubiquitin conjugating enzyme (Kim et al., 2009; Kim et al., 2005). H2B ubiquitylation does not appear to be required for transcription, but rather is proposed to be a consequence of transcription; H2B ubiquitylation may help to reassemble nucleosomes after the passage of the transcriptional apparatus (Fleming et al., 2008; Kim et al., 2009). H2A is ubiquitylated at K119 by the transcripitionally repressive Polycomb complex (PRC1), and by several ubiquitin ligases at sites of DNA damage, including Ring2, RNF8 and

$CRL4^{DDB2}$ (Bergink et al., 2006; Huen et al., 2007; Kapetanaki et al., 2006; Kolas et al., 2007; Wang et al., 2004). In response to double-strand breaks, H2A is ubiquitylated by RNF8 and this ubiquitylation is required for the subsequent recruitment of checkpoint proteins BRCA1 and 53BP1. Both Ring2 and $CRL4^{DDB2}$ have been shown to ubiquitylate H2A following UV damage, but for Ring2, this appears to occur after the assembly of the nucleotide excision repair factors as H2A could not be ubiquitylated in several cell lines deficient for nucleotide excision repair proteins (XP-A, XP-C, XP-G, and XP-F) (Bergink et al., 2006). The polycomb complex PRC1 contains two ubiquitin ligase subunits, Ring1 and Ring2. Both are genetically required during development to repress *Hox* genes (del Mar Lorente et al., 2000; Suzuki et al., 2002), but Ring2 appears to directly ubiquitylate H2A whereas Ring1 may function to enhance the catalytic activity of Ring2 (Cao et al., 2005; Wang et al., 2004). Intriguing new data suggest that Ring2 may function as part of the PRC1 complex in ubiquitylating H2A in both transcriptional repression and DNA repair (Ismail et al., 2010). Less is known about ubiquitylation of histones H3 and H4. However, recent evidence suggests that H3 may be ubiquitylated by the RAG1 complex during V(D)J recombination (Jones et al., 2011) and that H4 is ubiquitylated in response to DNA damage (Yan et al., 2009).

$CRL4^{DDB2}$ has been reported to ubiquitylate histone H3 and H4 (Wang et al., 2006) as well as H2A (Guerrero-Santoro et al., 2008; Kapetanaki et al., 2006) following ultraviolet irradiation. We collaborated with the Zhang lab in demonstrating a function for $CRL4^{DDB2}$ in histone ubiquitylation; $CRL4^{DDB2}$ was biochemically purified from nuclear fractions based on its histone ubiquitylation activity, and identified by mass spectrometry (Wang et al., 2006). H3 and H4 ubiquitylation were induced by UV, and RNAi depletion of DDB1, CUL4A or CUL4B abrogated this UV-induced ubiquitylation of histone H3 and H4 in vivo. Thus, $CRL4^{DDB2}$ plays a role in mono-ubiquitylating core histones in response to UV-induced DNA damage. Based on our observations that VprBP is

associated with chromatin in a cell cycle dependent manner and forms a CRL^{VprBP} complex, we hypothesized that $CRL4^{VprBP}$ may function to ubiquitylate core histones to facilitate cell cycle progression.

Experimental Procedures

Cell culture and plasmids

A stable HeLa cell line expressing HA-ubiquitin was previously generated (Wang et al., 2006). Cells were cultured in Dulbecco's Modified Eagle's Medium (DMEM) containing 10% fetal bovine serum (FBS) and 200 μg/ml hygromyocin B in a 37°C incubator with 5% CO_2.

Plasmids containing the *β-globin* intron and expressing Flag-tagged histone (H2A, H2B, H3, or H4) were kindly provided by Dr. Yi Zhang (Wang et al., 2006). Histones H1.1, which contains no introns, was cloned by PCR amplification from genomic DNA extracted from WI38 cells using the following primers (all primers are listed 5' to 3'): H1.1F GGATCCATGATGTCTGAAACAGTGCCTCCCG; H1.1R CTGAATTTACTTTTTCTTGGGTGCCGC. PCR products was ligated into pCR-2.1-TOPO using TA cloning (Invitrogen) and subsequently subcloned into pcDNA3-Flag using BamHI and EcoRI. Plasmids expressing VprBP, DDB1, and DDB2 were previously described (He et al., 2006; McCall et al., 2008).

Cell transfection and RNAi

RNAi oligonucleotides were transfected to HeLa-HA-Ub cells using Lipofectamine 2000 according to the manufacturer's instructions (Invitrogen). The sense sequence for oligonucleotides used to knockdown endogenous gene expression is as follows: DDB1 5' GUUUUUGGCAAUCAACAGGTT 3', VprBP1 5' UCACAGAGUAUCUUAGAGATT 3', VprBP2 5' GAAUACUCUUCAAGAAUGATT 3', and control 5' ACCUCAAGAAUUUAUUGAATT 3'. For VprBP knockdown, a pool containing VprBP1 and VprBP2 oligonucleotides was used. Transfection of HeLa-HA-Ub cells with pcDNA3-Flag- histone was carried out using a calcium-phosphate buffer 24h following RNAi transfection.

Mutagenesis

Lysine residues in histone H4 were mutated individually using the QuikChange Site-Directed Mutagenesis kit (Strategene) with the following primers:

H4K6R GGAATTCTGATGTCTGGCCGCGGTAGGGGCGGGAAGGGTTTG;

H4K9R CTGATGTCTGGCCGCGGTAGGGGCGGGAAGGGTTTGGGTAAGG;

H4K13R GGCGGGAAGGGTTTGGGCCGCGGAGGTGCCAAGCGC;

H4K17R GGTAAGGGGGGTGCCCGTCGACACCGCAAGGTGTTGC;

H4K21R GGGGGTGCCAAGCGCCACCGCAGAGTACTGCGTGACAACATC;

H4K32R ATCCAGGGCATCACCCGGCCAGCCATCCGGCGTCTG;

H4K45R GGCGTGGCGGTGTGAGGCGGATATCTGGTCTGATCTACG;

H4K60R CGCGGTGTGCTGCGGGTGTTCCTCGAGAATGTGATTCGG;

H4K78R GTCACCTACACCGAGCATGCCCGGCGCAAGACCGTCAC;

H4K80R ACCTACACCGAGCATGCCAAGCGCCGGACCGTCACAGCC;

H4K92R GTGGTCTACGCGCTTCGTCGACAGGGACGCACCCTTTATG.

Cellular lysis, immunoprecipitation and western blot analysis

Cells were harvested 72h after the RNAi transfection by scraping into phosphate buffered saline (PBS). Cell pellets were subsequently lysed in 1% SDS buffer containing 50 mM Tris-HCl, pH 7.5 and 0.5 mM EDTA and then boiled for 10 minutes. Lysates were diluted 1:10 in 0.1% NP-40 buffer (50 mM Tris-HCl, pH 7.5, 150 mM NaCl, 0.1% NP-40, 50 mM NaF) and histones were immunoprecipitated using Flag M2 antibody (Sigma). Proteins were resolved by SDS-PAGE and immunoblotted using Flag M2, Flag M2-HRP (both Sigma), HA 12CA5 (Boehringer-Mannheim) or HA-HRP (Roche).

For chromatin isolation, cells were lysed in CSK buffer (10 mM PIPES-KOH, pH 6.8, 100 mM NaCl, 300 mM sucrose, 3 mM $MgCl_2$, 0.5 mM phenylmethylsulfonyl

fluoride, 1 mM glycerophosphate, 50 mM NaF, 1 mM Na_3VO_4, and protease inhibitors) containing 0.5% Triton X-100 as described (Cook et al., 2004). Portions were reserved (whole-cell extracts) prior to fractionation by low-speed centrifugation. Detergent-insoluble pellets were treated for 5 min with 15 U of micrococcal nuclease (Roche) in CSK buffer supplemented with 2 mM $CaCl_2$ and then separated again by centrifugation. Proteins in the nuclease-soluble fractions of these digests were defined as chromatin bound.

Cell Cycle Synchronization and Flow Cytometry

Cells were synchronized by double thymidine treatment. In brief, subconfluent HeLa-HA-Ub cells were treated with 2mM thymidine (Sigma T1895) for 16h and then released into fresh medium for 8h. Cells were retreated with 2mM thymidine for 16h, released into fresh medium and collected at the indicated time points after release.

To analyze the cell cycle at each timepoint after release from synchronization, cells were fixed in 75% ethanol overnight at 4°C, washed once in 1× PBS plus 1% FBS, and then permeabilized in 1× PBS, 0.1 mg/ml RNase A, and 0.1% Triton X-100. The fixed and permeabized cells were stained with 50 µg/ml PI and analyzed on a CyAN (Dako Cytomation) flow cytometer. Data were analyzed using Summit software, version 4.3 (Dako Cytomation).

DNA Damage Induction

HeLa-HA-Ub cells were treated with 25 J/m^2 ultraviolet radiation (UV) 10 minutes prior to cell lysis. Alternatively, HeLa-HA-Ub cells were treated with 25µM etoposide for 4h prior to cell lysis.

Results

VprBP may regulate global levels of histone ubiquitylation.

To test the possibility that VprBP regulates ubiquitylation of core histones, we overexpressed Flag-tagged versions of the four major core histones in a stable HeLa cell line which expresses HA-ubiquitin (HeLa-HA-Ub) following RNAi for VprBP, DDB1 or control. Cells were lysed in 1 % SDS lysis buffer and boiled to disrupt chromatin, and lysates were immunoprecipitated with anti-Flag antibody. An apparent ubiquitylated H4 was observed in control cells, but not in cells knocked down for DDB1 or VprBP, suggesting that $CRL4^{VprBP}$ targets H4 for ubiquitylation (Fig. 2.1). H4 ubiquitylation has been scarcely reported, but has been reported in response to UV- and doxorubicin-induced DNA damage (Wang et al., 2006; Yan et al., 2009). Our preliminary results suggested that VprBP may play a role in H4 ubiquitylation.

VprBP promotes H4 modification, but inhibits H1.1 modification.

In addition to examining the role of VprBP in core histone ubiquitylation, we also asked whether VprBP might also affect the ubiquitylation of linker protein histone H1.1. As in the previous experiment, HeLa-HA-Ub cells were treated with RNAi oligos to VprBP, DDB1 or control and subsequently transfected with pcDNA3-Flag-Histone or pcDNA3-GFP plasmids. The efficiency of RNAi and equal loading was determined by western blotting of input cellular lysate. Following immunoprecipitation by Flag antibody, we examined the ubiquitylation of histone proteins by first probing for ubiquitin by western blotting for HA. We detected a ubiquitin band corresponding to ubiquitylated H2A in control cells and siVprBP cells, which verified that our assay worked as expected and established that VprBP plays no role in H2A ubiquitylation. No additional proteins were detected upon probing for ubiquitin. After striping the membrane and re-probing for histone proteins with Flag-HRP antibody, we detected all 5 histone proteins, and a

Figure 2.1

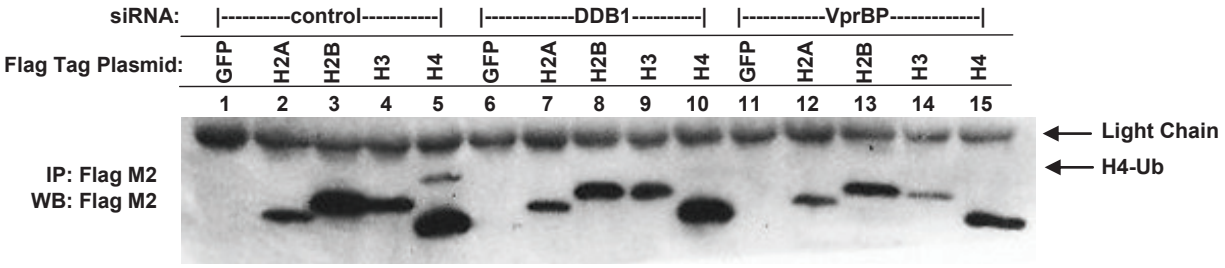

Figure 2.1. VprBP regulates global levels of H4 ubiquitylation.

A stable HeLa cell line expressing HA-ubiquitin (HeLa-HA-Ub) was transfected with pcDNA3-Flag-Histone or pcDNA3-GFP plasmids as indicated 24 hours following RNAi treatment. Cells were lysed in 1% SDS buffer and boiled. Histone proteins were immunoprecipitated from lysate using Flag antibody, resolved by SDS-PAGE and immunoblotted with Flag antibody. An apparent ubiquitylated H4 was observed in control cells, but not in cells knocked down for DDB1 or VprBP.

Figure 2.2

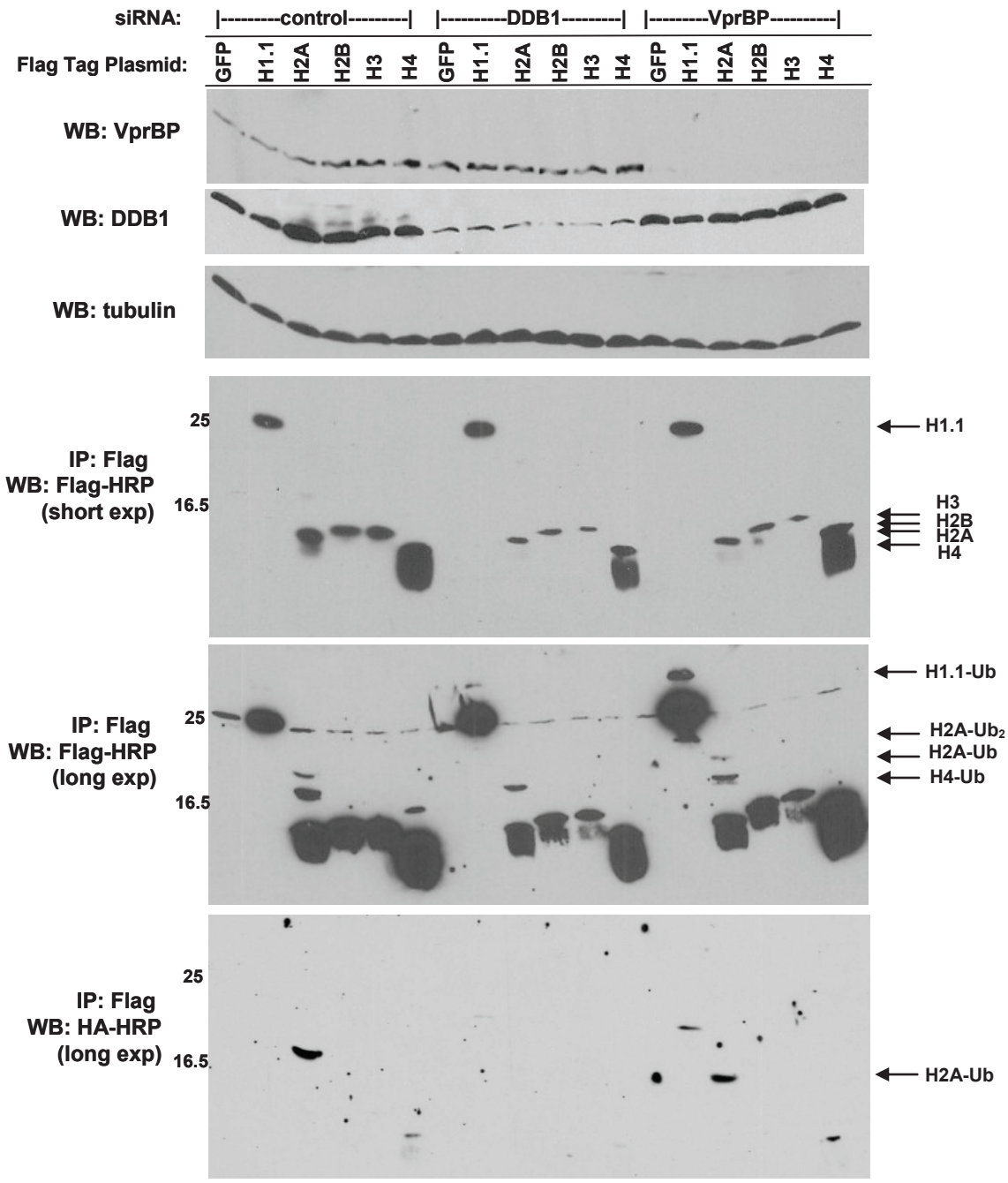
siRNA:
|---------control---------|
|----------DDB1---------|
|---------VprBP----------|
Flag Tag Plasmid:
GFP
H1.1
H2A
H2B
H3
H4
WB: VprBP
WB: DDB1
WB: tubulin
IP: Flag
WB: Flag-HRP
(short exp)
25
16.5
H1.1
H3
H2B
H2A
H4
IP: Flag
WB: Flag-HRP
(long exp)
H1.1-Ub
H2A-Ub2
H2A-Ub
H4-Ub
IP: Flag
WB: HA-HRP
(long exp)
H2A-Ub

Figure 2.2. VprBP promotes H4 modification, but inhibits H1.1 modification.

HeLa-HA-Ub cells were treated with RNAi oligos to VprBP, DDB1 or control as indicated and subsequently transfected with pcDNA3-Flag-Histone or pcDNA3-GFP plasmids as indicated. Histone proteins were immunoprecipitated from lysate using Flag antibody and resolved by SDS-PAGE. RNAi efficiency was confirmed by immunoblotting for VprBP and DDB1. The lower panel of the membrane was first blotted with HA-HRP, and detected ubiquitylated-H2A in control and siVprBP treated cells. The membrane was then stripped and probed with Flag-HRP. An increase in H1.1 modification and a decrease in H4 modification were observed following siVprBP treatment.

slower migrating form of histones H1.1, H2A, and H4. As was seen previously, loss of VprBP corresponded with loss of modified H4 protein. In addition, we now observed that loss of VprBP, and to a lesser extent, DDB1 depletion, correlated with an increase of modified histone H1.1. This unexpected result indicates that $CRL4^{VprBP}$ indirectly impacts the modification of histone H1.1 and suggests the possibility that there is cross-talk between H4 modification and H1.1 modification.

The fact that the modified version of both H1.1 and H4 were not detected by HA immunoblotting suggests one of two possibilities: (1) the level of modified histone was below the detection threshold for the HA antibody, but not for the highly sensitive Flag M2 antibody, or (2) the histone proteins have a post-translational modification which does not contain ubiquitin. Indeed sumoylated H4 has been noted in both *S. cerevisiae* and human cells using a system similar to ours, i.e. overexpression of Flag-tagged H4 and HA-tagged SUMO. However, SUMO, a ubiquitin-like protein with an apparent molecular weight of 15 kDa, runs at a significantly higher molecular weight than ubiquitin, which is 8.5 kDa; HA-sumoylated conjugated Flag-H4 migrates slower than antibody light chain while HA-ubiquitin conjugated Flag-H4 migrates faster than light chain (see (Shiio and Eisenman, 2003)). This suggests, but does not prove, that the level of HA-ubiquitylated H4 is below the detection limit of the HA antibody. Despite extensive efforts to scale up or modify the protocol (e.g. immunoprecipitate with HA antibody followed by Flag western blot), I was unsuccessful at positively identifying ubiquitylated H4 (data not shown). Thus I refer to this slower migrating form of H4 as modified rather than ubiquitylated.

H4 modification is potentially dependent on cell cycle phase.

To determine the biological significance of H4 modifications, I sought to determine cellular conditions which promoted ubiquitylation. Because VprBP binding to chromatin is cell cycle dependent, I hypothesized that if H4 ubiquitylation depended on VprBP, modification should also occur in a cell cycle-dependent manner. To test this idea, I synchronized HeLa-HA-Ub stable cells at the G1-S boundary using a double thymidine block following transfection with pcDNA3-Flag-H4 and collected at 0, 2, 4, 8, 12h after release. A 10 cm dish was used for each time point and cells collected were divided into two fractions: (1) cells were fixed with ethanol for flow cytometry, and (2) cells were lysed in SDS buffer and immunoprecipitated with Flag antibody. Flow cytometric analysis of propidium iodide stained cells demonstrates the cell cycle phase and synchrony of each time point (Fig. 2.3A). Input lysate for immunoprecipiation from each time point was resolved by SDS-PAGE, and immunoblotted for VprBP. Total VprBP showed a cell cycle-dependent expression pattern with low levels at the onset of S-phase and increasing protein levels through G2-phase (Fig. 2.3B and in agreement with (Maddika and Chen, 2009)). In addition, I examined the status of H4 modification, and observed very low levels of modified H4 in G2 phase cells at 8 and 12 h following release (Fig. 2.3B). This observation is consistent with a role for $CRL4^{VprBP}$ in modifying histone H4. These data also highlights the difficulty of detecting modified H4, suggesting that this modification is not very abundant or is readily lost during cell lysis, perhaps due to highly active deubiquitylase enzymes.

H4 modification and VprBP binding to chromatin is not induced by DNA damage.

To further probe for potential biological functions for VprBP-induced H4 modification, I tested if VprBP binding to chromatin or H4 modification can be induced by DNA damage. For DNA damage agents, I tested ultra-violet irradiation (UV), which

induces pyridimine dimers and (6-4) photoproducts, and etoposide, a topoisomerase II inhibitor which induces double and single strand DNA breaks. In contrast to published results (Wang et al., 2006), I did not see an increase in H4 ubiquitylation in response to UV treatment (Fig. 2.4A). Furthermore, I did not observe an increase in VprBP binding to chromatin in response to UV whereas DDB1 and CUL4A association with chromatin increased in response to UV (Fig. 2.4B) (consistent with (McCall et al., 2008)). This test serves as a positive control for UV treatment. In addition, I did not observe any increase in H4 ubiquitylation in response to etoposide-induced DNA damage, nor any increased association of VprBP, DDB1 or CUL4A with chromatin (Fig. 2.4A and 2.4B), indicating that $CRL4A^{VprBP}$ is not involved in mediating DNA damage response after etoposide-induced DNA breaks. Cumulatively, these results indicate that $CRL4^{VprBP}$ and histone H4 modification are not involved in the response to UV- or etoposide-induced DNA damage.

Figure 2.3

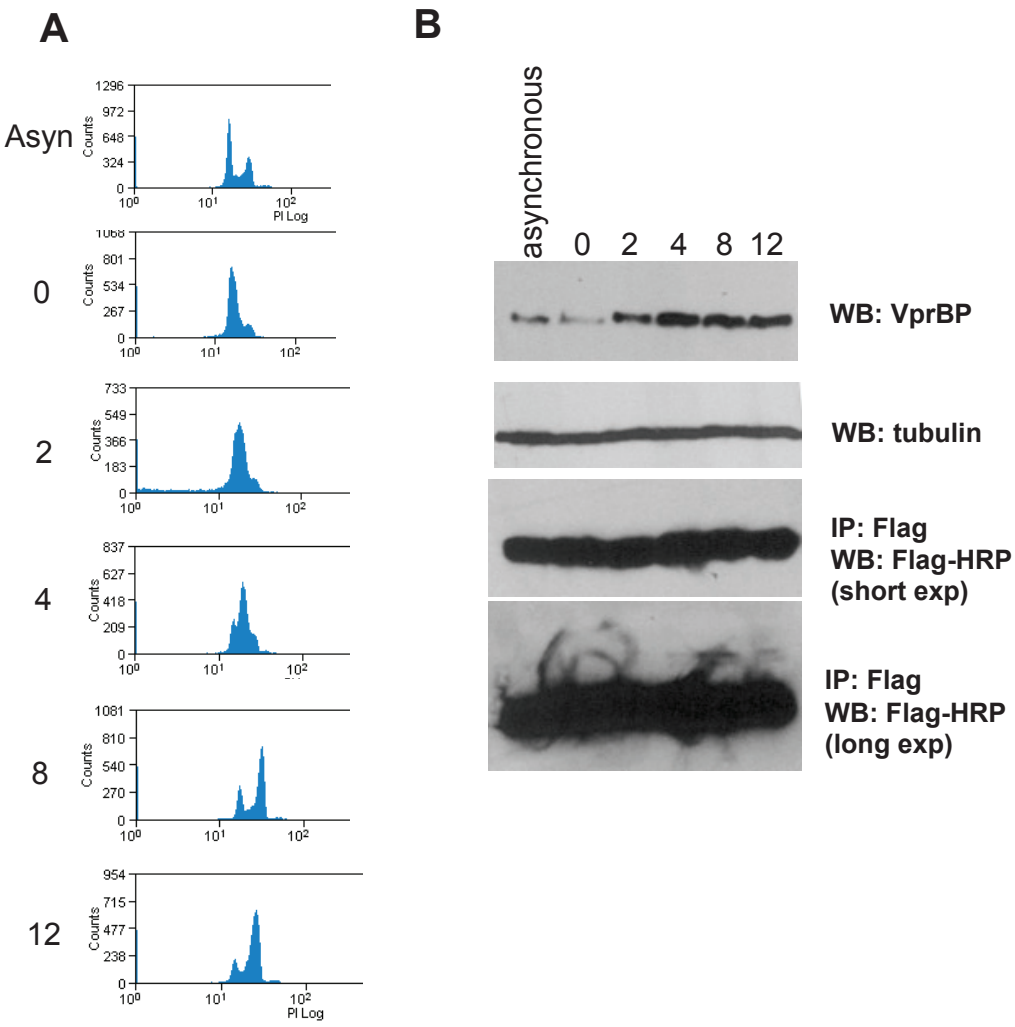

Figure 2.3. H4 modification is potentially dependent on cell cycle phase.

HeLa-HA-Ub cells transiently transfected with pcDNA3-Flag-H4 were synchronized at G1-S using a double thymidine block. (A) Flow cytometric analysis was used to verify synchronization at each time point collected.

(B) Whole cell lysate of a portion of synchronized cells was obtained, resolved by SDS-PAGE, and immunoblotted. A final portion of cells was lysed, immunoprecipated using Flag antibody, resolved by SDS-PAGE and immunoblotted with Flag antibody to detect histone H4.

Figure 2.4

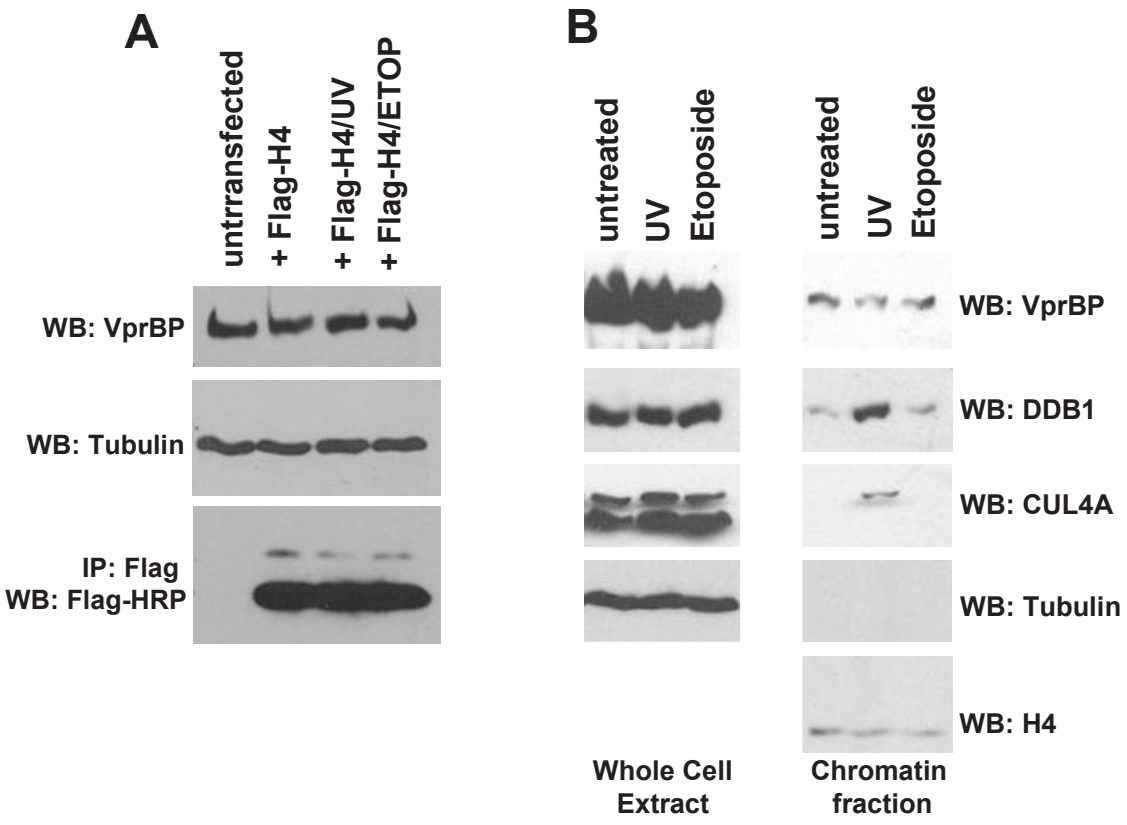

Figure 2.4. H4 modification and VprBP binding to chromatin is not induced by DNA damage.

(A) H4 ubiquitylation does not increase in response to UV or etoposide. HeLa-HA-Ub cells were transfected with pcDNA3-Flag-H4 as indicated and treated with 25 J/m^2 UV (10 min) or 25μM etoposide (4 h) as indicated.

(B) VprBP association with chromatin is not increased in response to DNA damage. HeLa cells were treated with UV or etoposide as indicated. Cells were lysed in CSK buffer, and the chromatin fraction was isolated. As a positive control, DDB1 binding to chromatin increases in response to UV treatment.

Mutagenesis of H4 indicates multiple sites affect H4 modification.

Several known post-translational modifications occur on the N-terminal tail of H4 (Fig. 2.5B). To better understand the nature of the histone H4 modification observed in this study, I sought to identify which residue on H4 was modified. Post-translational modification by both ubiquitin and SUMO require covalent conjugation to a lysine residue within the substrate protein. To determine which lysine is modified in H4, I individually mutated every lysine residue in histone H4 in both the N-terminal tail and the globular domain (K5, K8, K12, K16, K20, K31, K44, K59, K77, K79, K91) and substituted lysine with arginine by site-directed mutagenesis. After transient transfection into HeLa-HA-Ub cells, cells were lysed, Flag-H4 protein was immunoprecipitated, resolved by SDS-PAGE and detected by immunoblotting for Flag (Fig. 2.5). Surprisingly, I found that no single mutation completely abolished H4 modification. Typically mono-ubiquitylated or sumoylated proteins have a specific lysine residue which is targeted by modification. That lysine mutation did not disrupt H4 modification suggests that H4 can be mono-ubiquitylated (or sumoylated) at more than one residue.

VprBP does not readily bind core histones.

Observations that H4 modification correlated with previously-established timing of VprBP binding to chromatin suggested that VprBP may directly ubiquitylate H4. To test this possibility, Flag-H4 and Myc3-VprBP were transiently transfected into 293T cells and binding was probed by immunoprecipatation after micrococcal nuclease digestion. As a positive control, Flag-H2A and DDB2 were also co-expressed in 293T cells. As a negative control, Myc3-VprBP was overexpressed with Flag-H2A. Overexpression of DDB2 clearly increased the level of ubiquitylated H2A, and DDB2 could be detected in the Flag-H2A immunoprecipitation, though H2A was not detected in the reciprocal immunoprecipitation (Fig. 2.6). This finding is consistent with published results that

$CRL4^{DDB2}$ ubiquitylates histone H2A (Guerrero-Santoro et al., 2008; Kapetanaki et al., 2006). However, overexpression of VprBP had no effect on H4 ubiquitylation (Fig. 2.6). In addition, VprBP and H4 did not co-immunoprecipate. While it remains formally possible that active DUB activity prevented detection of ubiquitylated H4 and that binding between H4 and VprBP is too transient to be detected by immunoprecipitation, the most parsimonious explanation is that VprBP does not directly affect H4 modification.

Figure 2.5

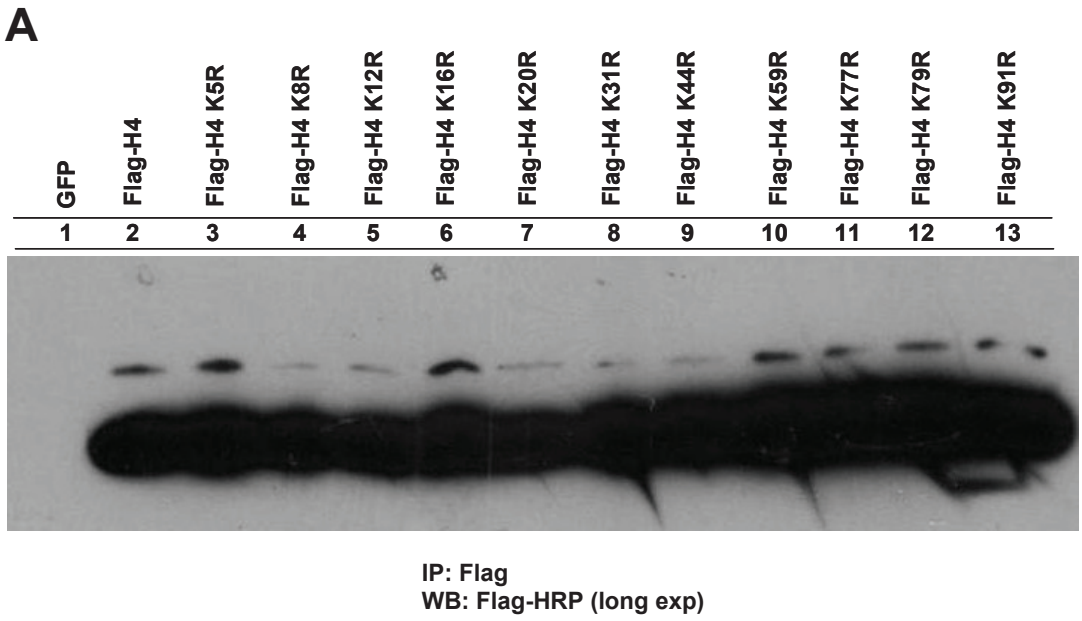

Figure 2.5. Mutagenesis of H4 indicates multiple sites affect H4 modification.

(A) Lysine residues in histone H4 were substituted with arginine using site-directed mutagenesis. pcDNA3-Flag-H4 constructs were transfected into HeLa-HA-Ub cells; cells were subsequently lysed, immunoprecipitated with Flag antibody, resolved by SDS-PAGE and immunoblotted with Flag to detect H4.

(B) Schematic of histone H4 highlighting known post-translation modifications in the N-terminal tail region.

Figure 2.6

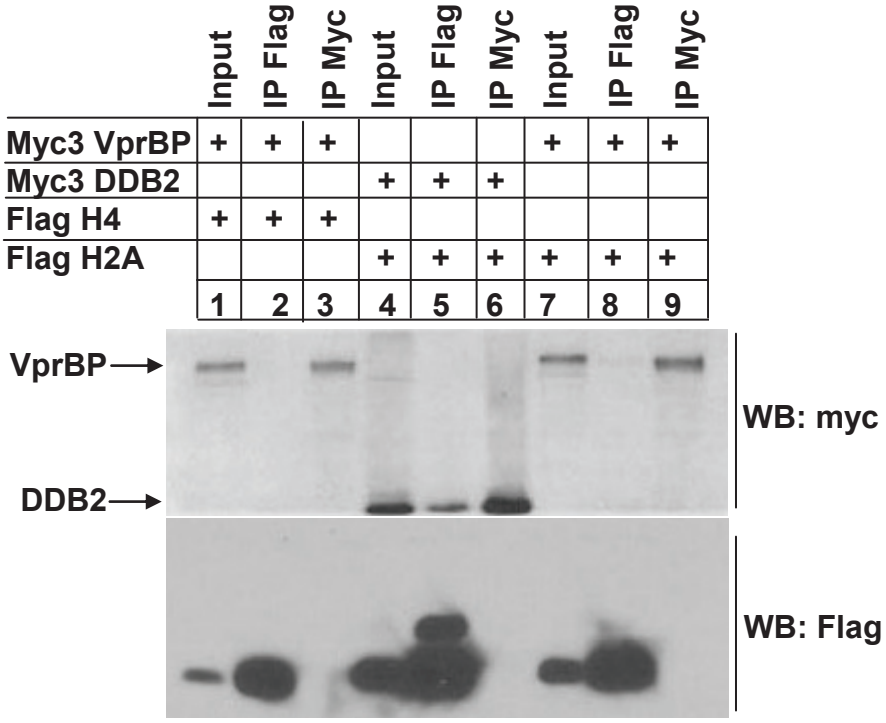

Figure 2.6. VprBP does not stably bind core histone H4.

293T cells were transiently transfected as indicated. Cells were lysed in CSK buffer containing micrococcal nuclease and subsequently immunoprecipitated for histone (Flag) or DWD protein (Myc). 5% inputs and immunoprecipitates were resolved by SDS-PAGE and immunoblotted as indicated.

Discussion

The experiments described in this chapter provided evidence that VprBP positively regulates modification of H4. The initial experiments were designed to detect ubiquitylation of histone proteins, though I was ultimately unable to definitively determine the identity of the modification. The size of the mobility shift, however, suggests that H4 is modified by ubiquitin in this assay rather than SUMO. Furthermore, I was not able to identify a specific lysine residue on H4 which was modified. These data suggest the possibility that H4 can be modified at more that one lysine residue. Throughout these studies, I had difficulties consistently detecting H4 ubiquitylation, suggesting that it is a rare event which is difficult to detect using the described methods. Attempts to identify biologically relevant conditions which enhanced H4 ubiquitylation suggested that H4 modification may increase in the G2-phase of the cell cycle, but did not increase in response to UV-treatment or etoposide treatment. This observation is particularly surprising given that H4 ubiquitylation by BBAP (B-lymphoma and BAL-associated protein) E3 ubiquitin ligase was reported in response to the topoisomerase II inhibitor doxorubicin (Yan et al., 2009). This discrepancy could suggest that the dose of etoposide used in my study was insufficient, or that doxorubicin is more potent at inducing H4 ubiquitylation. In the study by the Ship lab, depletion of BBAP delayed the recruitment of 53BP1 to sites of DNA damage whereas overexpression of BBAP increased H4 ubiquitylation in vivo (Yan et al., 2009). Given that I was unable to detect any increase in H4 ubiquitylation upon VprBP overexpression, I conclude that VprBP at best plays an indirect role in H4 ubiquitylation. This result is in contrast to my positive control which showed that DDB2 overexpression increased the ubiquitylation of H2A.

What is the role of core histone ubiquitylation in response to DNA damage? In the case of H4, ubiquitylation was suggested to trigger H4K20 methylation by PR-SET7/SET8 and 53BP1 recruitment to DNA damage (Yan et al., 2009). H2A

ubiquitylation by RNF8 also seems to trigger recruitment of repair factors such as 53BP1 and BRCA1 in response to double strand breaks (Mailand et al., 2007, Huen, 2007 #2255). My data, as well as studies by the Levine lab, support a role for $CRL4^{DDB2}$ in H2A ubiquitylation; DDB2-induced ubiquitylation was likewise suggested to function as a signal for the binding of repair factors to damaged DNA (Guerrero-Santoro et al., 2008; Kapetanaki et al., 2006).

The view that $CRL4^{DDB2}$ promotes the binding of other factors to the lesion is challenged by evidence that loss of $CRL4^{DDB2}$ activity enhances rather than inhibits DNA repair in cells lacking *Cul4A* (Liu et al., 2009). In addition to losing $CRL4^{DDB2}$ function toward H2A, DDB2 itself was accumulated following loss of *Cul4A* (Liu et al., 2009). Perhaps, ubiquitylation of DDB2 functions to restrict repair activity to the damaged DNA lesion instead of spreading to undamaged DNA. In the case of $CRL4^{VprBP}$, I suggest that this ubiquitin ligase is upstream of pathways that control H4 ubiquitylation, rather than serving as the direct E3 ubiquitin ligase for H4. It will be interesting to see if $CRL4^{VprBP}$ has any function in positively regulating BBAP and whether this regulation might account for the change in H4 modification observed in these studies.

CHAPTER III

ANALYSIS OF *VPRBP* DISRUPTION IN MOUSE EMBRYONIC FIBROBLASTS

Summary

VprBP, a WD40 domain-containing protein that binds to the DDB1-CUL4-ROC1 ubiquitin ligase, is required for cellular proliferation in immortalized cell lines and is required for embryonic development in mice. Merlin, a FERM-domain protein which represses growth in response to contact inhibition, was reported as a substrate for $CRL4^{VprBP}$. To further investigate the role of *Vprbp* in cellular proliferation, I disrupted *Vprbp* using a conditional allele in mouse embryonic fibroblasts (MEFs) and characterized these cells. I found that $Vprbp^{\Delta}$ was not a true null-allele, as small levels of a truncated VprBP protein were detected following Cre-mediated recombination. However, MEFs with $Vprbp^{\Delta}$ failed to proliferate, and were phenotypically similar to cultured cells depleted of VprBP by RNAi. I could not confirm a role for $CRL4^{VprBP}$ in Merlin degradation, however experiments designed to test this possibility unexpectedly uncovered abundant accumulation of VprBP protein in contact-inhibited and serum-starved wild-type MEFs. This accumulation was particularly pronounced in MEFs, but not in WI38 or MCF10A cells, suggesting this function of VprBP may be developmentally or cell-type regulated. Further, conditional disruption of *Vprbp* in MEFs was incompatible with survival in low-serum conditions, suggesting that VprBP may be required for quiescent MEFs or for tolerance of restrictive growth conditions.

Background

The *Vprbp* gene encodes a 175 kDa protein that contains LisH and WD40 domains, and a negatively charged C-terminal tail. VprBP was first described as a binding partner for the HIV1 Vpr protein (Zhao et al., 1994) and was subsequently noted as a transcriptional target of Sox9 (Zhao et al., 2002). However, its biological function remained largely obscure until the identification of VprBP by three independent lab groups as part of the CUL4A-DDB1 complex (Angers et al., 2006; He et al., 2006; Jin et al., 2006). VprBP contains two WDXR motifs, but not the larger DWD box sequence, and mutation of the conserved arginine residues in both WDXR motifs disrupts binding to DDB1. Through its interaction with DDB1, VprBP binds to CUL4A or CUL4B, suggesting that VprBP functions as a substrate receptor for CRL4 complexes. VprBP, like a subset of other substrate targeting receptors, has also been noted to bind the COP9 signalosome subunits (Hrecka et al., 2007; McCall et al., 2008; Olma et al., 2009), indicating that $CRL4^{VprBP}$ may exist in an unneddylated state until appropriately activated. In addition, VprBP complexes contain DDA1 (Hrecka et al., 2007; McCall et al., 2008; Olma et al., 2009), a protein of unknown function which associates with several chromatin-bound CRL4 complexes. Recent data indicate that two $CRL4^{VprBP}$ complexes may functionally cooperate in ubiquitylation through dimerization of the alpha-helical LisH domain of VprBP (Ahn et al., 2011). Cumulatively, these data provide the basis for a working model that the primary biochemical function of VprBP is to function as a substrate recruiting receptor for a CRL4-based complex. However the molecular targets and in vivo function of VprBP are still largely unknown.

VprBP knockdown arrests cell cycle progression in multiple cell lines and in primary cells, suggesting that VprBP is required for cellular proliferation (Hrecka et al., 2007; Li et al., 2010b; McCall et al., 2008). Overexpressed VprBP is primarily nuclear in localization (Li et al., 2010b), and a portion of endogenous VprBP associates with

chromatin (Belzile et al., 2010; McCall et al., 2008). These observations led to speculation that VprBP may function in DNA replication or repair. Indeed, VprBP knockdown modestly induced H2AX phosphorylation (Hrecka et al., 2007), but not phosphorylation of CHK1/2 (data not shown). Further, DNA damaging agents did not promote binding of VprBP to chromatin (Chapter 2). Thus any putative contribution of VprBP to the DNA repair process remains unclear at the present time.

To determine the in vivo function of *Vprbp* in a genetically controlled setting, I sought to characterize conditional *Vprbp* MEFs. In addition, I tested the model that $CRL4^{VprBP}$ promotes Merlin polyubiquitylation and degradation, as reported (Huang and Chen, 2008). Merlin, a tumor suppressor protein first identified in familial cases of schwanomas, is encoded by the *Nf2* gene (McClatchey and Fehon, 2009). Mice which are heterozygous for *Nf2* frequently develop osteosarcoma or a broad spectrum of other cancers including lymphoma and lung adenocarcinoma (McClatchey et al., 1998), while homozygous deletion of *Nf2* results in embryonic lethality around day 6.5 (McClatchey et al., 1997). Merlin has been suggested to mediate contact inhibition and inhibit proliferation in low serum by inhibiting a number of signaling pathways including Ras-ERK and Rac1 (Jung et al., 2005; Kissil et al., 2003; Morrison et al., 2007; Okada et al., 2005). The data reported here and elsewhere (Li et al., 2010b) do not confirm a role for $CRL4^{VprBP}$ in Merlin degradation, though we can confirm Merlin-VprBP binding. In addition, I found that *Vprbp* is essential for cellular proliferation in MEFs, and observed a massive VprBP protein accumulation in serum-starved or contact-inhibited MEFs. These data suggest that VprBP may also play a role in regulating the cellular response to contact inhibition and mitogen withdrawal.

Experimental Procedures

Animal maintenance and generation of mouse embryonic fibroblasts

Generation of the *Vprbp* conditional allele (*Vprbp*^{flox}) and Neo allele (*Vprbp*$^{-}$) by Dr. Paula Miliani de Marval was previously described (McCall et al. 2007). Mice were backcrossed into the C57BL/6 for at least four generations. Germline transmission of *Vprbp*$^{\Delta}$ was obtained by crossing *Vprbp* conditional mice with *EIIA-Cre*$^{+}$ mice (Jackson Laboratories, stock 003724). In addition, *Vprbp*$^{flox/flox}$ mice were crossed with *Ubc-CreERT2*$^{+}$ mice that were generously provided by Dr. Eric Brown (Ruzankina et al., 2007). *Vprbp*$^{flox/+}$*;Ubc-CreERT2*$^{+}$ were intercrossed and mouse embryonic fibroblasts (MEFs) were isolated from embryos at day 13.5 post coitus (E13.5). MEFs at early passage (passage 1-5) were used for all experiments described. Where specified, adenovirus-Cre-GFP (Vector Biolabs) at MOI 250 was used to transduce *Vprbp*$^{F/-}$ MEFs.

Genotyping

Primers for genotyping *Vprbp* alleles: 5' CTGGGTAGCTACTGTTGACTACTCACTGCG 3', 5' CAGTTAGAGAGTGACTTTGGACG 3', and 5' GCTGCCAACTATGGGTGC 3', which detected 434 bp, 468 bp and 280bp bands for the wild-type, flox and Δ alleles, respectively. Primers for genotyping *Cre-ERT2*: 5' GCTGGAGTTTCAATACCGGAG 3' and 5' CTTAGAGCGTTTGATCATGAGC 3'. *Il2* primers were included in the *CreERT2* PCR as an internal control: 5' CTAGGCCACAGAATTGAAAGATCT 3' and 5'GTAGGTGGAAATTCTAGCATCATC 3'. Primers for genotyping *Cre* for *EIIA-Cre*$^{+}$ mice: 5' GCGGTCTGGCAGTAAAAACTATC 3' and 5' GTGAAACAGCATTGCTGTCACTT 3'. PCR conditions were as follows: 94ºC for 2 min, 40 cycles of 94ºC for 1 min, 58ºC for 2 min, and 72ºC for 2 min followed by 72ºC for 5 min.

Cell Culture

MEFs were cultured in Dulbecco's Modified Eagle Medium (DMEM) containing 10% Fetal Bovine Serum (FBS). To induce CreERT2 translocation in *Ubc-CreERT2*$^{+}$ MEFs, 1 μM 4-Hydroxytamoxifen (Sigma H7904) was added to the culture medium and cells were assayed after 72h. To serum starve MEFs, cells were cultured in DMEM containing 0.1% FBS for 72h. WI38 cells were cultured in DMEM containing 10% FBS; MCF10A cells were cultured in DMEM F12 medium containing 5% Fetal Calf Serum, 20 ng/ml EGF, 0.05 μg/ml hydrocortisone and 10 μg/ml insulin.

Cell lysis and western blot analysis

Cells were lysed in 0.1% NP-40 buffer (50 mM Tris-HCl, pH 7.5, 150 mM NaCl, 0.1% NP-40, 50 mM NaF, 1 mM PMSF, 1 mM Na_3VO_4, and a cocktail of protease inhibitors containing 25 mg/L leupeptin, 25 mg/L aprotinin, 150 mg/L benzamidine, and 10 mg/L trypsin inhibitor) for co-immunoprecipitation experiments, or in RIPA buffer (50 mM Tris-HCl, pH 8.0, 150 mM NaCl, 0.1% SDS, 0.5% NP-40, 0.5% sodium deoxycholate, 1 mM PMSF, 1 mM Na_3VO_4, 1mM DTT, and a cocktail of protease inhibitors containing 25 mg/L leupeptin, 25 mg/L aprotinin, 150 mg/L benzamidine, and 10 mg/L trypsin inhibitor) for western blot analysis. Proteins were resolved by SDS-PAGE, transferred to PVDF membrane (Millipore) and proteins were probed with the following primary antibodies: VprBP (McCall et al. 2007), DDB1 (Zymed laboratories), Merlin (C-19 Santa Cruz), Tubulin (Neomarkers), Actin (Santa Cruz), p53 (Novocastra), p21 (Santa Cruz), phospho-Rb (Cell Signaling).

Flow Cytometry

To analyze DNA replication by bromodeoxyuridine (BrdU) labeling, cells were fixed in 75% ethanol overnight at 4°C. Nuclei were isolated by incubating cells in 0.08% pepsin

in 0.1 N HCl for 20 min at 37°C, and then DNA was denatured by incubating cells in 2 N HCl for a further 20 min at 37°C. After the HCl was neutralized with 2 volumes of 0.1 M sodium borate, pH 8.5, the cells were washed with immunofluorescence assay (IFA) buffer (10 mM HEPES [pH 7.3], 150 mM NaCl, 4% FBS, 0.1% sodium azide) plus 0.5% Tween-20. The cells were labeled with FITC-conjugated anti-BrdU (BD Biosciences). Cells were stained for DNA content by incubation with 0.1 mg/ml propidium iodide in IFA buffer containing RNase A. Stained cells were analyzed on a FACScan CyAN (Dako Cytomation) flow cytometer, and data were analyzed using Summit software (Dako Cytomation).

Results

Characterizing *Vprbp*$^{\Delta}$.

The *Vprbp* genomic locus spans approximately 60 kb on mouse chromosome 9 and contains 24 exons. Our previous work characterizing loss of *Vprbp* in mice and MEFs utilized a *Vprbp*$^{-}$ allele which contains a neomycin resistance cassette inserted after exon 6 of *Vprbp* and deletion of exons 7 and 8 (Figure 3.1). Loss of *Vprbp* (*Vprbp*$^{-/-}$) is embryonic lethal prior to day 7.5, necessitating the use of a conditional allele to study loss of *Vprbp* in MEFs. Our preliminary experiments, led by Dr. Paula Miliani de Marval, characterized *Vprbp*$^{F/-}$ MEFs following retroviral transduction of Cre. To avoid possible unintended effects of the neomycin cassette, I characterized *Vprbp*$^{F/F}$ MEFs following Cre-mediated recombination.

The *Ubc-CreERT2*$^{+}$ transgenic mice express a 4-OH-tamoxifen (4OHT)-inducible Cre driven by the *Ubiquitin C* promoter and provides a system to conditionally activate Cre recombinase in a wide range of tissues upon exposure to 4OHT (Ruzankina et al., 2007). Use of 4OHT-inducible Cre offers a unique advantage to my study as it avoids the potential complication of cell cycle arrest resulting from viral transduction. To optimize conditions for disrupting *Vprbp*, I treated MEFs with a range of doses of 4OHT and lysed cells 60 hours after drug treatment. I observed a dose-dependent loss of full-length VprBP, but surprisingly detected low-level expression of a truncated protein by immunoblotting with an antibody against the C-terminus of VprBP (Fig. 3.2A). The conditional allele used to disrupt *Vprbp* contains loxP sites flanking exons 7 and 8, and recombination at these sites is predicted to result in a frame-shift and premature stop-codon should splicing occur between exons 6 and 9 (Fig. 3.2D). The presence of a truncated, in-frame VprBP was therefore unexpected. I isolated cDNA from 4OHT-treated *Vprbp*$^{F/F}$*; CreERT2*$^{+}$ MEFs,

Figure 3.1

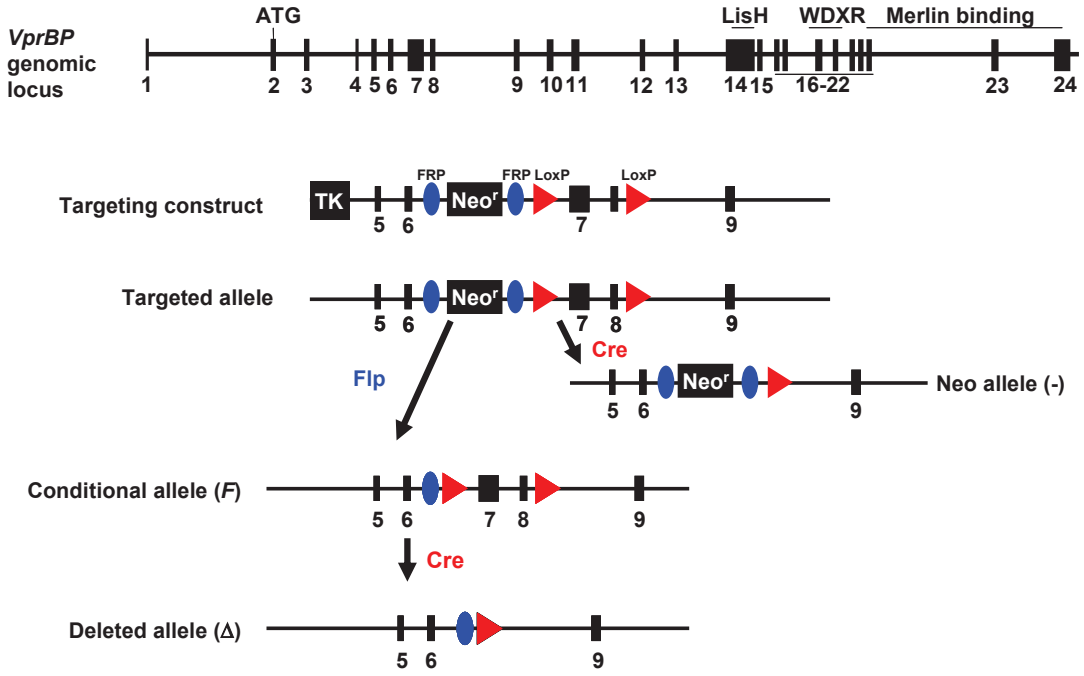

Figure 3.1. *Vprbp* genomic locus and alleles.

A schematic of the *Vprbp* genomic locus on mouse chromosome 9. Black boxes indicate exons; noteworthy protein features of VprBP are indicated above the exons which encode them. The targeting construct incorporated FRP sites (blue) flanking the neomycin resistance cassette and LoxP sites (red) flanking exons 7 and 8. Targeted ES cells were treated with Cre recombinase or Flipase to generate $Vprbp^{-}$ and $Vprbp^{F}$, respectively, as previously reported (McCall et al., 2008). Following Cre-mediated recombination, $Vprbp^{F}$ gives rise to $Vprbp^{\Delta}$, which differs from $Vprbp^{-}$ by the absence of the neomycin resistance cassette.

amplified the *Vprbp* transcript by PCR and submitted the gel-purified clone for sequencing (Fig. 3.2B). I found that exons 6 and 9 were spliced in an unconventional manner which resulted in an in-frame *Vprbp* transcript that lacks the coding sequence for amino acids 173-375 (Fig. 3.2C & D). The allele resulting from Cre recombination of conditional *Vprbp* is therefore not a null allele, but rather a hypomorphic allele which we have termed $Vprbp^{\Delta}$.

$Vprbp^{\Delta}$ is a severe hypomorphic allele.

To determine if $Vprbp^{\Delta/\Delta}$ mice were viable, I crossed $Vprbp^{F/F}$ mice with *EIIA-Cre*$^{+}$, which express Cre under the control of the adenovirus EIIA promoter in a broad range tissues, to generate germline transmission of $Vprbp^{\Delta}$. I found that subsequent intercrosses of $Vprbp^{\Delta/+}$ mice produced no viable $Vprbp^{\Delta/\Delta}$ pups (Fig. 3.3A) or embryonic day (E) 12.5 embryos (data not shown), indicating that homozygous *Vprbp* disruption causes embryonic lethality. To explore the cellular phenotype of $Vprbp^{\Delta/\Delta}$ MEFs, I examined cellular proliferation by a growth curve assay (Fig. 3.3B) and BrdU incorporation (Fig. 3.3D) in 4OHT-treated $Vprbp^{F/F}$; *CreERT2*$^{+}$ MEFs and found that disruption of *Vprbp* blocked cell cycle progression, mimicking results reported following VprBP knockdown (Hrecka et al., 2007; McCall et al., 2008). However, unlike previously published results for VprBP knockdown in U2OS cells and WI38 cells, I did not detect induction of p53 following disruption of *Vprbp* (Fig. 3.3C). Because VprBP has been established to bind chromatin, I tested if the hypomorphic VprBP$^{\Delta}$ protein could bind chromatin by isolating the chromatin fraction of MEFs following Cre-mediated recombination. Though VprBP$^{\Delta}$ was apparent in whole cell lysates, I was unable to detect VprBP$^{\Delta}$ on chromatin, suggesting that VprBP$^{\Delta}$ cannot functionally compensate for the chromatin-dependent

Figure 3.2

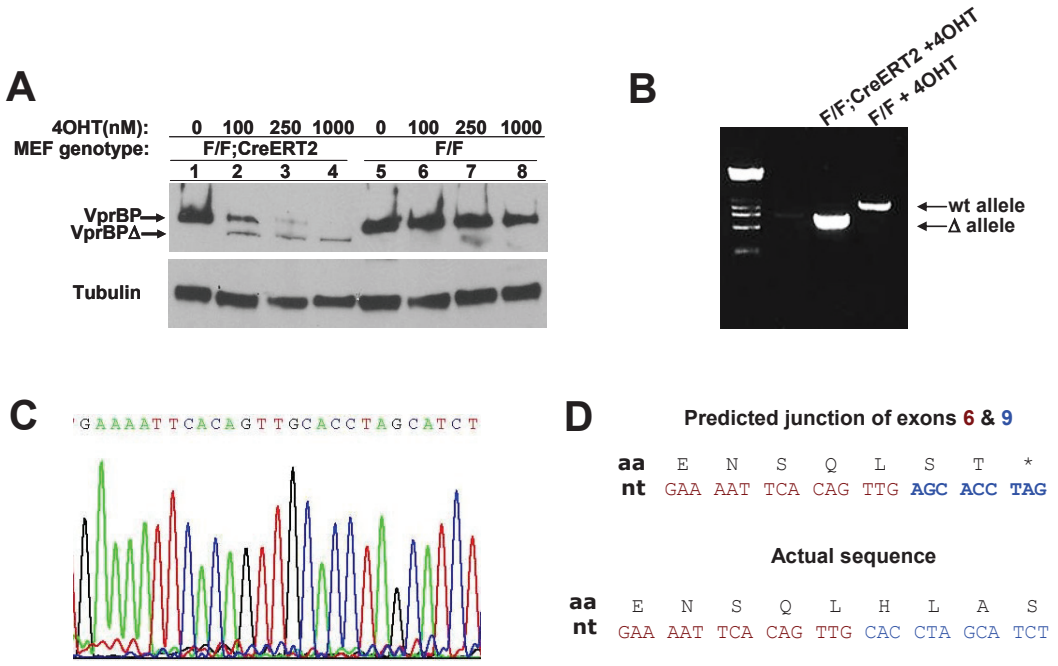

Figure 3.2. *Vprbp*$^{\Delta}$ is a hypomorphic allele.

(A) *Vprbp*$^{F/F}$*; CreERT2*$^{+}$ and *VprBP*$^{F/F}$ mouse embryonic fibroblasts (MEFs) were treated with 4-hydroxy-tamoxifen (4OHT). Cell lysates were resolved by SDS-PAGE and immunoblotted with an antibody against the C-terminus of VprBP or α-tubulin. Low-level expression of a truncated protein was noted.

(B) PCR of cDNA from 4OHT-treated *Vprbp*$^{F/F}$*; CreERT2*$^{+}$ and *VprBP*$^{F/F}$ MEFs using primers corresponding to sequences from exons 4 and 11 of *Vprbp*.

(C) Sequencing data of *Vprbp* cDNA cloned from 4OHT-treated *Vprbp*$^{F/F}$*; CreERT2*$^{+}$ MEFs showing the coding region spanning the exon 6 and exon 9 junction.

(D) Schematic of exon 6 to exon 9 junction following Cre-mediated recombination of conditional *Vprbp*. Excision of exons 7 and 8 is predicted to result in a frame-shift and premature stop codon. Shown here is the nucleotide (nt) sequence of the junction between exons 6 and 9 and the resulting amino acid (aa) sequence.

Figure 3.3

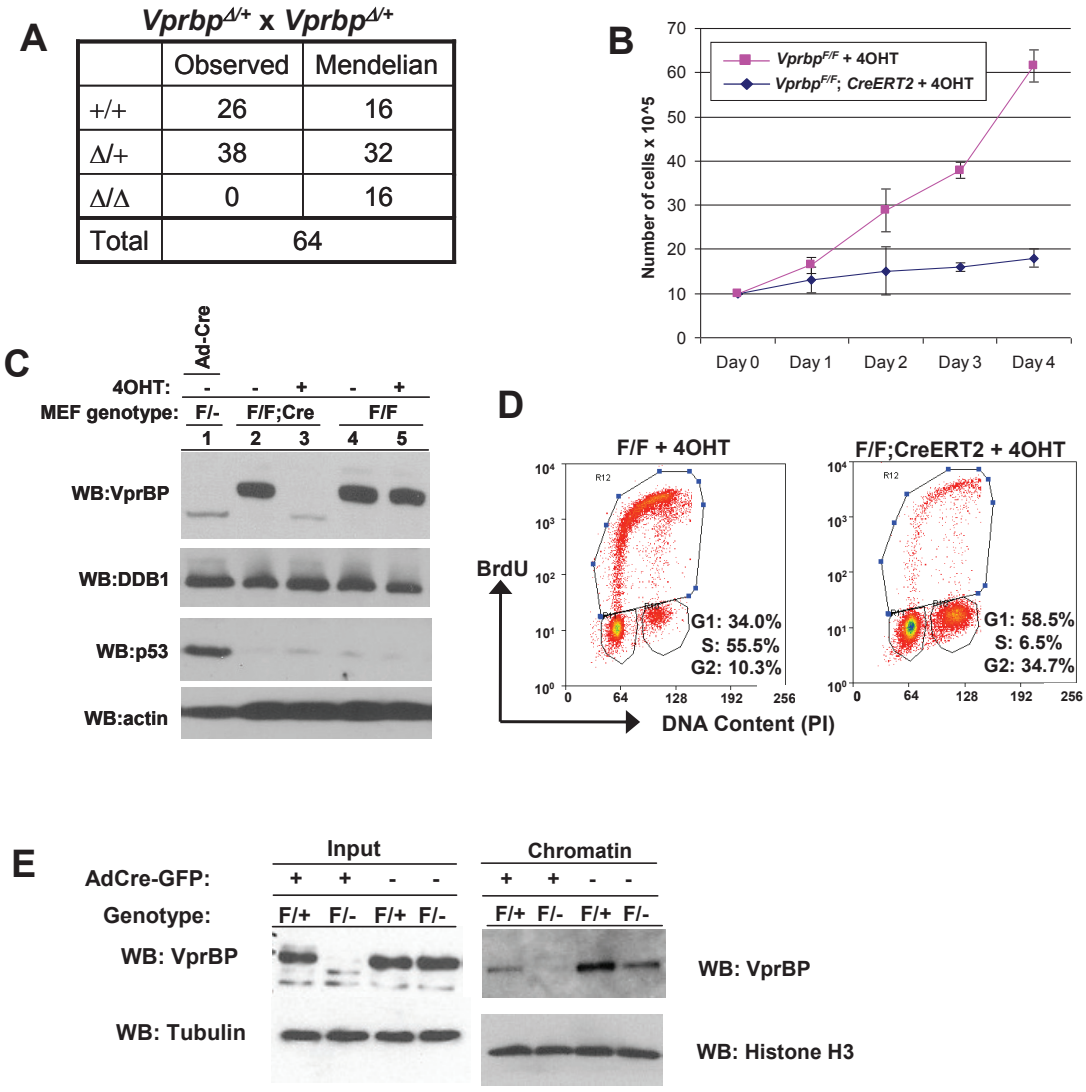

Figure 3.3. *Vprbp*$^{\Delta}$ mimics loss of function.

(A) *Vprbp*$^{\Delta/+}$ mice were intercrossed and the genotype of offspring at postnatal day 21 is shown. 'Mendelian' indicates the expected number based on Mendelian inheritance.

(B) Disruption of *Vprbp* impairs cell proliferation. 48 h after treatment with 1μM 4OHT, equal numbers of MEFs were plated and subsequently counted at the indicated time points. Experiment was performed in triplicate.

(C) *Vprbp* disruption does not induce p53. Western blot of cell lysates from MEFs as indicated. Adenovirus-Cre treated MEFs were used as a positive control for disruption of *Vprbp* and induction of p53.

(D) *Vprbp* disruption reduces 5'-bromo-2'-deoxyuridine (BrdU) incorporation. 60h after treatment with 1μM 4OHT, MEFs were pulse-labeled with BrdU for 6 h, fixed, stained with FITC-conjugated anti-BrdU antibody and propidium iodide, and detected by flow cytometry.

(E) VprBP$^{\Delta}$ does not bind to chromatin. *Vprbp*$^{F/+}$ or *VprBP*$^{F/-}$ MEFs were treated with Adenovirus-Cre or mock. Cells were lysed and chromatin fractions were isolated, resolved by SDS-PAGE, and immunoblotted as indicated.

functions of wild-type VprBP. Overall, these results demonstrate that *Vprbp*$^{\Delta}$ causes a similar cellular phenotype as VprBP knockdown in cultured cells.

Evidence for VprBP accumulation in quiescence.

I next sought to determine if VprBP regulates Merlin ubiquitylation, as reported (Huang and Chen, 2008). To first verify a relationship between VprBP and FERM-domain containing protein Merlin, my colleague Dr. Tadashi Nakagawa overexpressed wild-type Merlin or the patient-derived L64P point mutant of Merlin in 293T cells (Fig. 3.4A). We found that wild-type Merlin, but not L64P, binds with endogenous VprBP and DDB1 in agreement with published results (Huang and Chen, 2008; Li et al., 2010b). To determine if VprBP regulated global levels of Merlin in MEFs, I treated *Vprbp*$^{F/F}$*; CreERT2*$^{+}$ and *VprBP*$^{F/F}$ MEFs with 4OHT and examined Merlin by Western blot (Fig. 3.4B). I was unable to detect any change in total Merlin protein, despite apparent loss of full-length VprBP, suggesting VprBP does not regulate Merlin levels under these conditions.

Because previous work by the Chen lab indicated that VprBP degrades Merlin in response to serum stimulation in HeLa cells, I conducted a time course experiment in wild-type MEFs to determine the optimal time point of Merlin degradation in response to serum stimulation (Fig. 3.4C). While I could not see clear evidence for Merlin protein loss in response to serum stimulation, I unexpectedly uncovered a dramatic accumulation of VprBP protein in serum-starved cells (Fig. 3.4C). VprBP protein was decreased by 16h post-stimulation, which corresponded to phosphorylation of RB at serine 807/811. To verify VprBP accumulation in serum-starved MEFs, I performed the reciprocal experiment in which MEFs were cultured in DMEM containing 10% FBS, switched to 0.1% FBS-containing medium, and monitored at 12, 24, 36, 48, and 72 hours after culture in low-serum medium (Fig. 3.4D). In agreement with the previous

Figure 3.4

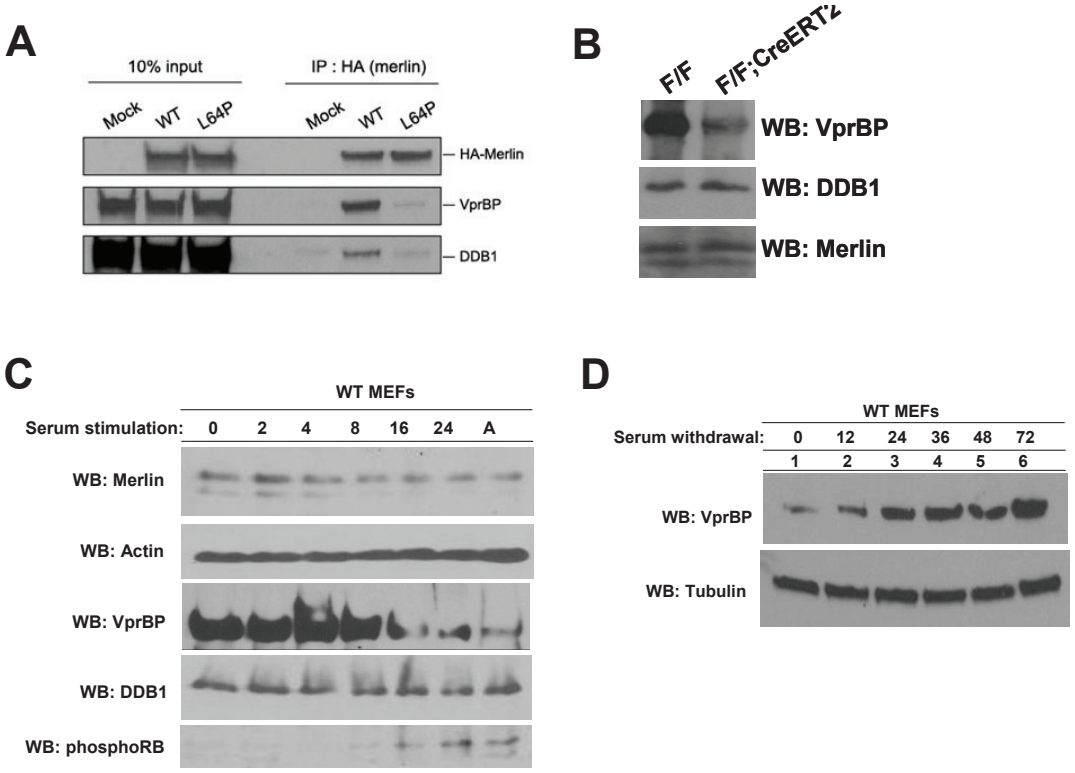

Figure 3.4. VprBP accumulates in serum starved MEFs.

(A) VprBP and Merlin interact. HA-tagged wild-type (WT) Merlin or patient-derived L64P mutant were transiently overexpressed in 293T cells. Immunoprecipitated WT, but not L64P, bound endogenous VprBP and DDB1.

(B) Western blot of whole cell lysate from 4OHT treated *Vprbp*$^{F/F}$ and *Vprbp*$^{F/F}$*; CreERT2*$^{+}$ MEFs. Disruption of *Vprbp* in MEFs did not cause a change in endogenous Merlin levels.

(C) Western blot of whole cell lysate from WT MEFs, which were starved for 3 days and stimulated with medium containing 10% FBS for the number of hours indicated.

(D) VprBP accumulates in WT MEFs in response to serum starvation. Western blot of cell lysates from WT MEFs, which were cultured in normal medium and subsequently switched to medium containing 0.1% FBS for the number of hours indicated.

experiment, VprBP protein abundantly accumulated 72h after culture in low-serum medium. Further, an increase in VprBP protein was evident as early as 24 hours after switching to low-serum medium, suggesting that VprBP protein accumulation correlated with exit from the cell cycle. Cumulatively, these experiments indicate that VprBP protein accumulation is induced by serum-starvation of wild-type MEFs. To determine if VprBP protein accumulation was specific to serum-starved cells or if other types of quiescent cells have increased VprBP levels, I examined the effects of cell density on VprBP. Wild-type MEFs, which are non-transformed cells that can be cell-cycle arrested in response to contact inhibition, were plated at low, medium and high density (Fig. 3.5). Western blotting indicated that VprBP protein levels were elevated when plated at increasingly higher density, as was also seen for Merlin protein. This suggests that accumulated VprBP protein in highly confluent MEFs does not function to promote proteolytic degradation of Merlin. Further, this supports a model that VprBP protein accumulates in quiescent cells.

To test if VprBP accumulation is specific to MEFs or is broadly observed in multiple cell types, I tested if VprBP accumulates in response to serum starvation or high density in WI38 and MCF10A cells. WI38 cells are a non-transformed, diploid cell line derived from normal embryonic lung fibroblasts which can undergo replication-induced senescence. MCF10A is also a non-transformed, diploid cell line which was derived from normal breast epithelium and is known to exhibit contact inhibition of cell proliferation. I found that VprBP protein levels were elevated in response to increasing cell density in both WI38 and MCF10A cells (Fig. 3.6A and 3.6C), though to a lesser extent than observed in WT MEFs. In contrast to observations in MEFs, serum starvation of WI38 or MCF10A cells resulted in very little increase in VprBP protein levels. This result suggests that while VprBP protein accumulation in response to contact inhibition is conserved, VprBP accumulation following serum-starvation may vary

Figure 3.5

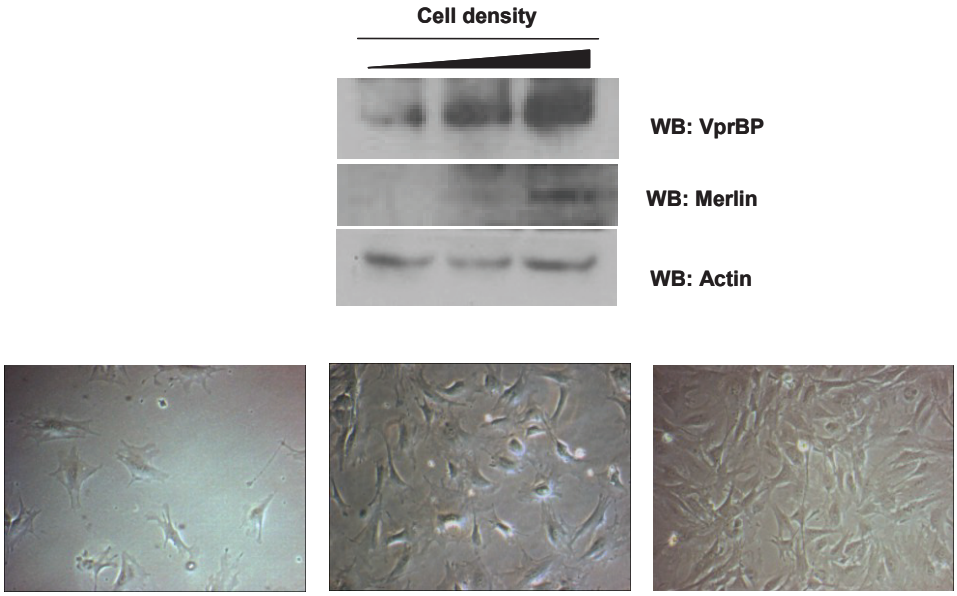

Figure 3.5. VprBP accumulates in highly confluent MEFs.

WT MEFs were cultured at low, medium, and high density, as shown in phase contrast images, for 16 h in DMEM containing 10% FBS. Cell lysates were resolved by SDS-PAGE and immunoblotted for VprBP, Merlin and Actin.

Figure 3.6

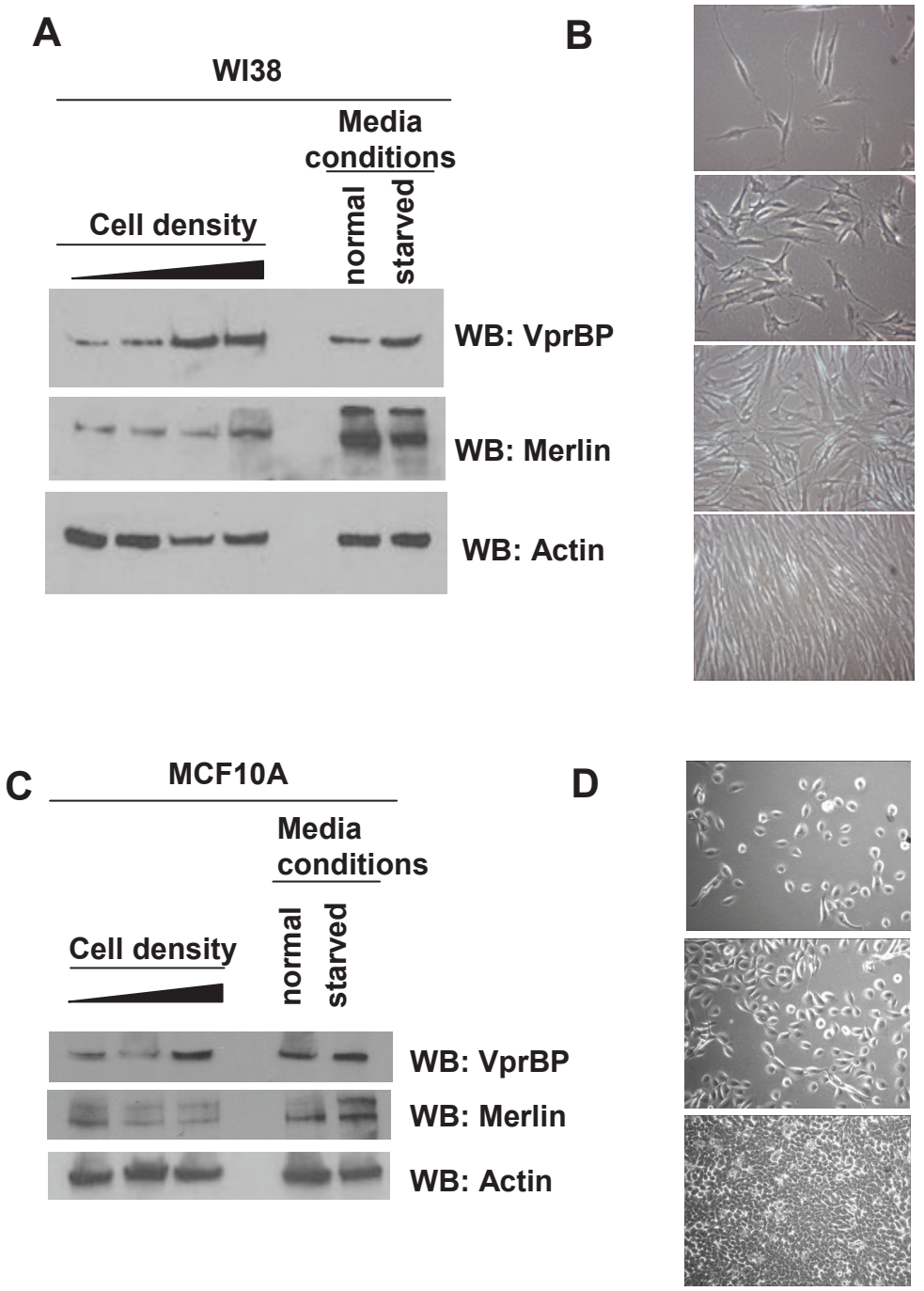
A
WI38
Media conditions
Cell density
normal
starved
WB: VprBP
WB: Merlin
WB: Actin
B
C
MCF10A
Media conditions
Cell density
normal
starved
WB: VprBP
WB: Merlin
WB: Actin
D

Figure 3.6. Accumulation of VprBP is dependent on cell type.

(A) WI38 cells were cultured at a range of densities or at medium density ± serum for three days.

(B) Phase contrast images of the WI38 cells used for the density experiment in (A).

(C) MCF10A cells were cultured at a range of densities or at medium density ± serum for three days.

(D) Phase contrast images of the MCF10A cells used for the density experiment in (C).

between cell lines. Further, MEFs appear to be the most sensitive system for detecting VprBP accumulation following serum starvation or contact inhibition, suggesting a possible developmental regulation of this response.

To determine if VprBP accumulation is required to maintain quiescence in MEFs, I designed experiments to examine cells following *Vprbp* disruption in conditional MEFs. Unfortunately, I could not obtain high density cultures of *Vprbp* disrupted MEFs by seeding plates with high numbers of mutant cells because of low efficiency of plate attachment (data not shown). Further, despite repeated attempts, I was unable to isolate *Vprbp* disrupted MEFs from low-serum conditions (data not shown). To optimize the timing of *Vprbp* disruption, I treated $Vprbp^{F/F}$ and $Vprbp^{F/F}$; $CreERT2^{+}$ MEFs with 1 μM 4OHT in 0.1% FBS and examined cells at 3d, 4d and 6d following 4OHT treatment; 4OHT treatment for 3 days in 10% FBS was included as a positive control (Fig. 3.7). I found that $Vprbp^{F/F}$; $CreERT2^{+}$ MEFs in 10% FBS-containing medium showed decreased VprBP protein levels as expected. However, conditional MEFs cultured in low-serum medium showed high levels of VprBP protein at 3 and 4 days following 4OHT treatment. Analysis of cell lysates from MEFs at 6 days after 4OHT showed a minor decrease in VprBP protein. However, very few of the $Vprbp^{F/F}$;$CreERT2^{+}$ MEF cells remained viable 6 days after 4OHT treatment. This observation suggests that VprBP may be required for cell survival in low-serum medium, and perhaps more broadly in quiescence because only cells which retain VprBP can survive. Further experiments are needed to test this model and specifically to identify a function for VprBP in maintaining quiescence.

Figure 3.7

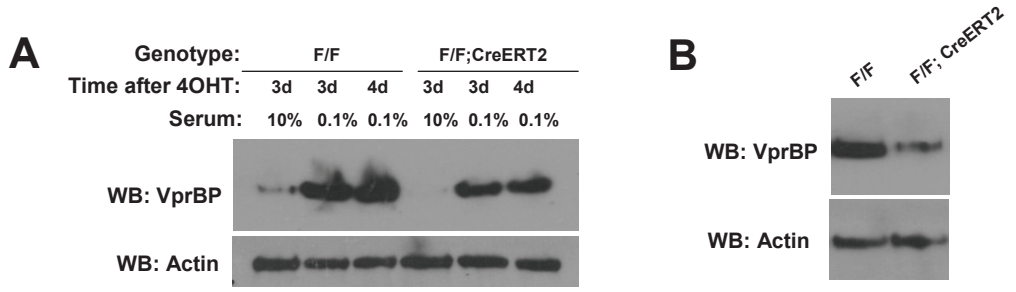

Figure 3.7. *Vprbp* disruption is inefficient following serum starvation.

(A) *Vprbp*$^{F/F}$ or *Vprbp*$^{F/F}$*;CreERT2*$^{+}$ MEFs were treated with 1 μM 4OHT in DMEM with 10% FBS or with 1 μM 4OHT in DMEM with 0.1% FBS for the number of days indicated. VprBP levels remained high despite induction of Cre.

(B) *Vprbp*$^{F/F}$ or *Vprbp*$^{F/F}$*;CreERT2*$^{+}$ MEFs were treated with 1 μM 4OHT in DMEM with 0.1% FBS, cultured for 6 days, and then lysed.

Discussion

In this chapter, I examined the function of VprBP in wild-type and conditional MEF cells. I found that Cre-mediated disruption of the conditional allele of *Vprbp* did not result in a complete loss of VprBP, but rather a loss of full-length VprBP and the appearance of very low levels of a truncated VprBP$^{\Delta}$ protein. My characterization of the *Vprbp*$^{\Delta}$ allele in MEFs demonstrated that *Vprbp* disruption was phenotypically similar to cultured cells depleted of VprBP by RNAi as assessed by cell proliferation and ability to enter S-phase. I was unable to verify Merlin as putative substrate for ubiquitylation by CRL4^{VprBP}, in agreement with a publication by the Giancotti lab (Li et al., 2010b). However, experiments designed to test for Merlin degradation following serum stimulation unexpectedly uncovered abundant accumulation of VprBP protein in contact inhibited and serum starved wild-type MEFs. This accumulation was particularly pronounced in MEFs, but was observed to a lesser extent in WI38 or MCF10A cells, suggesting this function of VprBP is possibly cell-type dependent. Further, disruption of *Vprbp* in conditional MEFs was incompatible with survival in low-serum conditions, suggesting that VprBP may be required for quiescent MEFs or for tolerance of restrictive growth conditions.

The results presented in this chapter provide a more complicated view of the function of *Vprbp* in cells than previously appreciated. I confirmed the essential role for *Vprbp* in cellular proliferation and now provide circumstantial evidence that *Vprbp* may also have a role in non-proliferative, quiescent cells. The observation that VprBP is increased in serum-starved and contact-inhibited cells is particularly intriguing in light of its interaction with Merlin. Some of the earliest research on Merlin showed that Merlin accumulates in response to contact inhibition and serum starvation in fibroblasts (Shaw et al., 1998). In contrast to VprBP, Merlin depletion causes loss of contact inhibition

(Lallemand et al., 2003; Morrison et al., 2001) which correlates with hyperactive RAC and MAPK signaling activity (Kaempchen et al., 2003; Morrison et al., 2007; Okada et al., 2005). The Giancotti lab recently demonstrated that RNAi to VprBP ablates the oncogenic activity associated with Merlin loss (Li et al., 2010b). This suggests that VprBP functions downstream of Merlin, perhaps in controlling mitogenic signaling. While the Giancotti lab provide evidence that Merlin and VprBP function in the nucleus to control an unknown transcription factor, I favor the long-held view that Merlin functions at or near the plasma membrane to inhibit mitogenic signaling (Li et al., 2010b; McClatchey and Fehon, 2009). Indeed, a recent paper finally provided a molecular mechanism for the long observed inhibition of RAC signaling by Merlin: Merlin binding to a tight-junction associated protein complex releases an inhibitor of RAC called RICH1 (Yi et al., 2011). RICH1, also known as ARHGAP17, is a GAP protein that stimulates the conversion of RAC-GTP to RAC-GDP, thereby inactivating it. The Kissil lab now suggest a model that RICH1 associates with the tight junction associated protein complex, but is displaced by binding of Merlin to the complex, and RICH1 is thought be activated upon its release (Yi et al., 2011).

In our lab, Dr. Tadashi Nakagawa has observed in conditional *Vprbp* MEFs and in RNAi depleted cells that depletion of VprBP results in an almost complete loss of GTP-bound RAC from cells (data not shown). Further, he found that co-depletion of Merlin by RNAi rescued this loss of RAC signaling (data not shown). This suggests that VprBP and Merlin may counterbalance each other to fine-tune RAC activity in cells. It will be interesting to determine if VprBP can bind with the tight junction associated protein complex (consisting of Angiomotin, PATJ, and PALS1) or RICH1, which would provide a direct role for VprBP in regulating RAC activity. In addition, it will be important to determine if loss of RAC signaling underlies the proliferation defect noted in cells without VprBP. Finally, it remains to be seen why VprBP accumulates to such a large

extent in quiescent MEFs. Do high levels of VprBP prime cells to re-enter the cell cycle or promote survival during quiescence? Is binding with Merlin required for VprBP function in quiescent cells? Does VprBP accumulation in contact-inhibited cells relate to RAC signaling? The lab will continue to explore the function of VprBP in proliferative and quiescent cells to understand the molecular mechanisms that underlie the requirement for VprBP.

CHAPTER IV

INDUCIBLE DISRUPTION OF *VPRBP* IN MOUSE IMPAIRS T-CELL DEVELOPMENT, PROLIFERATION AND SURVIVAL

Summary

Vprbp is an essential gene that encodes a putative substrate recruiting receptor for a CRL4-RING ubiquitin ligase complex. To investigate the role of *Vprbp* in an unbiased manner, we disrupted *Vprbp* in 5-week old mice using a ubiquitously expressed, 4-OH-tamoxifen-inducible Cre. We found that disruption of *Vprbp* results in severe thymic defects including a 90.4% reduction in total thymocytes, ablation of $CD4^+CD8^+$ cells, decreased 5'-bromo-2'-deoxyuridine incorporation and increased cleaved caspase-3 staining. We further observed defects in B-cell development with decreased immature and pre/pro- B-cell populations. In addition, we found that mature T-cells from *Vprbp* disrupted mice failed to proliferate in response to CD3/CD28 stimulation, suggesting that cell cycle defects underlie the observed phenotypes. Finally, we found that inducible loss of *Ddb1* results in a phenotype which considerably overlaps with *Vprbp* disruption, including a reduction in thymus size, decreased $CD4^+CD8^+$ population, and impaired B-cell development. Cumulatively, these data provide the first genetic evidence that *Vprbp* is required beyond embryonic development and demonstrate a specific role for *Vprbp* in lymphocyte development and T-cell proliferation. Further, observations that *Ddb1* or *Vprbp* disruption cause similar defects in lymphocyte development provide genetic support for the established biochemical interaction between DDB1 and VprBP.

Background

Ubiquitylation, a post-translational modification best-known for mediating proteasomal degradation, is critically involved in regulating a wide range of diverse cellular processes. The largest family of E3s is the cullin-based ubiquitin ligase complexes which target numerous substrates by associating with different substrate recruiting receptors. Cullin 4-RING E3 ligases (CRL4s), which use CUL4A or its paralog CUL4B as a scaffold, bind linker protein DDB1 (damaged DNA binding) and a family of substrate receptors containing a specialized WD40 repeat (Jackson and Xiong, 2009a). Here, we describe genetic characterization of mouse *Vprbp* which encodes a putative CRL4 substrate receptor of unknown function.

VprBP was first identified as the HIV1 viral protein r binding protein, and was subsequently shown to associate with CRL4 (Zhang et al., 2001; Zhao et al., 1994; He et al., 2006). Vpr can associate with $CRL4^{VprBP}$ (Belzile et al., 2007; Hrecka et al., 2007; Le Rouzic et al., 2007; Tan et al., 2007; Wen et al., 2007) and may hijack the complex to degrade UNG2 (Ahn et al. 2010), a uracil DNA glycosylase that removes uracil from DNA as part of the base excision repair pathway. It is unclear if Vpr directs ubiquitylation of additional substrates or if Vpr might also function to modulate normal $CRL4^{VprBP}$ activity. $CRL4^{VprBP}$ cannot ubiquitylate UNG2 in the absence of Vpr and its normal physiological substrate(s) are unknown.

The function of VprBP as a substrate recruiting receptor for CRL4 is inferred from binding with the CUL4-DDB1-ROC1 complex and the presence of the WDXR motif that is shared in other experimentally demonstrated CRL4 substrate receptors. Without any known substrate, the in vivo function of $CRL4^{VprBP}$ remains obscure, but a possible function in DNA replication has been proposed. Knocking down VprBP resulted in defective progression through S phase and inhibited proliferation (McCall et al., 2008),

(Hrecka et al., 2007), indicating that VprBP is required for normal cell cycle progression in cultured cells.

Genetic studies in several model organisms have established a role for *Vprbp* in embryonic development. Loss of *VPRBP* in *Arabidopsis* led to early embryonic lethality at the globular stage, and reduced expression of *VPRBP* disrupted multiple developmental pathways, indicating broad functions in development (Zhang et al., 2008). In *Drosophila*, *vprbp/mahjong* is required for embryogenesis, but zygotic mutants (which have maternally supplied Vprbp) develop normally, suggesting that unlike plants, *vprbp* is only essential for early embryogenesis in *Drosophila* (Tamori et al. 2010). We previously generated a strain of *Vprbp* knockout mouse, and found that loss of *Vprbp* causes early embryonic lethality (prior to E7.5) whereas conditional ablation of *Vprbp* in mouse embryonic fibroblasts (MEFs) resulted in cell cycle arrest and apoptosis (McCall et al., 2008). Collectively, these studies demonstrate an evolutionarily conserved, essential role for *Vprbp* in early embryonic development. In this study, we sought to genetically examine the in vivo function of *Vprbp* in adult mice by using a broadly expressed, tamoxifen-inducible Cre to drive *Vprbp* disruption. This unbiased approach uncovered a novel role for *Vprbp* in the development and proliferation of lymphocytes in mice.

Cell proliferation and apoptosis are both critical for proper lymphocyte development. Developing B- and T-cells have several selection points to ensure that gene rearrangement has yielded a productive receptor that responds to specific antigens but is not self-reactive. In the case of thymocytes, $CD4^{-}CD8^{-}$ cells undergo β selection following T-cell receptor β (TCRβ) gene rearrangement, which dimerizes with the proTCRα to express the pro-TCR. Cells which can relay intra-cellular TCR signals survive, undergo a rapid proliferative burst (Vasseur et al., 2001) and further

differentiate, while those that fail undergo apoptosis (Zhang et al., 2005). The TCRα gene locus is rearranged at the CD4+CD8+ stage and cells are subjected to both positive selection (selection for T cells with TCR$\alpha\beta$ binding to self MHC molecules) and negative selection (selection against self-reactive cells) before committing to $CD4^+$ or $CD8^+$ lineages (Starr et al., 2003). Many double-positive cells fail to successfully signal through TCR$\alpha\beta$ at this stage and consequently undergo apoptosis within a few days (Carpenter and Bosselut, 2010 ; Starr et al., 2003). Thus, thymocytes are poised to die by apoptosis at several developmental stages and rely on proliferation at distinct stages of the differentiation process.

Loss of function of many essential genes required for proliferation (e.g. *Rac1/2*, *Csn5* (Dumont et al., 2009; Guo et al., 2008; Panattoni et al., 2008)), survival (e.g. c*Flip*, *Bcl2* (Chau et al., 2005; Veis et al., 1993)) or cellular metabolism (e.g. *Pdk1*, *Lkb1* (Hinton et al., 2004; Tamas et al., 2010)) results in severe phenotypes in lymphocyte development . For example, loss of cyclin D3 (*Ccnd3*), which drives the G1 to S-phase cell cycle transition in lymphocytes, blocked B-cell development by inhibiting proliferation of pre-B-cells (Cooper et al., 2006). In addition, T-cell development was inhibited; loss of cyclin D3 led to reduced thymus size with a decrease in the number of double positive and single positive thymocytes (Sicinska et al., 2003).

The *Ubiquitin C* promoter-driven *CreERT2*$^+$ I chose for my study was previously used to characterize inducible deletion of the essential gene *Atr* in adult mice (Ruzankina et al., 2007). The Brown lab found that loss of *Atr* in adult mice led to pronounced phenotypes in a number of proliferative tissues including thymus, bone marrow, intestine and skin (Ruzankina et al., 2007). Given the established requirement for *Vprbp* in normal cell cycle progression and survival, we hypothesized that disruption of *Vprbp* would broadly cause defects in proliferating tissues. I report here that

inducible disruption of *Vprbp* causes defects in B- and T-cell development and decreased the survival and cell proliferation of lymphocytes.

Experimental Procedures

Mice

Mice were bred and maintained strictly in the University of North Carolina Animal Care Facility under protocol approved by the Institutional Animal Care and Use Committee. All efforts were made to minimize animal suffering. The generation of conditional *Vprbp* mice was previously described (McCall et al., 2008). Conditional *Ddb1* mice were previously described (Cang et al., 2006). All mice were backcrossed to C57BL/6 for at least 4 generations. Germline transmission of $Vprbp^{\Delta}$ and $Ddb1^{-}$ was obtained by crossing conditional mice with $EIIA\text{-}Cre^{+}$ mice (Jackson Laboratories, stock 003724). $Ubc\text{-}CreERT2^{+}$ mice were previously described and kindly provided by Dr. Eric Brown (Ruzankina et al., 2007). All experiments were performed using gender-matched, littermate controls. 5-week-old mice were injected intraperitoneally (i.p.) once per day for five consecutive days with 0.4 μmol/g body weight tamoxifen (Sigma, T5648) prepared in solution as described (Feil et al., 2009). For BrdU incorporation experiment, 50 μg BrdU (Sigma, B5002) in PBS per g body weight was i.p. injected 4 hours prior to sacrifice.

Genotyping

Primers for genotyping *Vprbp* alleles: 5' CTGGGTAGCTACTGTTGACTACTCACTGCG 3', 5' CAGTTAGAGAGTGACTTTGGACG 3', and 5' GCTGCCAACTATGGGTGC 3', which detected 434 bp, 468 bp and 280bp bands for the wild-type, flox and Δ alleles, respectively. Primers for genotyping conditional *Ddb1*:

5'CGGGACTGGAGCATTTTTGACTAC 3' and 5' ATTTTCTGTGTATGGAGGGGAGTG 3'. Primers for genotyping conditional *Ddb1*$^{-}$: 5' CCCACTTAAAGGACTGGTG 3' and 5' GGACAATGGAAACATAGGG 3'. Primers for genotyping *Cre-ERT2*: 5' GCTGGAGTTTCAATACCGGAG 3' and 5' CTTAGAGCGTTTGATCATGAGC 3'. *Il2* primers were included in the *CreERT2* PCR as an internal control: 5' CTAGGCCACAGAATTGAAAGATCT 3' and 5'GTAGGTGGAAATTCT AGCATCATC 3'.

Immunohistochemistry and Immunoblotting

Mouse tissue was removed, fixed in 10% neutral buffered formalin, embedded in paraffin and cut into 3-μm sections. Primary antibodies for immunohistochemistry included p53 (1:500, Novocastra NCL-p53-505), BrdU (1:100, Amersham Pharmacia Biotech BU-1), and cleaved caspase-3 (1:400, Cell Signaling 9661) and were detected by diaminobenzidine (DAB) staining (Vector Laboratories, Vectastain Elite ABC reagent) after unmasking by heating in 10 mM sodium citrate buffer (pH 6.0).

For immunoblotting, tissue or cells were lysed in RIPA buffer (50 mM Tris-HCl [pH 8.0], 150 mM NaCl, 1% NP-40, 0.5% DOC, 0.1% SDS, 1 mM Na_3VO_4, supplemented with 1 mM DTT, 1 mM PMSF, and a cocktail of protease inhibitors containing 25 mg/L leupeptin, 25 mg/L aprotinin, 150 mg/L benzamidine, and 10 mg/L trypsin inhibitor), resolved by SDS-PAGE and transferred to 0.2 μm PVDF (Millipore). Antibodies to VprBP and DDB1 were previously described (McCall et al., 2008). Antibodies for immunoblotting included Actin (Santa Cruz, sc-1616), α-tubulin (NeoMarkers, Ab-2), PARP (Cell Signaling, 9542) pRB (Cell Signaling, 9308), and RB (BD Pharmingen, G3-245).

Flow Cytometry

All cells were analyzed at the University of North Carolina School of Medicine Flow Cytometry Facility on a CyAN (Dako Cytomation) flow cytometer, and data were analyzed using Summit software, version 4.3 (Dako Cytomation). To examine BrdU incorporation in MEFs, cells were prepared as previously described (McCall et al., 2008). For thymocyte, splenocyte, and bone marrow cells, single cell suspensions were prepared in PBS containing 2% FBS (FACS buffer) after red blood cells lysis in 4 parts 0.8% NH_4Cl, 0.1 mM EDTA, pH 7.45 and 1 part FACS buffer. 10^6 live cells were stained in FACS buffer containing Fc block (BioLegend, Trustain fcX, 1:200) with the antibodies indicated: Pacific Blue-conjugated CD8a (BioLegend, 1:400), APC-AF750-conjugated CD4 (Caltag,1:50), PE-conjugated B220 (BD Biosciences, 1:100), or FITC-conjugated IgM (eBioscience, 1:100), and immediately analyzed by flow cytometry.

For in vitro T-cell proliferation experiments, primary lymphocytes were labeled with 5 μM carboxyfluorescein diacetate succinimidyl ester (CFSE, Molecular Probes, Inc) in PBS at room temperature for 10 min; labeling was quenched with the addition of an equal volume of FBS followed by two washes in RPMI-10. T-cells were then stimulated by CD3 and CD28 antibodies (Caltag) and cultured in RPMI-10 for the indicated time. 10^6 cells were then labeled with Pacific Blue-conjugated CD4 (Biolegend, 1:100) and Pacific Blue-conjugated CD8a (Biolegend, 1:400), and subsequently stained with APC-conjugated Annexin V (eBioscience, 1:20) and 7AAD before flow cytometry analysis.

Cell Culture

Primary mouse embryo fibroblasts (MEF) were isolated on embryonic day 13.5 and grown in a 37°C incubator with 5% CO_2 in DMEM supplied with 10% FBS and penicillin-streptomycin. All experiments were performed at passage 4 or earlier. For BrdU

incorporation, a final concentration of 10 μM BrdU was added to the culture medium for 6 hours before harvesting and fixing cells. 4-OH-Tamoxifen (Sigma, H7904) was dissolved in 100% ethanol and added to the culture medium as indicated.

Primary lymphocytes from mouse lymph nodes and spleen were obtained from 6-week-old tam-treated mice 6 days following the first injection. After red blood cell lysis, cells were cultured in RMPI (Gibco) supplemented with 10% FBS, penicillin-streptomycin, 2 mm L-glutamine, 50μM β-mercaptoethanol, and 100nM 4-OHT. Cells were cultured for 18h before CFSE labeling and T-cell activation.

qPCR

Total RNA was extracted by RNeasy (Qiagen), and used for cDNA synthesis primed with Oligo(dT)20 primers (Invitrogen, Superscript III). The cDNA was added to a qPCR mixture that contained 1× SYBR Green PCR master mix (Applied Biosystems) and 500 nM gene-specific primers. Assays were performed in triplicate on a 7900 HT sequence detection system (Applied Biosystems). The PCR protocol comprised incubations for 2 min at 50°C and for 10 min 95°C, followed by 40 cycles, each consisting of 15 sec at 95°C and 1 min at 60°C. The expression level of each gene was normalized with glyceraldehyde-3-phosphate dehydrogenase (*Gapdh*). The specific PCR pairs were as follows: *Vprbp*: 5' GCCGGGCCTAGAAACCGCAG 3', 5' TGTCCTGCCGCAAAGCCACT; *Ddb1*: 5' GCAGAGCCCAAGCAGGGTCG 3', 5'GCCGCACCGTGCTATTGATGC ; *Gapdh*: 5' AGCCTCGTCCCGTAGACAA 3', 5' AATCTCCACTTTGCCACTGC 3'. For qPCR of genomic DNA from paraffin-embedded tissue, the following primers for *Vprbp* were used: 5' TGCAGGTCACTCCTGATTAAGGGT 3' (in intron 7-8) and 5'

GAGTGCCTCAAAAGTAAGCAGGACA 3' (in exon 8). Detection of *Vprbp* was normalized to *Il2*, which was unaffected by Cre recombination: 5' CTAGGCCACAGAATTGAAAGATCT 3' and 5'GTAGGTGGAAATTCT AGCATCATC 3'.

Results

Inducible disruption of *Vprbp* results in marked thymic atrophy

To genetically examine the in vivo function of *Vprbp* in mice, we administered tamoxifen (tam) to $Vprbp^{F/\Delta};CreERT2^{+}$ and littermate control $Vprbp^{F/+};CreERT2^{+}$ mice and observed loss of full-length VprBP in multiple tissues including heart, liver, kidney and brain (Fig. 4.1A). We found that 43.8% (14/32) of mutant mice became moribund within 7 to 14 days after initial tam injection, indicating that disruption of *Vprbp* is poorly tolerated in adult mice. Further, the appearance of this severe phenotype correlated closely with the efficiency of *Vprbp* disruption as assessed by immunoblotting or qRT-PCR, suggesting that the variation between animals reflects varying degrees of Cre-mediated recombination in mice (data not shown). In the course of analyzing these mice, we noted obvious thymic atrophy in tam-treated $Vprbp^{F/\Delta};CreERT2^{+}$ mice (Fig. 4.1B) and have therefore chosen to focus our efforts on characterizing in detail the effects of *Vprbp* disruption in thymus. In addition to reduced size, histological analysis of thymus from a $Vprbp^{F/\Delta};CreERT2^{+}$ mouse after tam treatment revealed a clear lack of typical cortico-medullary architecture (Fig. 4.1C), suggesting T-cell developmental defects.

Figure 4.1

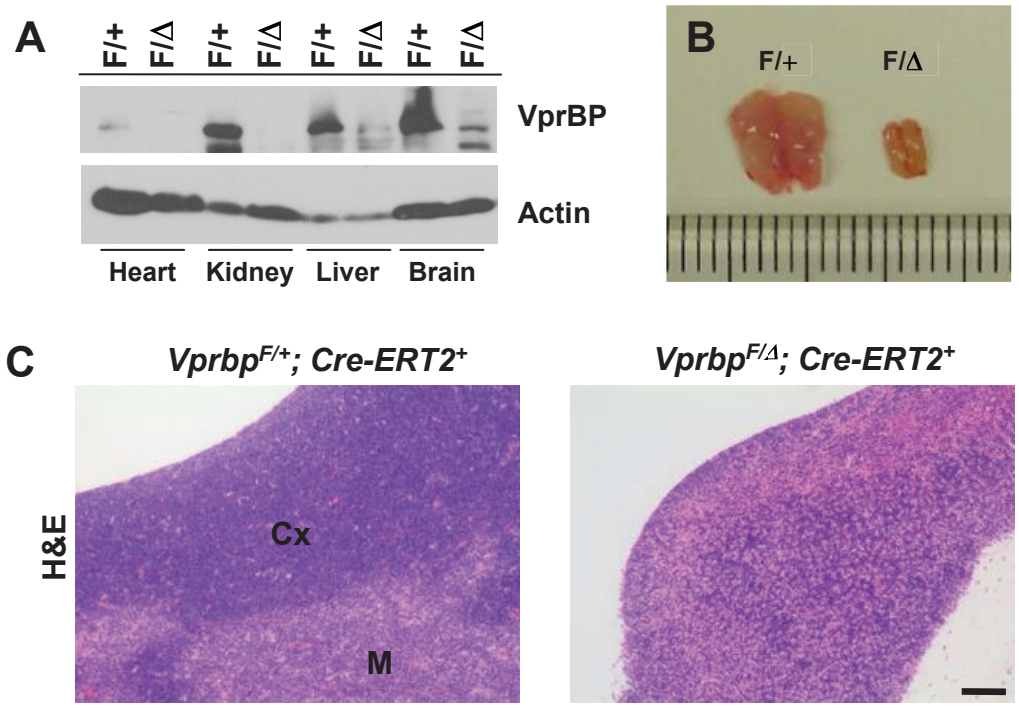

Figure 4.1. Inducible disruption of *Vprbp* results in marked thymic atrophy

(A) Tamoxifen administration resulted in loss of VprBP protein in a broad range of tissues. Tissue lysates from tamoxifen-treated *Vprbp*$^{F/+}$*;CreERT2*$^{+}$ or *Vprbp*$^{F/\Delta}$*;CreERT2*$^{+}$ mice were prepared, resolved by SDS-PAGE and immunoblotted as indicated.

(B) Disruption of Vprbp resulted in a visibly smaller thymus. Thymi were isolated from 6-week-old *Vprbp*$^{F/+}$*;CreERT2*$^{+}$ or *Vprbp*$^{F/\Delta}$*;CreERT2*$^{+}$ mice, 7 d after tamoxifen injection.

(C) Disruption of Vprbp caused disorganized thymic structure. Sections of formalin-fixed, paraffin-embedded thymus tissue were stained with hematoxylin and eosin. Cortex (Cx) and medulla (M) are indicated in thymus from tamoxifen-treated *Vprbp*$^{F/+}$*;CreERT2*$^{+}$, but are not well-defined in thymus tissue from a *Vprbp*$^{F/\Delta}$*;CreERT2*$^{+}$ mouse. Scale bar = 200 μm.

Defects in T-lymphocyte development following inducible disruption of *Vprbp*

Total thymocyte cell counts were significantly reduced in thymus from tam-treated *Vprbp*$^{F/\Delta}$*;CreERT2*$^{+}$ mice (1.36 ± 0.67 × 10^7 in mutant vs. 15.52 ± 1.37 × 10^7 in control animals 7-10 days after tam treatment, p=0.0005; Fig. 4.2A), indicating a severe T-cell developmental defect. To further probe the nature of the T-cell developmental defect, flow cytometric analysis of CD4 and CD8 cell surface markers was performed on thymocytes from tam-treated *Vprbp*$^{F/\Delta}$*;CreERT2*$^{+}$ mice compared with tam-treated *Vprbp*$^{F/+}$*;CreERT2*$^{+}$ control mice. T-cell precursors migrate to the thymus as double negative ($CD4^-$ $CD8^-$, DN), mature into double positive ($CD4^+$ $CD8^+$, DP) cells, and subsequently commit to become single positive ($CD4^+$ or $CD8^+$) cells. In the mutant thymus, CD4/CD8 staining notably revealed a near complete loss of the DP cells, with a corresponding relative increase in the percentage of DN and SP cells (Fig. 4.2B-C). While this result could suggest a block in the DN to DP transition (with residual SP cells developed before tam-treatment), the absolute number of DN and SP cells was also greatly reduced (Fig. 4.2D), indicating decreased survival at all developmental stages, with DP cells being the most profoundly affected. RT-PCR analysis of thymic tissue indicated that the majority of remaining cells retained full length *Vprbp* mRNA (Fig. 4.2E), indicative of a strong selection pressure against cells with Cre-mediated recombination in thymus despite good recombination in other tissues in the same mice (Fig. 4.2E and data not shown).

Figure 4.2

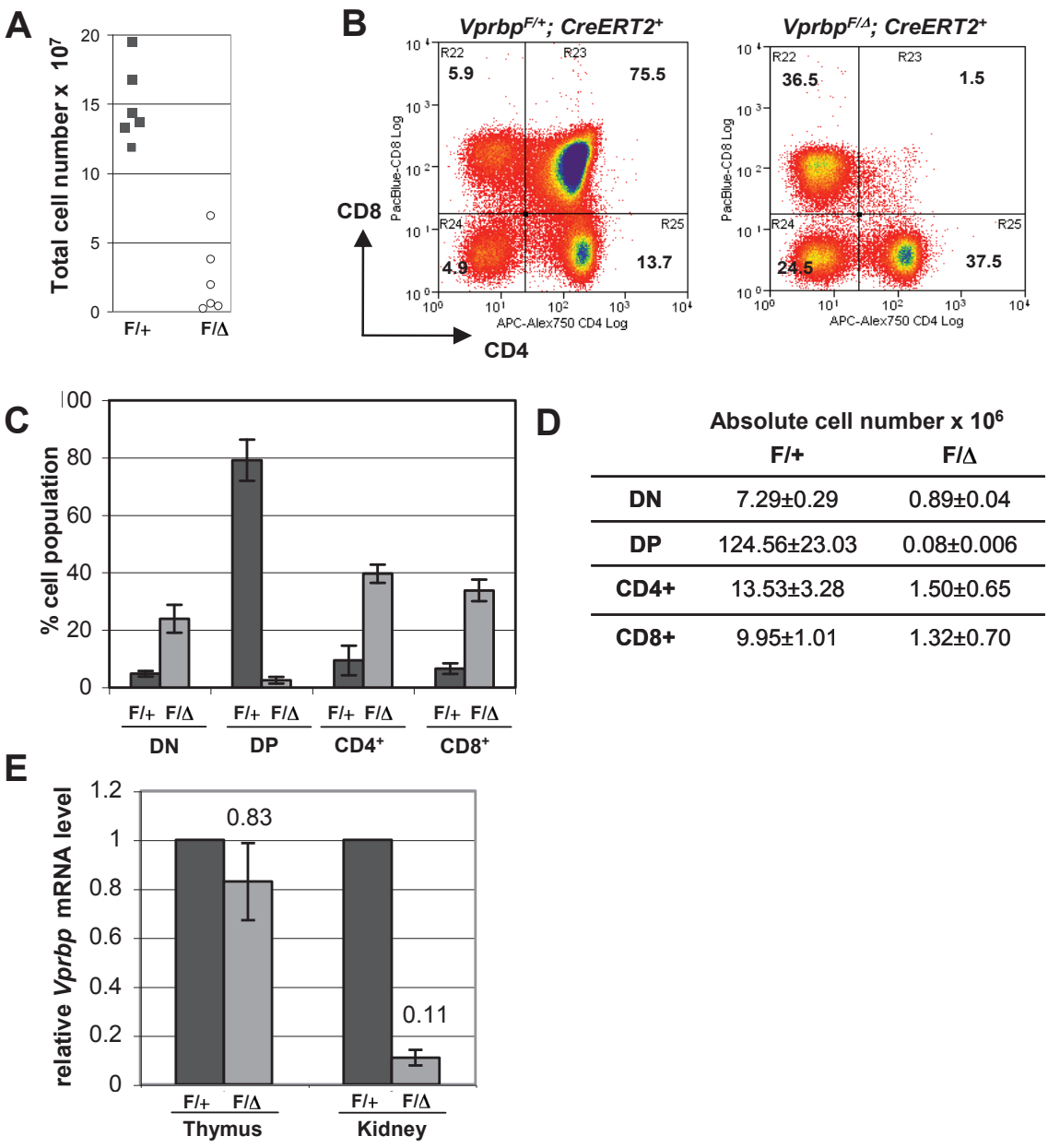
A
Total cell number x 10^7
20
15
10
5
0
F/+
F/Δ
B
Vprbp^F/+; CreERT2+
Vprbp^F/Δ; CreERT2+
R22
R23
R24
R25
5.9
75.5
4.9
13.7
36.5
1.5
24.5
37.5
PacBlue-CD8 Log
APC-Alex750 CD4 Log
CD8
CD4
C
% cell population
100
80
60
40
20
0
F/+ F/Δ
DN
DP
CD4+
CD8+
D
Absolute cell number x 10^6
F/+
F/Δ
DN 7.29±0.29 0.89±0.04
DP 124.56±23.03 0.08±0.006
CD4+ 13.53±3.28 1.50±0.65
CD8+ 9.95±1.01 1.32±0.70
E
relative Vprbp mRNA level
1.2
1
0.8
0.6
0.4
0.2
0
0.83
0.11
F/+ F/Δ
Thymus
Kidney

Figure 4.2. Defects in T-lymphocyte development following disruption of *Vprbp*

(A) Total thymic cellularity (x10^6) in 6-wk-old *Vprbp$^{F/+}$;CreERT2$^+$* and *Vprbp$^{F/\Delta}$;CreERT2$^+$* mice 6-10 days after tamoxifen treatment. Single cell suspensions prepared from thymus were quantified using a hemacytometer (n=6 for *Vprbp$^{F/+}$;CreERT2$^+$* and n=6 for *Vprbp$^{F/\Delta}$;CreERT2$^+$* mice).

(B) Flow cytometric analysis of thymocytes from *Vprbp$^{F/+}$;CreERT2$^+$* and *Vprbp$^{F/\Delta}$;CreERT2$^+$* mice 6 d after tamoxifen injection, stained with Pacific Blue-conjugated CD8 antibody and APC-AF750-conjugated CD4 antibody.

(C) Bar diagram showing average percentages for CD4$^-$ CD8$^-$ (DN), CD4$^+$ CD8$^+$ (DP), CD4$^+$ SP and CD8$^+$ SP subpopulations from 6-wk-old mice 7 d after initial tamoxifen treatment (n=3 for *Vprbp$^{F/+}$;CreERT2$^+$* and n=3 for *Vprbp$^{F/\Delta}$;CreERT2$^+$* mice). Values represent the mean ± SE.

(D) Absolute cell numbers (x10^6) for thymocyte subsets in C were calculated by multiplying percentages by total cell number. Values represent the mean ± SE.

(E) Thymus tissue remaining in *Vprbp$^{F/\Delta}$;CreERT2$^+$* mice following tamoxifen treatment has largely escaped Cre-mediated recombination. The mRNA level of full length Vprbp transcript from kidney and thymus tissue from the same mice was determined by quantitative real-time reverse transcriptase PCR (qRT-PCR). Data are expressed relative to the corresponding values for *Vprbp$^{F/+}$;CreERT2$^+$* thymus or kidney. Each experiment was performed in triplicate; mean value and standard deviations were calculated from three independent experiments.

Disruption of *Vprbp* decreased proliferation and induced apoptosis in thymus.

To examine how *Vprbp* disruption effects cell survival and cell proliferation, we examined the histology of thymus sections from more moderately affected animals (6 d after tam), at which time there was robust recombination at the *Vprbp* loci as assessed by qPCR analysis of genomic DNA from thymic tissue (data not shown). Incorporation of the thymidine analog BrdU was almost undetectable in thymus from mutant mice, indicating a strong inhibition of proliferation (Fig. 4.3A). In addition, cleaved caspase-3 and p53 are more abundantly detected following *Vprbp* disruption, indicating that, in addition to proliferation inhibition, apoptosis also contributes to the reduction in thymus size in mutant mice (Fig. 4.3A). Consistent with these observations, western blot analysis revealed an increase in p53 protein and reduced proliferation, as assessed by lack of phosphorylated-RB protein, in thymocytes from tam-treated *Vprbp*$^{F/\Delta}$*;CreERT2*$^{+}$ mice compared to control animals (Fig. 4.3B). Furthermore, we noted an increase in apoptotic and dead cells in the mutant DP population compared with control DP cells, as assessed by Annexin V+ and 7AAD staining (Fig. 4.3C), indicating that disruption of *Vprbp* promotes apoptosis of DP thymocytes.

Inducible disruption of *Vprbp* disrupts B-cell development.

Having observed a clear requirement for *Vprbp* in T-cell development, we sought to determine if *Vprbp* also played a role in B-cell development by examining the effect of *Vprbp* disruption on bone marrow. We assessed the efficiency of *Vprbp* disruption by qRT-PCR analysis of isolated bone marrow cells (Fig. 4.4B). We found that the total number of bone marrow cells from femurs was reduced ($7.76 \pm 1.60 \times 10^6$ in mutant versus $13.94 \pm 1.41 \times 10^6$ in control animals 6-10 days after tam treatment; Fig. 4.4C), though this difference was not statistically significant. Histological analysis of bone

Figure 4.3

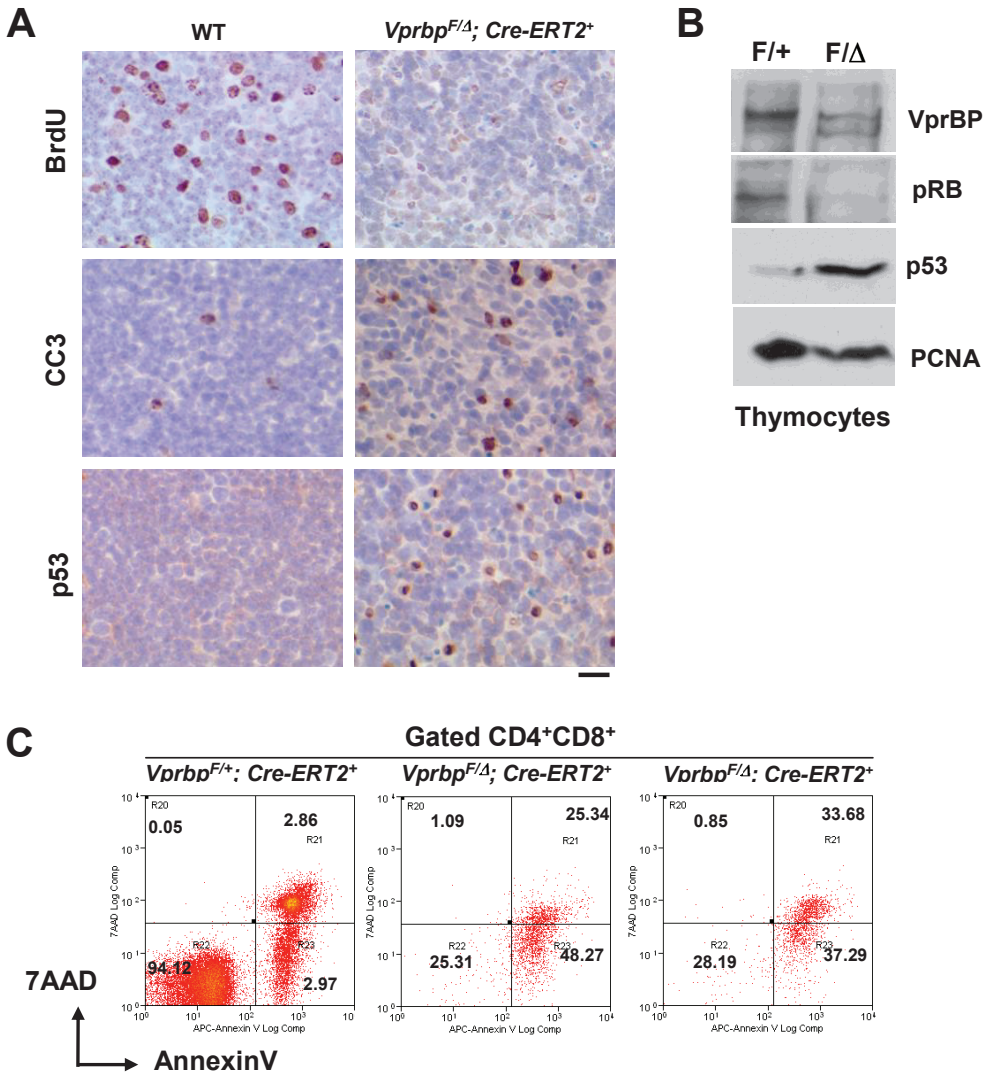

Figure 4.3. *Vprbp* disruption decreased proliferation and induced apoptosis in thymus

(A) Immunostaining of BrdU, cleaved caspase-3 and p53 from sections of formalin-fixed, paraffin-embedded thymus tissue following tamoxifen treatment. Positive staining is indicated by brown color; sections were counter-stained with hematoxylin. Scale bar = 20 μm.

(B) Immunoblot analysis, using the indicated antibodies, of thymocyte lysate from *Vprbp*$^{F/+}$*;CreERT2*$^{+}$ and *Vprbp*$^{F/\Delta}$*;CreERT2*$^{+}$ mice 6d after initial tamoxifen treatment

(C) Flow cytometric analysis of apoptotic cells by 7AAD and Annexin V staining, gated by the CD4^{+}CD8^{+} population.

Figure 4.4

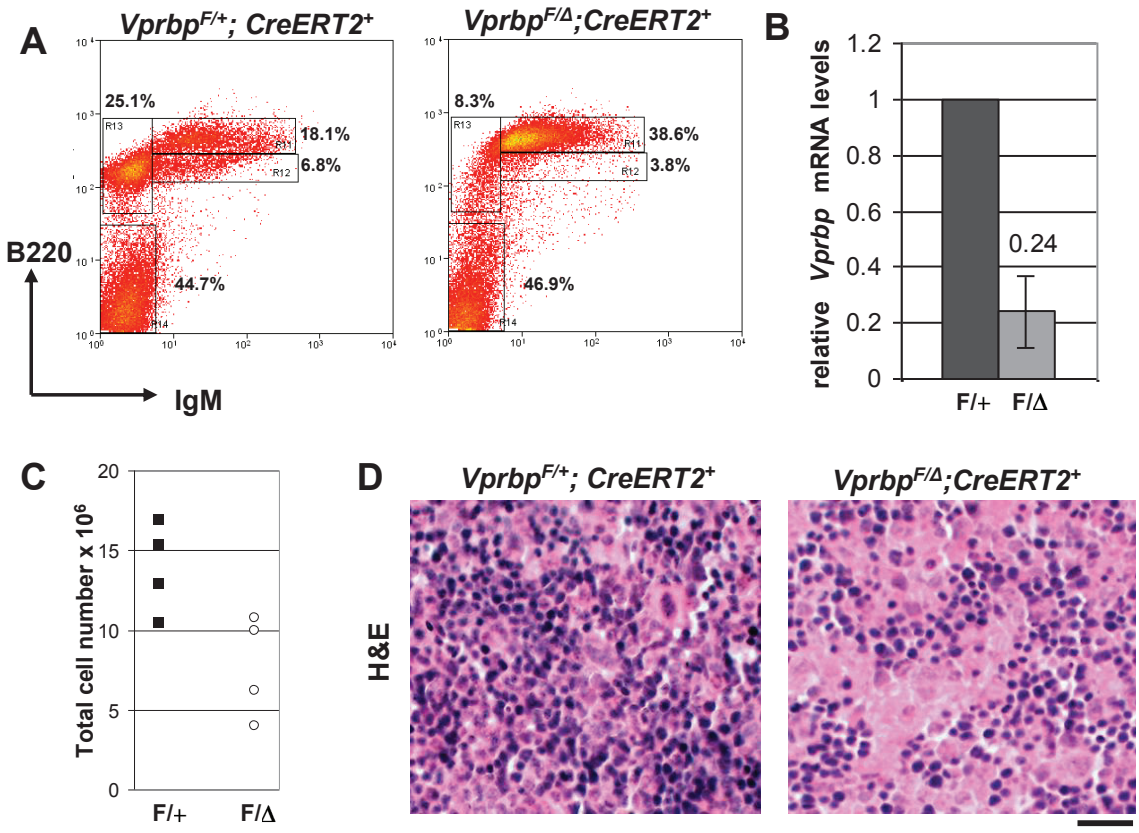

Figure 4.4. Inducible disruption of *Vprbp* impairs B-cell development

(A) Bone marrow cells from one femur of *Vprbp*$^{F/+}$;*CreERT2*$^{+}$ and *Vprbp*$^{F/\Delta}$;*CreERT2*$^{+}$ mice were isolated 6 d after tamoxifen injection, stained with PE-conjugated B220 antibody and FITC-conjugated IgM antibody, and analyzed on a flow cytometer.

(B) *Vprbp* mRNA levels from bone marrow were determined by quantitative real-time reverse transcriptase PCR (qRT-PCR). Data are expressed relative to the corresponding values for *Vprbp*$^{F/+}$;*CreERT2*$^{+}$. Each experiment was performed in triplicate; mean value and standard deviations were calculated from three independent experiments.

(C) Total bone marrow cellularity (x10^{6}) in 6-wk-old *Vprbp*$^{F/+}$;*CreERT2*$^{+}$ and *Vprbp*$^{F/\Delta}$;*CreERT2*$^{+}$ mice 6 days after tamoxifen treatment. Single cell suspensions were quantified using a hemacytometer (n=4 for *Vprbp*$^{F/+}$;*CreERT2*$^{+}$ and n=4 for *Vprbp*$^{F/\Delta}$;*CreERT2*$^{+}$ mice).

(D) Sections of decalcified, paraffin-embedded bone marrow tissue were stained with hematoxylin and eosin. Scale bar = 20 μm.

marrow tissue supported the notion that bone marrow cellularity decreased following tam injection in *Vprbp*$^{F/\Delta}$*;CreERT2*$^{+}$ mice (Fig. 4.4D). To examine how *Vprbp* disruption specifically affects B-cell development, we analyzed the B-cell subpopulations of isolated bone marrow cells from femurs by staining the cell surface for B-cell markers B220 and IgM. We found that the B220^{+}IgM^{-} cells, which represents pre- and pro-B-cell populations, were reduced in tam-treated *Vprbp*$^{F/\Delta}$*;CreERT2*$^{+}$ mice (8.3% in mutant versus 25.1% in control) as were the B220^{lo}IgM^{+} cells, which represents immature B-cells (3.8% in mutant versus 6.8% in control; Fig. 4.4A). Concomitantly, a relative increase in the percentage of recirculating, mature B-cells which are B220^{hi}IgM^{+} was found in bone marrow of in tam-treated *Vprbp*$^{F/\Delta}$*;CreERT2*$^{+}$ mice (38.6% in mutant versus 18.1% in control bone marrow; Fig. 4.4A). This finding suggests that B-cells which matured prior to tam injection in *Vprbp*$^{F/\Delta}$*;CreERT2*$^{+}$ mice were largely unaffected by *Vprbp* disruption, but new B-cell development in bone marrow was inhibited. Thus, we conclude that disruption of *Vprbp* impairs the development of both B- and T-cells in mice.

Mature T-cells with disrupted *Vprbp* fail to proliferate in response to activation.

To examine the effects of *Vprbp* disruption on mature, rather than developing lymphocytes, we examined B- and T- cell populations from spleen tissue. We found a decrease in spleen size (Fig. 4.5A) and splenocyte cellularity following inducible disruption of *Vprbp* ($8.18 \pm 0.89 \times 10^7$ in mutant vs. $13.52 \pm 0.98 \times 10^7$ in control animals 6-10 days after tam treatment, p=0.014; Fig. 4.5B). However, flow cytometric analysis of the B- and T-cell populations from spleen showed no change in the relative percentage of lymphocytes following *Vprbp* disruption. This observation suggests that developing B-

Figure 4.5

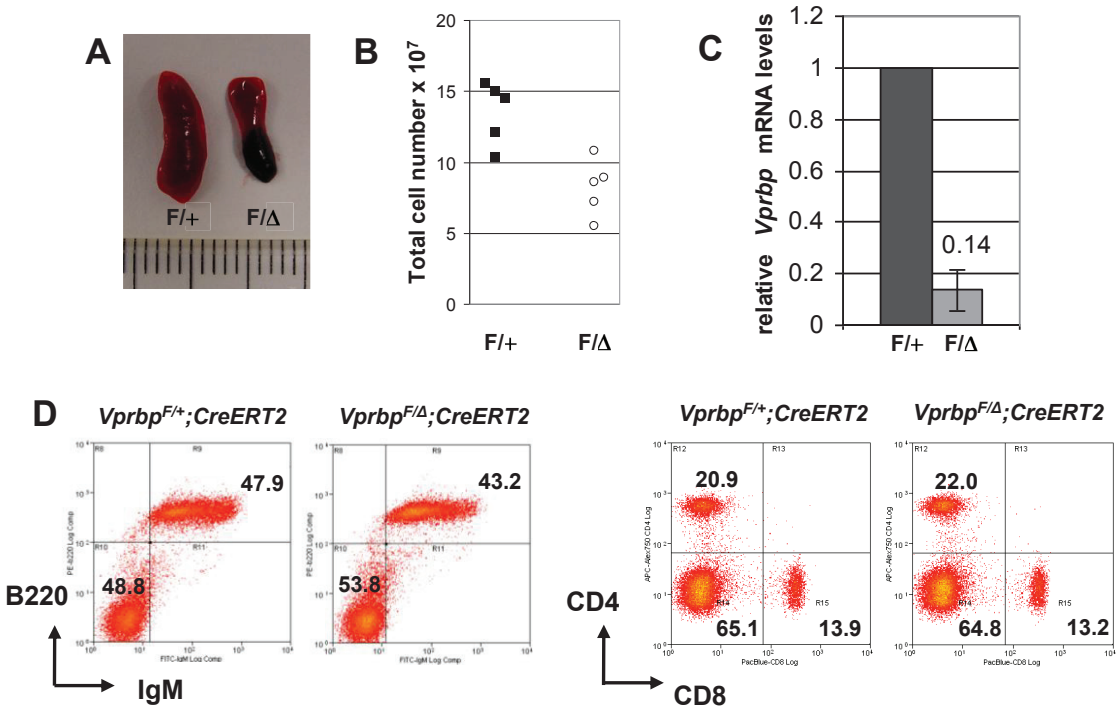

Figure 4.5. Disruption of Vprbp did not impact the distribution of splenocytes.

(A) Gross morphology of spleen 6 d after tamoxifen treatment in 6-wk-old *Vprbp*$^{F/+}$*;CreERT2*$^{+}$ and *Vprbp*$^{F/\Delta}$*;CreERT2*$^{+}$ mice.

(B) Total splenocyte cellularity (x10^{7}) in 6-wk-old *Vprbp*$^{F/+}$*;CreERT2*$^{+}$ and *Vprbp*$^{F/\Delta}$*;CreERT2*$^{+}$ mice 6-10 days after tamoxifen treatment. Single cell suspensions were quantified following red blood cell lysis using a hemacytometer (n=5 for *Vprbp*$^{F/+}$*;CreERT2*$^{+}$ and n=5 for *Vprbp*$^{F/\Delta}$*;CreERT2*$^{+}$ mice).

(C) *Vprbp* mRNA levels from spleen tissue were determined by quantitative real-time reverse transcriptase PCR (qRT-PCR). Data are expressed relative to the corresponding values for *Vprbp*$^{F/+}$*;CreERT2*$^{+}$. Each experiment was performed in triplicate; mean value and standard deviations were calculated from three independent experiments.

(D) Flow cytometric analysis of the B-cell population in spleen was determined by staining splenocytes with PE-conjugated B220 antibody and FITC-conjugated IgM antibody. Flow cytometric analysis of the T-cell population in spleen was determined by staining splenocytes with stained with Pacific Blue-conjugated CD8 antibody and APC-AF750-conjugated CD4 antibody.

and T-cells are more severely affected by *Vprbp* disruption than mature lymphocytes, possibly reflecting the G0 state of naïve, mature T- and B-cells.

We hypothesized that the developmental defect present in T-cells was likely due to a failure of thymocytes to proliferate, rather than a requirement for *Vprbp* in pathways specific to T-cell development (e.g. V(D)J recombination or positive or negative selection). To test for a requirement of *Vprbp* in cell proliferation independent of its role in T-cell development, we stimulated mature T-cell proliferation in vitro and subsequently monitored cell divisions. We isolated mature lymphocytes from tam-treated *Vprbp*$^{F/\Delta}$;*CreERT2*$^{+}$ mice and control *Vprbp*$^{F/+}$;*CreERT2*$^{+}$ and confirmed a decrease in VprBP by immunoblotting (Fig. 4.6A). In addition, we saw no evidence for PARP cleavage, indicative of apoptosis, in mutant lymphocytes suggesting disruption of *Vprbp* did not affect the survival of resting lymphocytes (Fig. 4.6A). In addition, we saw no evidence for apoptosis in mutant lymphocytes, suggesting disruption of *Vprbp* did not affect the survival of resting lymphocytes (Fig. 4.6A). To follow cell divisions, lymphocytes were labeled with CFSE (carboxyfluorescein succinimidyl ester), a fluorescent dye that forms stable adducts on intracellular proteins and provide a quantitative measurement of cell division by using flow cytometry as it is diluted by half following each cell division. T-cell proliferation was activated by anti-CD3 in the presence of anti-CD28 co-stimulation followed by in vitro culture. We collected cells at 42h, 54h, and 66h after stimulation or mock treatment and monitored the proliferation of T-cells by flow cytometry. We found that whereas control cells showed continued, robust proliferation in response to activation, very few mutant T-cells proliferated in response to activation 42h and 54h and less than half had undergone any proliferation at 66h (Fig. 4.6C). These data indicate that *Vprbp* is required for normal T-cell proliferation in response to CD3/CD28 stimulation. In agreement with this observation, the total cell number following T-cell stimulation was decreased in *Vprbp* disrupted primary

Figure 4.6

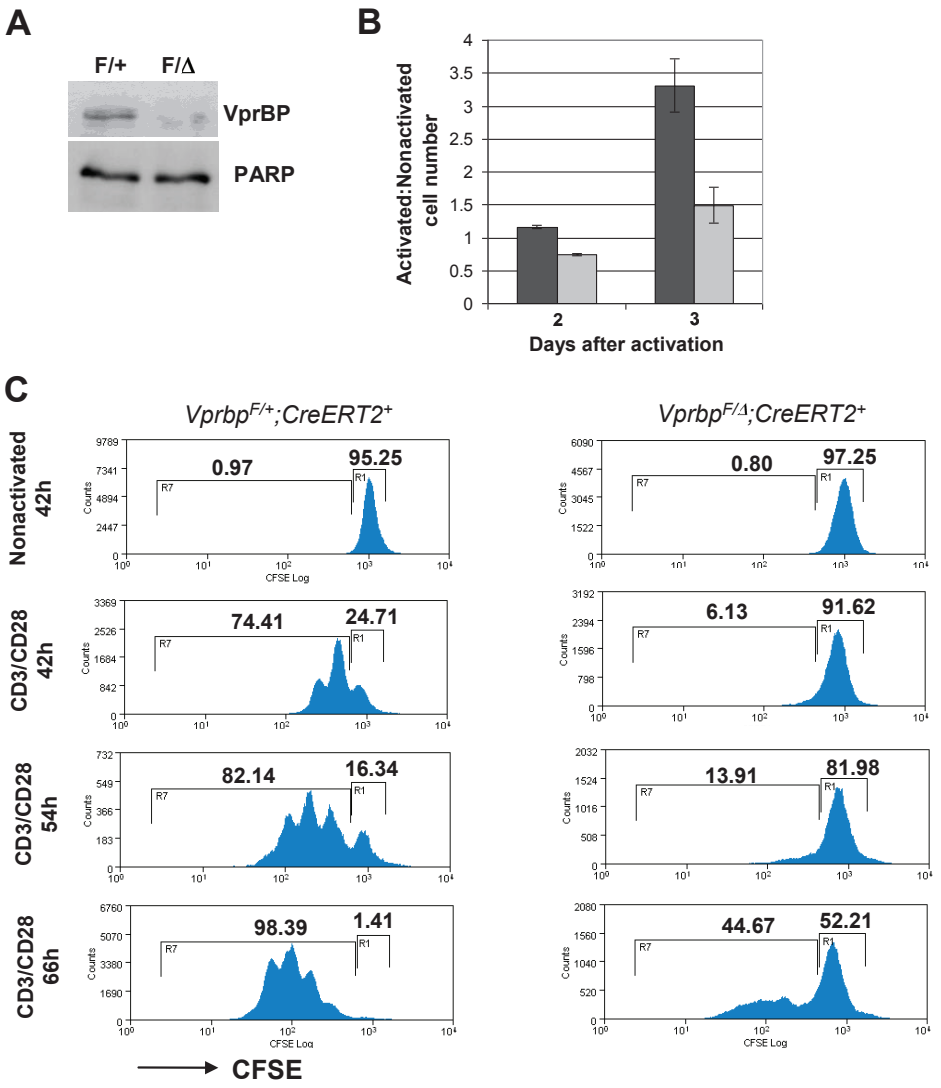

Figure 4.6. *Vprbp* disruption impairs mature T-cell proliferation

(A) Immunoblotting of cell lysates from primary lymphocytes derived from tam-treated *Vprbp*$^{F/+}$*;CreERT2*$^{+}$ and *Vprbp*$^{F/\Delta}$*;CreERT2*$^{+}$ mice 6 days after initial tam-treatment.

(B) T-cells in primary lymphocyte cultures from tam-treated *Vprbp*$^{F/+}$*;CreERT2*$^{+}$ and *Vprbp*$^{F/\Delta}$*;CreERT2*$^{+}$ mice were stimulated with CD3/CD28 or mock treated and plated at equal cell numbers. The total cell number following activation, expressed relative to the number of mock treated cells, is reported at 2 and 3 days after CD3/28 stimulation.

(C) Primary lymphocytes labeled with CFSE, followed by CD3/CD28 stimulation or mock. Cells were cultured in vitro for 42h, 54h, or 66h before collection. Flow cytometric analysis for CFSE was used to determine the proliferation, gated by 7AAD^{-} T-cells.

lymphocytes versus control primary lymphocytes following T-cell activation (Fig. 4.6B). Therefore, we conclude that *Vprbp* is required for the proliferation of mature T-cells and suggest that decreased proliferative capacity may account for the developmental defects observed in B- and T-cells.

Loss of *Ddb1* disrupts B- and T-cell development.

VprBP is thought to function as part of a CRL4 ligase through binding to the linker protein DDB1. We therefore predicted that loss of *Ddb1* should phenocopy *Vprbp* disruption. To test this notion, we induced conditional loss of *Ddb1* using *Ubc-Cre-ERT2* to drive Cre expression in 5-week-old mice and confirmed broad loss of DDB1 in a variety of tissues by immunoblotting (Fig. 4.7A). We found that inducible loss of *Ddb1* typically caused death 5 to 8 days after initial tam injection (data not shown). In addition, we observed a pronounced reduction in thymus size, suggesting that loss of Ddb1 also impacts T-cell development (Fig. 4.7B). We further examined T-cell development following inducible loss of *Ddb1* by CD4/8 staining of thymocytes and found a marked decrease of DP cells (17.9% in mutant thymus versus 71.3% in control) with a concurrent increase in $CD4^+$ and $CD8^+$ cells (Fig. 4.7C), similar to observations in *Vprbp* disrupted thymus. Disruption of *Ddb1* was confirmed by immunoblotting of thymocyte cell lysate for DDB1 (Fig. 4.7C). These results suggest that *Ddb1* is required for normal T-cell development in vivo. Likewise, we observed that B-cell development, as monitored by B220 and IgM surface staining of femur-derived bone marrow cells, was also disrupted following inducible loss of *Ddb1*, with a decrease in pre-/pro-B-cells (14.6% in mutant versus 30.0% in control) and an increase in the population of mature $B220^{hi}IgM^+$ cells (39.4% in mutant versus 23.6% in control; Fig. 4.7D). We interpret these results to indicate that new B-cell development is impaired following *Ddb1* loss, but B-cells which matured prior to tam-treatment survive loss of *Ddb1*. This phenotype,

Figure 4.7

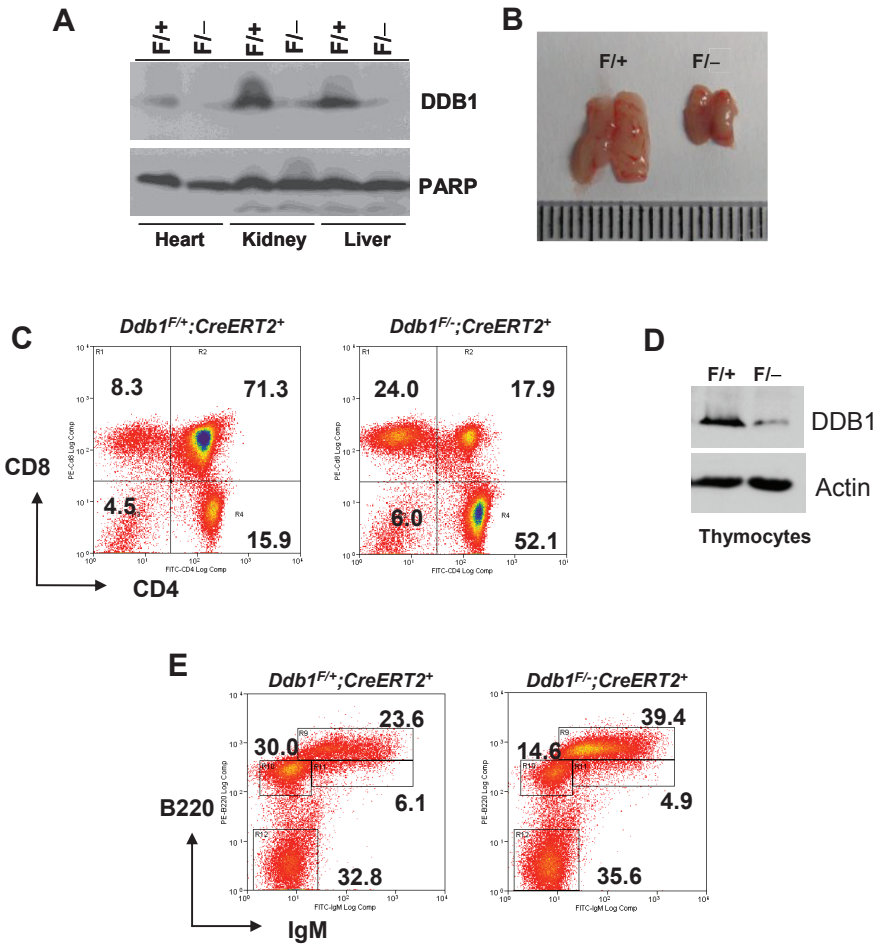

Figure 4.7. Loss of *Ddb1* impairs lymphocyte development.

(A) Tamoxifen administration resulted in loss of DDB1 protein in a broad range of tissues. Tissue lysates from tamoxifen-treated *Ddb1*$^{F/+}$*;CreERT2+* or *Ddb1*$^{F/-}$*;CreERT2*$^{+}$ mice were prepared 6 d after tamoxifen injection, resolved by SDS-PAGE and immunoblotted as indicated.

(B) Gross morphology of thymus in 6-wk-old *Ddb1*$^{F/+}$*;CreERT2*$^{+}$ and *Ddb1*$^{F/-}$*;CreERT2*$^{+}$ mice 6 d after tamoxifen treatment.

(C) Representative flow cytometric analysis of thymocytes from *Ddb1*$^{F/+}$*;CreERT2*$^{+}$ and *Ddb1*$^{F/-}$*;CreERT2*$^{+}$ mice stained with Pacific Blue-conjugated CD8 antibody and APC-AF750-conjugated CD4 antibody.

(D) Immunoblot of cellular lysate of thymocytes in (C).

(E) Representative flow cytometric analysis of bone marrow cells from *Ddb1*$^{F/+}$*;CreERT2*$^{+}$ and *Ddb1*$^{F/-}$*;CreERT2*$^{+}$ mice stained with FITC-conjugated IgM antibody and PE-conjugated B220 antibody.

which largely overlaps with observations following *Vprbp* disruption, provides genetic support for the biochemically established interaction between VprBP and DDB1.

Discussion

In this paper, we provide the first genetic evidence that *Vprbp* is required in adult mice. Using a broadly expressed, tamoxifen-inducible Cre, we showed that disruption of *Vprbp* causes defects in B- and T-cell development and decreased the survival and cell proliferation of thymocytes. Inducible loss of *Vprbp* significantly decreased thymocyte cellularity, nearly completely ablated the $CD4^{+}CD8^{+}$ population of thymocytes, severely disrupted thymic structure, inhibited BrdU incorporation, and increased cleaved caspase 3 staining. Further, we found that *Vprbp* disruption severely inhibited the proliferation of mature T-cells in response to CD3/CD28 stimulation. We suggest that *Vprbp* is broadly required for cell proliferation, and that developmental defects in T-cells reflect a requirement for *Vprbp* in the cell cycle of developing lymphocytes. Supporting this notion, we observed depletion of the absolute number of all stages of thymocytes, but did not observe an accumulation of $Vprbp^{\Delta/\Delta}$ cells at any specific developmental timepoint, a finding that would argue against a specific role for *Vprbp* during thymocyte development. Given that cell proliferation and apoptosis are both critical for proper lymphocyte development and that significant proliferative defects and apoptosis in *Vprbp*-deficient thymus, we further suggest that VprBP plays a role required for *both* cell cycle progression and survival during T-cell development.

We also provide the first genetic evidence supporting the biochemical finding that VprBP is a component of and may functionally depend on the DDB1-mediated E3 ligase. We found that loss of *Ddb1* caused similar defects in thymus as VprBP-deficient thymus. *Ddb1* has previously been established to play an essential role in proliferation, survival, and development in multiple tissue types. Genetic analysis following loss of *Ddb1* in

developing mouse brain or skin both demonstrated that *Ddb1* is essential for proper development and that loss of *Ddb1* induces p53-dependent apoptosis in proliferating cells (Cang et al., 2006; Cang et al., 2007). Further, albumin-Cre driven deletion of *Ddb1* was recently shown to result in obligatory proliferation of DDB1 expressing hepatocytes to replace dying *Ddb1*-deleted cells confirming a function for *Ddb1* in cell survival (Yamaji et al.). Our studies of conditional deletion of *Ddb1* in thymus reveal a new function of *Ddb1* in T-cell proliferation and development and support the notion that CUL4-DDB1 E3 ligase, via interacting with multiple DWD/DCAF proteins, may target ubiquitylation of multiple proteins and play broad functions in vivo.

Our studies also provide a new mechanistic insight regarding Vpr-VprBP interaction. Although not essential for HIV-1 replication in cell culture, the Vpr accessory protein plays an important function for lentivirus pathogenesis as evidenced by its conservation in HIV-1, HIV-2 and SIV viruses and by the attenuated progression of AIDS in rhesus monkeys infected with SIV missing Vpr and the very similar accessory protein Vpx (Gibbs et al., 1995). How Vpr facilitates HIV pathogenesis, however, remains unclear. One consistent effect on host cells upon ectopic expression of Vpr has been its ability to cause G2 cell cycle arrest (Jowett et al., 1995; Rogel et al., 1995). Our finding that the function of VprBP is required for both T-cell proliferation and survival can be reconciled with previous findings by a model that Vpr binds to and activates the function of VprBP to benefit HIV propagation. Given that a G2 cell cycle arrest can only be achieved during active cell proliferation, not in quiescent cells, we speculate that during this activation of VprBP's function to promote cell proliferation, Vpr hijacks $CRL4^{VprBP}$ E3 ligase to degrade a protein(s) which causes G2 arrest.

While we have firmly established a role for *Vprbp* in cellular proliferation in vivo, the underlying molecular mechanism remains obscure. Although the tumor suppressor protein Merlin was initially reported as a substrate for the $CRL4^{VprBP}$ complex (Huang and

Chen, 2008), it was also proposed to function as an upstream inhibitor of VprBP (Li et al., 2010b). At present, neither targeting Merlin for ubiquitylation nor the inhibition of VprBP-mediated E3 ligase(s) by Merlin provides a clear molecular model for the function of VprBP in T cell proliferation and survival. In addition to Merlin, VprBP and DDB1 were identified as components of a novel EDD1 HECT E3 ligase complex that targets Katanin p60, the catalytic subunit of the microtubule-severing AAA ATPase katanin complex, for ubiquitylation (Maddika and Chen, 2009). Katanin has previously been established to play a role in severing microtubles during mitosis (McNally and Thomas, 1998; McNally et al., 2006), and overexpression of katanin p60 is associated with an accumulation of 4N cells and increased phospho-H3 staining, indicative of mitotic defects (Maddika and Chen, 2009). Unfortunately, we were unable to detect accumulation of endogenous katanin p60 following disruption of *Vprbp* due to lack of specificity of the katanin p60 antibody for mouse katanin p60 (data not shown). Inducible disruption of *Vprbp* in MEFs (Fig. 4.1), like reported results following knockdown experiments (Hrecka et al., 2007; McCall et al., 2008), resulted in cell cycle arrest, but was not associated specifically with a G2/M arrest, suggesting that, at a minimum, katanin p60 is not the sole target of VprBP in vivo. Thus, future efforts will focus on the identification of $CRL4^{VprBP}$ substrate(s).

CHAPTER V

CONCLUSIONS AND PERSPECTIVES

Over the course of the last several years, I have extensively focused on the in vivo function of VprBP, and uncovered definitive evidence for a role of *Vprbp* in the proliferation and survival of developing of B- and T-cells in mice. Furthermore, my studies in mouse embryonic fibroblasts correlatively suggest that VprBP may also function in maintaining quiescent cells and contact inhibition. Despite numerous studies of VprBP from many different perspectives (e.g. HIV1 research, association with tumor suppressor Merlin, as well as genetic studies in *Arabidopsis*, *Drosophila* and mice), we still know surprisingly little about the in vivo functions of VprBP. Genetic studies consistently demonstrate a function in early embryonic development, and human cell culture studies consistently indicate a function in cellular proliferation. In addition, VprBP is abundantly expressed throughout the body and is readily detected in CRL4 complexes. We infer that the biochemical mechanism of VprBP is through ubiquitylation of substrate proteins via a CRL4 complex. However, the identity and in vivo function of such substrates remains completely obscure. In this final chapter, I provide a perspective on the key outstanding questions in the field of VprBP research, and conclude by suggesting possible experiments to identify potential substrates and genetically address the in vivo function of *Vprbp*.

Does VprBP have CRL4-independent functions?

Maddika and Chen identified VprBP and DDB1 as components of a novel E3 ligase that uses DYRK2 (a member of evolutionarily conserved dual-specificity tyrosine (Y)-regulated kinases) as a scaffold for the assembly of a HECT E3 complex, indicating that VprBP functions outside of the CRL4 complex (Maddika and Chen, 2009; Jackson and Xiong, 2009b). This finding was particularly unexpected given the central role established for DDB1 as the key adaptor protein for recruiting substrate to CRL4s (He et al., 2006; Higa et al., 2006b; Angers et al., 2006; Jin et al., 2006). The DYRK2-DDB1-

VprBP complex also contained EDD (E3 identified by differential display), a large protein containing multiple domains linked to ubiquitylation, including an N-terminal ubiquitin associated (UBA) domain, a UBR box (a motif important for the targeting of N-end rule substrates) and a C-terminal HECT domain.

Genetic studies in *C. elegans* previously demonstrated the DYRK2 homolog MBK-2 regulates the meiotic protein, MEI-1/katanin, the catalytic subunit of the microtubule-severing AAA ATPase complex (Lu and Mains, 2007). This finding prompted Maddika and Chen to test whether mammalian katanin p60 was a substrate for the DYRK2 E3 complex, referred to as EDVP (EDD–DDB1–VprBP). In vitro binding and in vivo ubiquitylation assays demonstrated that katanin p60 associates with and is polyubiquitylated by the EDVP E3 ligase complex. Further, VprBP was required for association of katanin p60 with other complex subunits. Notably, no CUL4A, CUL4B or ROC1 was detected in the complex. Silencing individual components of EDVP, but not CUL4A and CUL4B, severely impaired katanin polyubiquitylation.

The authors did not, however, investigate a potential role for the WD40 protein katanin p80, the major cellular binding partner for katanin p60 which contains a single WDXR motif. Previous studies of the microtubule severing activity of the katanin complex indicated that the WD40 domain of katanin p80 negatively regulates the enzymatic activity of katanin p60 (McNally et al., 2000). It remains possible that insufficient knockdown of CUL4A/B masked the role of CUL4 and minimally suggests that possible involvement of katanin p80 in a CRL4 complex merits exploration. In my own hands, I have verified that a small percentage of endogenous VprBP can indeed associate with DYRK2 in cultured cells (data not shown), consistent with published results on the EDVP complex. However, I was unable to verify accumulation of endogenous katanin p60 following loss of *Vprbp* in MEFs or VprBP knockdown in cultured cells due to lack of specificity of the katanin p60 antibody. In addition, Maddika

and Chen showed that ectopic expression of katanin caused an increase in cells with 4N DNA content and positive for phopho-histone H3, indicative of mitotic defects (Maddika and Chen, 2009). Depletion of VprBP results in cell cycle arrest, but is not associated specifically with a G2/M arrest, suggesting that katanin p60 is minimally not the sole target of VprBP in vivo. I favor a model whereby the primary functions of VprBP are mediated by CRL4, based in part on the abundant binding of VprBP to CRL4 and CSN components in vivo, and I suggest that involvement in the EDVP complex accounts for a minor portion of VprBP function.

VprBP likely targets a diverse set of substrates

A single CRL complex can target multiple different substrates for ubiquitylation, as has been demonstrated for SCF^{SKP2}, $SCF^{\beta TRCP}$, SCF^{FBW7}, $CRL4^{DDB2}$, and $CRL4^{CDT2}$ (Frescas and Pagano, 2008; Welcker and Clurman, 2008; Jackson and Xiong, 2009a). In the case of $CRL4^{CDT2}$, substrate polyubiquitylation requires binding to PCNA on chromatin and is tightly coupled with DNA replication and/or repair. For example, proper $CRL4^{CDT2}$-mediated destruction of CDT1, p21, *Drosophila* E2f1, and SET8 during S-phase is required for proper cell cycle progression, while UV-induced DNA damage triggers ubiquitylation of CDT1 and p21, to restrict DNA licensing, as well as polymerase η and PCNA to facilitate proper translesion synthesis (Arias and Walter, 2006; Hu and Xiong, 2006; Senga et al., 2006; Abbas et al., 2008; Kim et al., 2008; Nishitani et al., 2008; Shibutani et al., 2008; Abbas et al., 2010; Centore et al. 2010; Jorgensen et al., 2011; Oda et al., 2010; Terai et al., 2010). Thus, it appears that as a whole, degradation of $CRL4^{CDT2}$ substrates facilitates S-phase progression and DNA repair and that substrates may be targeted in a coordinated manner. In contrast, substrates of $SCF^{\beta TRCP1}$ and $SCF^{\beta TRCP2}$ (collectively referred to as $SCF^{\beta TRCP}$) appear to be much more

diverse with functions in distinct pathways resulting in, at times, contradictory effects on the cell cycle. $SCF^{\beta TRCP}$ substrates include IκB (NFκB signaling), WEE1 (CDK1 inhibitor), CDC25 (CDK1 activator), β-catenin (Wnt signaling), REST (neural transcription repressor), PDCD4 (translation inhibitor), claspin (DNA replication/repair) and Pro-casapase 3 (pro-apoptotic protein) (Busino et al., 2003; Dorrello et al., 2006; Peschiaroli et al., 2006; Tan et al., 2006; Tan et al., 1999; Watanabe et al., 2004; Westbrook et al., 2008). While clusters of substrates which function in coordinately regulated pathways emerge (e.g. degradation of CDC25A and claspin at the end of G2), other substrates appear quite unrelated, and would require degradation at distinct time points. The disparate nature of substrates suggests that the regulatory kinases, which function to phosphorylate substrates and thus control substrate binding to βTRCP, play a dominant role in determining the timing of substrate degradation, rather than activation of ubiquitin ligase activity of $SCF^{\beta TRCP}$ itself. Thus $SCF^{\beta TRCP}$ can regulate diverse substrates, as long as these substrates contain the required phospho-degron.

I suggest that $CRL4^{VprBP}$ function is likely more analogous to the $SCF^{\beta TRCP}$ complex, rather than $CRL4^{CDT2}$. I base this on evidence from my own work, including the accumulation of VprBP in quiescent cells (Chapter 3) and a requirement for VprBP in cell proliferation (Chapters 3 and 4), indicating that VprBP may have functions at multiple phases of the cell cycle and may play apparently contradictory roles in promoting proliferation and maintaining quiescence. Furthermore, VprBP is quite abundantly detected in virtually all adult mouse tissues, both in proliferative tissues such as intestine and bone marrow and in largely post-mitotic tissues including adult kidney, liver and brain. While this is correlative evidence, expression patterns suggest multiple functions for VprBP in a wide variety of tissues. Furthermore, VprBP has been identified in protein complexes with binding partners of diverse and seemingly unrelated function such as

Merlin, LGL1/2, and DYRK2 (Huang and Chen, 2008;Tamori et al., 2010; Maddika and Chen, 2009). Because my model is that VprBP largely functions as part of a CRL4 complex, I suggest that $CRL4^{VprBP}$ targets multiple proteins of diverse functions for degradation.

Identification of bona fide $CRL4^{VprBP}$ substrates

Perhaps the greatest limitation for understanding the function of VprBP is the lack of validated $CRL4^{VprBP}$ substrates. The Xiong lab has pursued several different avenues to identify substrate proteins including yeast two hybrid and mass spectrometry to identify co-immunoprecipitated proteins of the endogenous VprBP complex. Unfortunately, VprBP was auto-reactive in the yeast two hybrid assay. Further, no novel VprBP-interacting proteins were identified in two separate mass spectrometry experiments examining the endogenous complex; only DDB1, CUL4A/B and CSN subunits were identified. Because the sensitivity of mass spectrometry has increased significantly since the previous experiments in 2004 and 2007, we recently renewed efforts to identify VprBP substrates by TAP-purification of the VprBP complex. This work is being directed by Dr. Tadashi Nakagawa, a post-doctoral researcher in the lab, who has purified the full-length VprBP construct, a mutant containing disrupted WDXR motifs, and a mutant lacking the C-terminal 598 amino acids ($VprBP^{N909}$). Preliminary results from these TAP experiment found a much larger number of proteins associated in these complexes than were uncovered in our previous mass spectrometry experiments. However, a number of published VprBP-binding proteins were not detected in the complex including Merlin, DYRK2, LGL1 and LGL2. We have already validated Merlin and DYRK2 binding with VprBP by co-immunoprecipitation experiments, indicating that mass spectrometry of the TAP-VprBP complex is still missing known interactions. Furthermore, a survey of the literature finds relatively few examples where a substrate

has been identified by mass spectrometry of the E3 ubiquitin ligase complex (D'Angiolella et al., 2010); rather the vast majority of E3-substrate interactions are identified by mass spectrometry of the substrate complex. I suspect this limitation has to do with the very transient nature of the interaction between E3 and substrate which greatly impairs attempts to co-purify substrate and ligase. We hope that mutations which disrupt binding between DDB1 and VprBP (such as $VprBP^{N909}$ and $VprBP^{WDXA}$) will effectively trap VprBP-substrate interactions. In addition to mass spectrometry-based approaches, future efforts could utilize an RNAi-based screen to search for proteins whose co-depletion rescues the cellular defects of loss of *Vprbp* (e.g. apoptosis and inhibition of cellular proliferation).

An alternative hypothesis for VprBP function is that VprBP is not a substrate receptor for CRL4, but rather functions as an inhibitor of the complex, thus explaining why no substrates for VprBP have been discovered. VprBP does appear to be unique among DWD proteins in that it is one of the largest DDB1-associated proteins and one of the most abundant, with stochiometric levels DDB1 in the VprBP immunocomplex. Could the function of VprBP be to regulate access of other DWD proteins to CUL4-DDB1? This model is indeed quite possible, though my prediction is that VprBP does function as a substrate receptor based on two lines of evidence: (1) The VprBP compex has been demonstrated by several groups to have ubiquitin ligase activity in vitro and in in vivo (Huang and Chen, 2008, Li et al., 2010), and (2) Viral proteins Vpr and Vpx have clearly been demonstrated to hijack the complex to polyubiquitylate UNG2 and SAMHD1, respectively (Ahn et al. 2010, Hrecka et al. 2011). While several ubiquitin ligases have been reported to be hijacked by viral proteins (discussed in Chapter 1), to the best of my knowledge, no viral protein has been established to convert a ubiquitin ligase inhibitor into a substrate receptor. I suggest that VprBP does indeed function as a substrate receptor and that current experimental approaches, including mass

spectrometric analysis of the VprBP complex, have simply not yet identified the targeted substrate(s).

Another approach that has effectively identified CRL substrates is through genetic analysis of phenotypes. For example, depletion of CUL4 or DDB1 in *C. Elegans* resulted in a massive re-replication phenotype that led to the identification of CDT1 targeting by CRL4 (Zhong et al., 2003). For this approach to be effective, a phenotype needs to be associated with the accumulation of a dominant substrate in vivo. We had hoped that the genetic studies I initiated would provide phenotypic clues to the identity of a $CRL4^{VprBP}$ substrate. However, our observations in the developing immune system are largely consistent with cellular phenotypes observed following VprBP knockdown in cultured cells and did not provide a significant breakthrough in substrate identification. Clearly, a single genetic study is insufficient to fully investigate the diverse in vivo functions of a pleiotropic gene such a *Vprbp*. Because VprBP likely targets multiple, varied substrates, we may find that loss of *Vprbp* in mice in a highly proliferative tissue such as the hematopoietic system yields a distinct phenotype from loss of *Vprbp* in brain, a largely post-mitotic tissue with high levels of *Vprbp* expression in adult animals. I would predict that loss of *Vprbp* in proliferative tissues results in defects in DNA replication/repair or mitogenic signaling, whereas in brain, katanin p60, which has microtubule-severing functions associated with axon formation, may be more significant. Thus, a thorough understanding of *Vprbp* in mice ultimately cannot be addressed by one genetic study, but will require examination of several different systems. I suggest here two lines of research which could be conducted to address the function of murine *Vprbp* in vivo.

Future Genetic Studies

Vprbp in hematopoiesis. The data I presented in Chapter 4 provided solid evidence that *Vprbp* functions in the development of lymphocytes, and suggest perhaps a broader role in hematopoiesis. Therefore, I suggest here experiments to examine the function of VprBP in hematopoiesis. Ubc-CreERT2 is an appropriate driver for Cre expression because it is apparently quite well expressed in hematopoietic lineages (Ruzankina et al., 2007, Lum et al., 2007, Maillard et al., 2009, Thiel et al., 2010, Rahman, 2011 #2272) .

To test for a role for VprBP in hematopoiesis, I would recommend modifying the genetic system I used by crossing conditional *Vprbp* mice with a reporter strain that express YFP following Cre-mediated excision, which are readily available from Jackson labs (Stock No. 006148). This would significantly improve the existing system by allowing identification by flow cytometry or immunohistochemistry of individual cells which have been disrupted by Cre. By specifically examining cells with active Cre (out of a mosaic population), this system would avoid diluting phenotypic effects that result from analyzing total tissue. Furthermore, once individual mutant cells could be identified, the dose of tamoxifen administered could be reduced thereby decreasing tam-associated toxicity, as well as lessening the severity of phenotypes due to disruption of *Vprbp* in other tissues.

Our current model posits that VprBP is generally required for cell proliferation. If so, I would predict that disruption of *Vprbp* would prevent proliferation in myeloid lineage, in addition to lymphoid lineages. To test this model, the proliferative capacity of myeloid cells, such as neutrophils should be examined. Neutrophil granulocytes, which are an essential component of the innate immune systems, have a notably short half-life (2-5 days or less) and undergo constant generation in the bone marrow (Barreda et al., 2004). To test if *Vprbp* is required for neutrophil proliferation in bone marrow, I would

identify *Vprbp* disrupted neutrophils (YFP+, Gr-1+, Mac1+ cells) following BrdU injection and determine if *Vprbp* disruption impairs neutrophil cell division by flow analysis. I would predict that analyzing YFP^+, *Vprbp* disrupted neutrophils after acute gene disruption (1-2 weeks following tam treatment) would demonstrate that these cells fail to incorporate BrdU and show increased apoptosis. Further, I predict that mice analyzed at later timepoints (greater than one month following tam) would show a lack of *Vprbp* disrupted Gr-1+ Mac1+ cells due to selection pressure to retain an intact *Vprbp* locus.

The predicted results for the neutrophil experiments would be consistent with my observations in B- and T-cell lineages. It's important to experimentally test this prediction, however, as results in *Drosophila* suggest that *Vprbp* is not required for proliferation, per se. In addition, in my own experiments in 2-week-old mice, I did not see a change in BrdU incorporation in kidney, despite near complete absence of VprBP protein in the tissue (data not shown). Thus, if neutrophil proliferation is not affected by *Vprbp* disruption, this finding would suggest that *Vprbp* is specifically required for proliferation of lymphoid lineages in adult mice and indicate that we should examine a role in lymphocyte-specific processes such as T-cell receptor and B-cell receptor signaling. In contrast, a function for *Vprbp* in both myeloid and lymphoid lineages would suggest a broader function in hematopoesis. In that case, I would recommend specifically examining upstream progenitor and stem cell populations.

Hematopoietic stem cells (HSCs), which give rise to both myeloid and lymphoid lineages and have the capacity for self-renewal, primarily reside in bone marrow (Kawamoto and Katsura, 2009). To test if disruption of *Vprbp* more broadly affects hematopoesis by preventing HSC proliferation, I would examine the HSC population in bone marrow by $Lin^- Kit^+ Sca^+$ staining (negative for lineage specific markers, positive for c-kit and Sca-1). I predict there would be increased apoptosis and lack of proliferation in YFP^+, *Vprbp* disrupted HSCs. To definitively prove a requirement for *Vprbp* in HSC

proliferation and differentiation, a reconstitution experiment, in which YFP^{+}, *Vprbp* disrupted HSCs are transplanted into irradiated recipient mice, should be conducted. Further, a parallel analysis of $Vprbp^{F/F};VavCre^{+}$ mice should be conducted to rigorously show a role for *Vprbp* during hematopoeisis in embryonic mice.

Once the cell populations which exhibit proliferation defects are identified, the molecular mechanisms which underlie the failure to proliferate could be addressed using the $CreERT2^{+}$ system. For example, we observe that loss of VprBP is associated with a complete loss RAC activity in cultured cells (Tadashi Nakagawa, personal communication). In addition, previous genetic studies have established that loss of *Rac1* and *Rac2* causes a partial block of T-cell development at the $CD4^{-}CD8^{-}$ stage (Dumont et al., 2009; Guo et al., 2008), largely consistent with the phenotypes I observed following disruption of *Vprbp*. By sorting for YFP^{+} cells (e.g. thymocytes), it could be determined if acute *Vprbp* disruption causes loss of GTP bound RAC in vivo. Further, viral expression of a constitutively active form of RAC (L61RAC-1) in *Vprbp* disrupted mature T-cells could be tested for rescue of cell proliferation defects in vitro following T-cell activation.

While it remains to be seen if RAC-dependent signaling accounts for the major proliferation defect in *Vprbp* disrupted mice, the ability to isolate *Vprbp* disrupted cell from a mosaic population would significantly improve our ability to determine the molecular mechanisms underling the phenotypes observed following *Vprbp* disruption. The hematopoietic system is an attractive system to functionally examine potential substrates or molecular pathways of VprBP because of the plethora of established cell markers to monitor each developmental stage, the relative ease of isolating hematopoietic cells, and the ability to conduct rescue experiments using in vitro culture systems.

Vprbp in the Hippo pathway. The Hippo signal transduction pathway is an evolutionarily conserved pathway that constrains organ size during development and promotes cell contact inhibition (Saucedo and Edgar, 2007). The Hippo pathway was first discovered in *Drosophila*; mutations in the key pathway kinases Hippo (homologous to mammalian MST1/2) and Warts (homologous to mammalian LATS1/2) were noted to cause significant overgrowth of epithelial tissue (Harvey et al., 2003; Wu et al., 2003) (Fig. 5.1). The Hippo kinase cascade results in phosphorylation and nuclear exclusion of the transcription factor Yorkie (homologous to mammalian YAP) (Huang et al., 2005). A putative function for VprBP in the Hippo pathway is indicated by its binding with Merlin, which has been suggested to transmit signals from membrane receptors to Hippo in *Drosophila* (Hamaratoglu et al., 2006). In addition, VprBP has been noted to bind with *Drosophila* Lgl (lethal giant larvae), which is also linked to the Hippo pathway and appears to genetically function as an inhibitor to Hippo activity (Parsons et al., 2010; Tamori et al., 2010). In mammalian cells, all of the components of Hippo signaling are conserved, though the mammalian pathway appears more complicated and to vary depending on the context studied (Zhao et al., 2009). Further, the role of Merlin in the mammalian Hippo pathway is less clearly defined and somewhat contentious (Benhamouche et al., 2010; Zhang et al., 2010). In this section, I propose genetic experiments to determine if VprBP regulates the mammalian Hippo pathway.

The best studied genetic system for examining the mammalian Hippo pathway is mouse liver. Several groups have taken advantage of liver specific deletion of Hippo

Figure 5.1

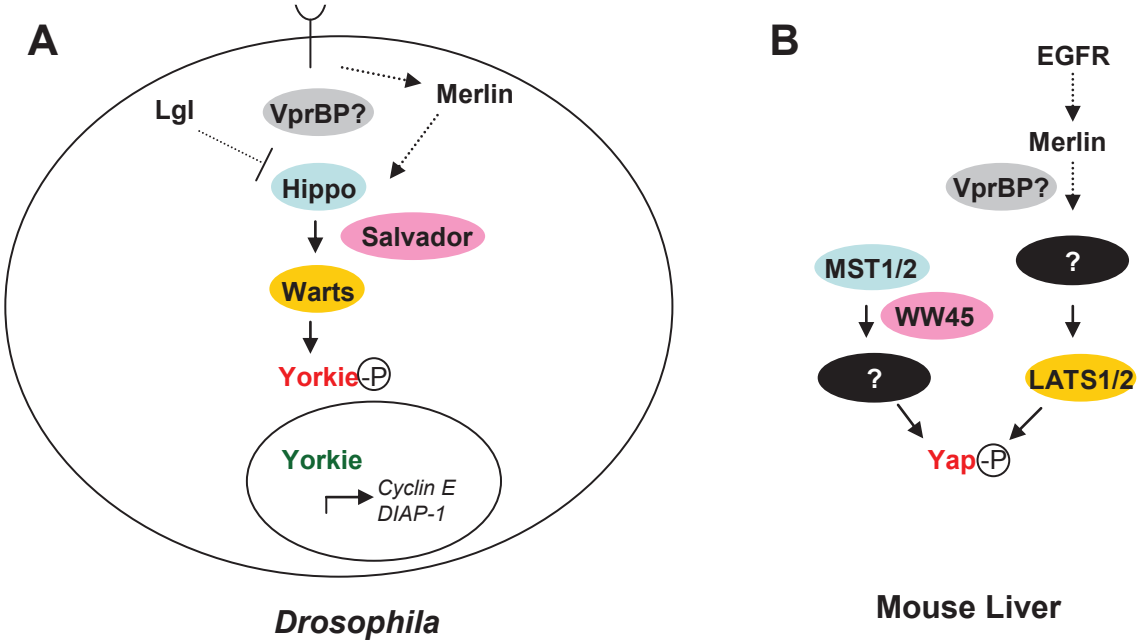

Figure 5.1. Model for the Hippo Pathway.

(A) In *Drosophila*, genetic evidence indicates that the kinases Hippo and Warts regulate size control by inhibiting the transcription factor Yorkie, which is excluded from the nucleus when phosphorylated. Merlin may function upstream of Hippo, potentially by mediating signals from membrane receptors. Lgl, a known regulator of cell polarity, is proposed to inhibit the Hippo pathway. VprBP has been found in separate studies to bind Merlin and to bind Lgl. Overexpression of VprBP or constitutively active Yorkie can both rescue loss of *Lgl* in mosaic tissue analysis.

(B) In mouse liver, the homologs of Hippo, MST1 and MST2 function to promote YAP1 phosphorylation in a LATS1/2-independent manner (LATS1/2 are homologous to Warts; YAP1 is homologous to Yorkie). Based on cell fractionation experiments, a YAP1 kinase downstream of MST1/2 is proposed to exist. LATS1/2 phosphorylates YAP1 in a parallel pathway which requires an activating phosphorylation on LATS1/2 by an unknown upstream kinase. Loss of Merlin reduces LATS1/2 phosphorylation, and can be rescued by heterozygosity for *Yap1* or by EGFR inhibitors. I suggest experiments to test if VprBP inhibits Hippo signaling.

components including *Mst1/2* double knockout, *Ww45* (homologous to Salvador) and *Nf2* (which encodes Merlin) (Lee et al., 2010b; Zhang et al., 2010; Zhou et al., 2009). In all three cases, gene deletion resulted in liver enlargement, oval cell expansion, and eventually led to hepatocellular carcinoma. Further, transgenic expression of *Yap1* in liver likewise increased liver size and eventually promoted hepatocellular carcinoma (Camargo et al., 2007; Dong et al., 2007). Despite several phenotypic similarities, there are some key differences in how gene deletion impacts the Hippo pathway: loss of *Mst1/2* led to a complete loss of phosphorylated YAP1, whereas loss of Merlin only partially reduced the amount of phosphorylated YAP1 (Zhang et al., 2010; Zhou et al., 2009). Further, loss of *Mst1/2* did not change the phosphorylation of LATS1/2, which suggests that LATS1/2 is not required for MST1/2 signaling in liver (Zhou et al., 2009). In contrast, loss of Merlin reduced LATS1/2 phosphorylation, but not MST1/2, indicating that Merlin possibly functions upstream of YAP1 via LATS rather than MST1/2.

To examine a role for *Vprbp* in repressing Hippo signaling, I would generate $Vprbp^{F/F}$; $Albumin\text{-}Cre^{+}$ mice to induce disruption of *Vprbp* in liver. If *Vprbp* is indeed an inhibitor of the Hippo pathway, I would predict constitutive inhibition of YAP1 as well as reduced liver size and increased hepatocyte apoptosis. Indeed, loss of *Yap1* in liver was shown to cause increased apoptosis, increased proliferation (apparently to replace dying cells), and a failure to form functional bile ducts (Zhang et al., 2010).

I would expect *Vprbp* disruption to result in similar phenotypes, if its major function is in regulating the mammalian Hippo pathway. Liver to body weight ratio should be closely monitored and cytokeratin staining of liver tissue should be conducted to examine the formation of bile ducts. Most importantly, YAP1 protein should be examined by both western blot and immunohistochemistry to determine if changes to YAP1 levels, phosphorylation or localization occur in *Vprbp* disrupted livers. The levels of phosphorylated MST1/2 and LATS1/2 should likewise be examined to determine

through which signaling pathway *Vprbp* functions. If indeed analysis of *Vprbp*$^{F/F}$; *Albumin-Cre*$^{+}$ mice indicates that VprBP is a critical regulator of Hippo in mice, then overexpression of a S112A mutant of YAP1 (which cannot be phosphorylated and is therefore constitutively active) should rescue proliferation or cell death phenotypes in primary *Vprbp* disrupted hepatocytes.

These experiments would definitively indicate if VprBP is a regulator of mammalian Hippo signaling, but would not reveal if this effect was due to its putative interaction with Merlin or LGL1/2. To test this possibility, I would turn to primary hepatocyte cell culture to examine the role of Merlin in the *Vprbp* disrupted phenotype. The Merlin binding domain of VprBP has been mapped to residues 1311-1507 of VprBP. I would test if lentiviral expression of VprBP$^{\Delta C}$ can rescue disruption of *Vprbp* by examining apoptosis, proliferation and YAP1 localization in cultured hepatocytes. Rescue of *Vprbp* disruption by VprBP$^{\Delta C}$ expression would indicate that Merlin interaction does not mediate the effect of VprBP in the Hippo pathway. In that case, I would instead focus on the role of VprBP-LGL interaction in controlling Hippo signaling.

A possible caveat of these suggested experiments to genetically address *Vprbp* function in Hippo signaling is the possibility that pleiotropic phenotypes might mask the role of VprBP in this pathway. If indeed *Vprbp* does have multiple, critical functions in most tissues, as is the case for *Ddb1*, pleiotrophic effects will be a complication in any genetic study. Further genetic studies will still be invaluable for experimentally determining the in vivo function, but may not provide a crystal clear view of the underlying molecular mechanism. In addition to thorough biochemical studies, the generation of knock-in mice with mutations that abrogate specific VprBP functions, but do not destroy the entire protein, may someday provide a more precise picture of the precise in vivo functions of *Vprbp*. Ultimately, multi-pronged efforts combining

biochemical, molecular, and genetic approaches will be needed to fully uncover the function and mechanism of VprBP.

REFERENCES

Abbas, T., Shibata, E., Park, J., Jha, S., Karnani, N., and Dutta, A. (2010). CRL4(Cdt2) regulates cell proliferation and histone gene expression by targeting PR-Set7/Set8 for degradation. Mol Cell *40*, 9-21.

Abbas, T., Sivaprasad, U., Terai, K., Amador, V., Pagano, M., and Dutta, A. (2008). PCNA-dependent regulation of p21 ubiquitylation and degradation via the CRL4Cdt2 ubiquitin ligase complex. Genes Dev *22*, 2496-2506.

Ahn, J., Novince, Z., Concel, J., Byeon, C.H., Makhov, A.M., Byeon, I.J., Zhang, P., and Gronenborn, A.M. (2011). The Cullin-RING E3 ubiquitin ligase CRL4-DCAF1 complex dimerizes via a short helical region in DCAF1. Biochemistry *50*, 1359-1367.

Ahn, J., Vu, T., Novince, Z., Guerrero-Santoro, J., Rapic-Otrin, V., and Gronenborn, A.M. (2010). HIV-1 Vpr loads uracil DNA glycosylase-2 onto DCAF1, a substrate recognition subunit of a cullin 4A-ring E3 ubiquitin ligase for proteasome-dependent degradation. J Biol Chem *285*, 37333-37341.

Al Khateeb, W.M., and Schroeder, D.F. (2009). Overexpression of Arabidopsis damaged DNA binding protein 1A (DDB1A) enhances UV tolerance. Plant Molecular Biology *70*, 371-383.

Alekseev, S., Kool, H., Rebel, H., Fousteri, M., Moser, J., Backendorf, C., de Gruijl, F.R., Vrieling, H., and Mullenders, L.H. (2005). Enhanced DDB2 expression protects mice from carcinogenic effects of chronic UV-B irradiation. Cancer Res *65*, 10298-10306.

Andrejeva, J., Poole, E., Young, D.F., Goodbourn, S., and Randall, R.E. (2002). The p127 subunit (DDB1) of the UV-DNA damage repair binding protein is essential for the targeted degradation of STAT1 by the V protein of the paramyxovirus simian virus 5. J Virol *76*, 11379-11386.

Angers, S., Li, T., Yi, X., MacCoss, M.J., Moon, R.T., and Zheng, N. (2006). Molecular architecture and assembly of the DDB1-CUL4A ubiquitin ligase machinery. Nature *443*, 590-593.

Arias, E.E., and Walter, J.C. (2005). Replication-dependent destruction of Cdt1 limits DNA replication to a single round per cell cycle in Xenopus egg extracts. Genes Dev *19*, 114-126.

Arias, E.E., and Walter, J.C. (2006). PCNA functions as a molecular platform to trigger Cdt1 destruction and prevent re-replication. Nat Cell Biol *8*, 84-90.

Bai, C., Sen, P., Hofmann, K., Ma, L., Goebl, M., Harper, J.W., and Elledge, S.J. (1996). SKP1 connects cell cycle regulators to the ubiquitin proteolysis machinery through a novel motif, the F-box. Cell *86*, 263-274.

Barreda, D.R., Hanington, P.C., and Belosevic, M. (2004). Regulation of myeloid development and function by colony stimulating factors. Developmental and Comparative Immunology *28*, 509-554.

Belzile, J.P., Abrahamyan, L.G., Gerard, F.C., Rougeau, N., and Cohen, E.A. (2010). Formation of mobile chromatin-associated nuclear foci containing HIV-1 Vpr and VPRBP is critical for the induction of G2 cell cycle arrest. PLoS Pathog *6*, e1001080.

Belzile, J.P., Duisit, G., Rougeau, N., Mercier, J., Finzi, A., and Cohen, E.A. (2007). HIV-1 Vpr-Mediated G2 Arrest Involves the DDB1-CUL4A(VPRBP) E3 Ubiquitin Ligase. PLoS Pathog *3*, e85.

Benhamouche, S., Curto, M., Saotome, I., Gladden, A.B., Liu, C.H., Giovannini, M., and McClatchey, A.I. (2010). Nf2/Merlin controls progenitor homeostasis and tumorigenesis in the liver. Genes Dev *24*, 1718-1730.

Bergink, S., Salomons, F.A., Hoogstraten, D., Groothuis, T.A., de Waard, H., Wu, J., Yuan, L., Citterio, E., Houtsmuller, A.B., Neefjes, J.*, et al.* (2006). DNA damage triggers nucleotide excision repair-dependent monoubiquitylation of histone H2A. Genes Dev *20*, 1343-1352.

Bernhardt, A., Lechner, E., Hano, P., Schade, V., Dieterle, M., Anders, M., Dubin, M.J., Benvenuto, G., Bowler, C., Genschik, P.*, et al.* (2006). CUL4 associates with DDB1 and DET1 and its downregulation affects diverse aspects of development in Arabidopsis thaliana. Plant J *47*, 591-603.

Bhaumik, S.R., Smith, E., and Shilatifard, A. (2007). Covalent modifications of histones during development and disease pathogenesis. Nat Struct Mol Biol *14*, 1008-1016.

Bondar, T., Ponomarev, A., and Raychaudhuri, P. (2004). Ddb1 is required for the proteolysis of the Schizosaccharomyces pombe replication inhibitor Spd1 during S phase and after DNA damage. J Biol Chem *279*, 9937-9943.

Bosu, D.R., Feng, H., Min, K., Kim, Y., Wallenfang, M.R., and Kipreos, E.T. (2010). C. elegans CAND-1 regulates cullin neddylation, cell proliferation and morphogenesis in specific tissues. Developmental Biology *346*, 113-126.

Braun, S., Garcia, J.F., Rowley, M., Rougemaille, M., Shankar, S., and Madhani, H.D. (2011). The Cul4-Ddb1(Cdt)(2) ubiquitin ligase inhibits invasion of a boundary-associated antisilencing factor into heterochromatin. Cell *144*, 41-54.

Busino, L., Donzelli, M., Chiesa, M., Guardavaccaro, D., Ganoth, D., Dorrello, N.V., Hershko, A., Pagano, M., and Draetta, G.F. (2003). Degradation of Cdc25A by beta-TrCP during S phase and in response to DNA damage. Nature *426*, 87-91.

Camargo, F.D., Gokhale, S., Johnnidis, J.B., Fu, D., Bell, G.W., Jaenisch, R., and Brummelkamp, T.R. (2007). YAP1 increases organ size and expands undifferentiated progenitor cells. Curr Biol *17*, 2054-2060.

Cang, Y., Zhang, J., Nicholas, S.A., Bastien, J., Li, B., Zhou, P., and Goff, S.P. (2006). Deletion of DDB1 in mouse brain and lens leads to p53-dependent elimination of proliferating cells. Cell *127*, 929-940.

Cang, Y., Zhang, J., Nicholas, S.A., Kim, A.L., Zhou, P., and Goff, S.P. (2007). DDB1 is essential for genomic stability in developing epidermis. Proc Natl Acad Sci U S A *104*, 2733-2737.

Cao, R., Tsukada, Y., and Zhang, Y. (2005). Role of Bmi-1 and Ring1A in H2A ubiquitylation and Hox gene silencing. Mol Cell *20*, 845-854.

Carpenter, A.C., and Bosselut, R. (2010). Decision checkpoints in the thymus. Nature Immunology *11*, 666-673.

Centore, R.C., Havens, C.G., Manning, A.L., Li, J.M., Flynn, R.L., Tse, A., Jin, J., Dyson, N.J., Walter, J.C., and Zou, L. (2010). CRL4(Cdt2)-mediated destruction of the histone methyltransferase Set8 prevents premature chromatin compaction in S phase. Mol Cell *40*, 22-33.

Chau, H., Wong, V., Chen, N.J., Huang, H.L., Lin, W.J., Mirtsos, C., Elford, A.R., Bonnard, M., Wakeham, A., You-Ten, A.I.*, et al.* (2005). Cellular FLICE-inhibitory protein is required for T cell survival and cycling. The Journal of Experimental Medicine *202*, 405-413.

Chen, H., Shen, Y., Tang, X., Yu, L., Wang, J., Guo, L., Zhang, Y., Zhang, H., Feng, S., Strickland, E.*, et al.* (2006). Arabidopsis CULLIN4 Forms an E3 Ubiquitin Ligase with RBX1 and the CDD Complex in Mediating Light Control of Development. Plant Cell *18*, 1991-2004.

Chen, X., Zhang, Y., Douglas, L., and Zhou, P. (2001). UV-damaged DNA-binding Proteins Are Targets of CUL-4A-mediated Ubiquitination and Degradation. J Biol Chem *276*, 48175-48182.

Chew, E.H., Poobalasingam, T., Hawkey, C.J., and Hagen, T. (2007). Characterization of cullin-based E3 ubiquitin ligases in intact mammalian cells--evidence for cullin dimerization. Cell Signal *19*, 1071-1080.

Choe, K.P., Przybysz, A.J., and Strange, K. (2009). The WD40 repeat protein WDR-23 functions with the CUL4/DDB1 ubiquitin ligase to regulate nuclear abundance and activity of SKN-1 in Caenorhabditis elegans. Mol Cell Biol *29*, 2704-2715.

Choi, S.H., Wright, J.B., Gerber, S.A., and Cole, M.D. (2010). Myc protein is stabilized by suppression of a novel E3 ligase complex in cancer cells. Genes Dev *24*, 1236-1241.

Clark, S.H., and Chovnick, A. (1986). Studies of normal and position-affected expression of rosy region genes in Drosophila melanogaster. Genetics *114*, 819-840.

Cook, J.G., Chasse, D.A., and Nevins, J.R. (2004). The regulated association of Cdt1 with minichromosome maintenance proteins and Cdc6 in mammalian cells. J Biol Chem *279*, 9625-9633.

Cooper, A.B., Sawai, C.M., Sicinska, E., Powers, S.E., Sicinski, P., Clark, M.R., and Aifantis, I. (2006). A unique function for cyclin D3 in early B cell development. Nature Immunology *7*, 489-497.

Cope, G.A., and Deshaies, R.J. (2003). COP9 signalosome: a multifunctional regulator of SCF and other cullin-based ubiquitin ligases. Cell *114*, 663-671.

Cope, G.A., and Deshaies, R.J. (2006). Targeted silencing of Jab1/Csn5 in human cells downregulates SCF activity through reduction of F-box protein levels. BMC biochemistry *7*, 1.

Cox, B.J., Vollmer, M., Tamplin, O., Lu, M., Biechele, S., Gertsenstein, M., van Campenhout, C., Floss, T., Kuhn, R., Wurst, W.*, et al.* (2010). Phenotypic annotation of the mouse X chromosome. Genome Research *20*, 1154-1164.

D'Angiolella, V., Donato, V., Vijayakumar, S., Saraf, A., Florens, L., Washburn, M.P., Dynlacht, B., and Pagano, M. (2010). SCF(Cyclin F) controls centrosome homeostasis and mitotic fidelity through CP110 degradation. Nature *466*, 138-142.

DeHart, J.L., Zimmerman, E.S., Ardon, O., Monteiro-Filho, C.M., Arganaraz, E.R., and Planelles, V. (2007). HIV-1 Vpr activates the G2 checkpoint through manipulation of the ubiquitin proteasome system. Virol J *4*, 57.

del Mar Lorente, M., Marcos-Gutierrez, C., Perez, C., Schoorlemmer, J., Ramirez, A., Magin, T., and Vidal, M. (2000). Loss- and gain-of-function mutations show a polycomb group function for Ring1A in mice. Development *127*, 5093-5100.

Dong, J., Feldmann, G., Huang, J., Wu, S., Zhang, N., Comerford, S.A., Gayyed, M.F., Anders, R.A., Maitra, A., and Pan, D. (2007). Elucidation of a universal size-control mechanism in Drosophila and mammals. Cell *130*, 1120-1133.

Dorrello, N.V., Peschiaroli, A., Guardavaccaro, D., Colburn, N.H., Sherman, N.E., and Pagano, M. (2006). S6K1- and betaTRCP-mediated degradation of PDCD4 promotes protein translation and cell growth. Science *314*, 467-471.

Dumont, C., Corsoni-Tadrzak, A., Ruf, S., de Boer, J., Williams, A., Turner, M., Kioussis, D., and Tybulewicz, V.L. (2009). Rac GTPases play critical roles in early T-cell development. Blood *113*, 3990-3998.

El-Mahdy, M.A., Zhu, Q., Wang, Q.E., Wani, G., Praetorius-Ibba, M., and Wani, A.A. (2006). Cullin 4A-mediated proteolysis of DDB2 protein at DNA damage sites regulates in vivo lesion recognition by XPC. J Biol Chem *281*, 13404-13411.

Feil, S., Valtcheva, N., and Feil, R. (2009). Inducible Cre mice. Methods in Molecular Biology *530*, 343-363.

Fleming, A.B., Kao, C.F., Hillyer, C., Pikaart, M., and Osley, M.A. (2008). H2B ubiquitylation plays a role in nucleosome dynamics during transcription elongation. Mol Cell *31*, 57-66.

Freemont, P.S. (2000). RING for destruction? Curr Biol *10*, R84-87.

Frescas, D., and Pagano, M. (2008). Deregulated proteolysis by the F-box proteins SKP2 and beta-TrCP: tipping the scales of cancer. Nature Reviews *8*, 438-449.

Fukumoto, Y., Dohmae, N., and Hanaoka, F. (2008). Schizosaccharomyces pombe Ddb1 recruits substrate-specific adaptor proteins through a novel protein motif, the DDB-box. Mol Cell Biol *28*, 6746-6756.

Furukawa, M., He, Y.J., Borchers, C., and Xiong, Y. (2003). Targeting of protein ubiquitination by BTB-Cullin 3-Roc1 ubiquitin ligases. Nat Cell Biol *5*, 1001-11007.

Galan, J.M., and Peter, M. (1999). Ubiquitin-dependent degradation of multiple F-box proteins by an autocatalytic mechanism. Proc Natl Acad Sci U S A *96*, 9124-9129.

Geyer, R., Wee, S., Anderson, S., Yates, J., and Wolf, D.A. (2003). BTB/POZ domain proteins are putative substrate adaptors for cullin 3 ubiquitin ligases. Mol Cell *12*, 783-790.

Gibbs, J.S., Lackner, A.A., Lang, S.M., Simon, M.A., Sehgal, P.K., Daniel, M.D., and Desrosiers, R.C. (1995). Progression to AIDS in the absence of a gene for vpr or vpx. J Virol *69*, 2378-2383.

Goldenberg, S.J., Cascio, T.C., Shumway, S.D., Garbutt, K.C., Liu, J., Xiong, Y., and Zheng, N. (2004). Structure of the Cand1-Cul1-Roc1 complex reveals regulatory mechanisms for the assembly of the multisubunit cullin-dependent ubiquitin ligases. Cell *119*, 517-528.

Gong, L., and Yeh, E.T. (1999). Identification of the activating and conjugating enzymes of the NEDD8 conjugation pathway. J Biol Chem *274*, 12036-12042.

Groisman, R., Kuraoka, I., Chevallier, O., Gaye, N., Magnaldo, T., Tanaka, K., Kisselev, A.F., Harel-Bellan, A., and Nakatani, Y. (2006). CSA-dependent degradation of CSB by the ubiquitin-proteasome pathway establishes a link between complementation factors of the Cockayne syndrome. Genes Dev *20*, 1429-1434.

Groisman, R., Polanowska, J., Kuraoka, I., Sawada, J., Saijo, M., Drapkin, R., Kisselev, A.F., Tanaka, K., and Nakatani, Y. (2003). The ubiquitin ligase activity in the DDB2 and CSA complexes is differentially regulated by the COP9 signalosome in response to DNA damage. Cell *113*, 357-367.

Groth, A., Rocha, W., Verreault, A., and Almouzni, G. (2007). Chromatin challenges during DNA replication and repair. Cell *128*, 721-733.

Guerrero-Santoro, J., Kapetanaki, M.G., Hsieh, C.L., Gorbachinsky, I., Levine, A.S., and Rapic-Otrin, V. (2008). The cullin 4B-based UV-damaged DNA-binding protein ligase binds to UV-damaged chromatin and ubiquitinates histone H2A. Cancer Res *68*, 5014-5022.

Guo, F., Cancelas, J.A., Hildeman, D., Williams, D.A., and Zheng, Y. (2008). Rac GTPase isoforms Rac1 and Rac2 play a redundant and crucial role in T-cell development. Blood *112*, 1767-1775.

Hamaratoglu, F., Willecke, M., Kango-Singh, M., Nolo, R., Hyun, E., Tao, C., Jafar-Nejad, H., and Halder, G. (2006). The tumour-suppressor genes NF2/Merlin and

Expanded act through Hippo signalling to regulate cell proliferation and apoptosis. Nat Cell Biol *8*, 27-36.

Harvey, K.F., Pfleger, C.M., and Hariharan, I.K. (2003). The Drosophila Mst ortholog, hippo, restricts growth and cell proliferation and promotes apoptosis. Cell *114*, 457-467.

Havens, C.G., and Walter, J.C. (2009). Docking of a specialized PIP Box onto chromatin-bound PCNA creates a degron for the ubiquitin ligase CRL4Cdt2. Mol Cell *35*, 93-104.

He, Q., Cheng, P., He, Q., and Liu, Y. (2005). The COP9 signalosome regulates the Neurospora circadian clock by controlling the stability of the SCFFWD-1 complex. Genes Dev *19*, 1518-1531.

He, Y.J., McCall, C.M., Hu, J., Zeng, Y., and Xiong, Y. (2006). DDB1 functions as a linker to recruit receptor WD40 proteins to CUL4-ROC1 ubiquitin ligases. Genes Dev *20*, 2949-2954.

Higa, L.A., Banks, D., Wu, M., Kobayashi, R., Sun, H., and Zhang, H. (2006a). L2DTL/CDT2 interacts with the CUL4/DDB1 complex and PCNA and regulates CDT1 proteolysis in response to DNA damage. Cell Cycle *5*, 1675-1680.

Higa, L.A., Mihaylov, I.S., Banks, D.P., Zheng, J., and Zhang, H. (2003). Radiation-mediated proteolysis of CDT1 by CUL4-ROC1 and CSN complexes constitutes a new checkpoint. Nat Cell Biol *5*, 1008-1015.

Higa, L.A., Wu, M., Ye, T., Kobayashi, R., Sun, H., and Zhang, H. (2006b). CUL4-DDB1 ubiquitin ligase interacts with multiple WD40-repeat proteins and regulates histone methylation. Nat Cell Biol *8*, 1277-1283.

Higa, L.A., Yang, X., Zheng, J., Banks, D., Wu, M., Ghosh, P., Sun, H., and Zhang, H. (2006c). Involvement of CUL4 ubiquitin E3 ligases in regulating CDK inhibitors Dacapo/p27Kip1 and cyclin E degradation. Cell Cycle *5*, 71-77.

Hinton, H.J., Alessi, D.R., and Cantrell, D.A. (2004). The serine kinase phosphoinositide-dependent kinase 1 (PDK1) regulates T cell development. Nature Immunology *5*, 539-545.

Holmberg, C., Fleck, O., Hansen, H.A., Liu, C., Slaaby, R., Carr, A.M., and Nielsen, O. (2005). Ddb1 controls genome stability and meiosis in fission yeast. Genes Dev *19*, 853-862.

Horn, P.J., Bastie, J.N., and Peterson, C.L. (2005). A Rik1-associated, cullin-dependent E3 ubiquitin ligase is essential for heterochromatin formation. Genes Dev *19*, 1705-1714.

Hrecka, K., Gierszewska, M., Srivastava, S., Kozaczkiewicz, L., Swanson, S.K., Florens, L., Washburn, M.P., and Skowronski, J. (2007). Lentiviral Vpr usurps Cul4-DDB1[VprBP] E3 ubiquitin ligase to modulate cell cycle. Proc Natl Acad Sci U S A *104*, 11778-11783.

Hrecka, K, Hao, C, Gierszewska, M, Swanson, SK, Kesik-Brodacka, M, Srivastava, S, Florens, L, Washburn, MP, and Skowronski, J. (2011). Vpx relieves inhibition of HIV-1 infection of macrophages mediated by the SAMHD1 protein. Nature. *474*, 658-61.

Hu, J., McCall, C.M., Ohta, T., and Xiong, Y. (2004). Targeted ubiquitination of CDT1 by the DDB1-CUL4A-ROC1 ligase in response to DNA damage. Nat Cell Biol *6*, 1003-1009.

Hu, J., and Xiong, Y. (2006). An evolutionarily conserved function of proliferating cell nuclear antigen for Cdt1 degradation by the Cul4-Ddb1 ubiquitin ligase in response to DNA damage. J Biol Chem *281*, 3753-3756.

Hu, J., Zacharek, S., He, Y.J., Lee, H., Shumway, S., Duronio, R.J., and Xiong, Y. (2008). WD40 protein FBW5 promotes ubiquitination of tumor suppressor TSC2 by DDB1-CUL4-ROC1 ligase. Genes Dev *22*, 866-871.

Huang, J., Wu, S., Barrera, J., Matthews, K., and Pan, D. (2005) The Hippo signaling pathway coordinately regulates cell proliferation and apoptosis by inactivating Yorkie, the Drosophila Homolog of YAP. Cell *122*, 421-34.

Huang, J., and Chen, J. (2008). VprBP targets Merlin to the Roc1-Cul4A-DDB1 E3 ligase complex for degradation. Oncogene.

Huen, M.S., Grant, R., Manke, I., Minn, K., Yu, X., Yaffe, M.B., and Chen, J. (2007). RNF8 transduces the DNA-damage signal via histone ubiquitylation and checkpoint protein assembly. Cell *131*, 901-914.

Huibregtse, J.M., Scheffner, M., Beaudenon, S., and Howley, P.M. (1995). A family of proteins structurally and functionally related to the E6-AP ubiquitin-protein ligase. Proc Natl Acad Sci USA *92*, 2563-2567.

Ismail, I.H., Andrin, C., McDonald, D., and Hendzel, M.J. (2010). BMI1-mediated histone ubiquitylation promotes DNA double-strand break repair. J Cell Biol *191*, 45-60.

Jackson, S., and Xiong, Y. (2009a). CRL4s: the CUL4-RING E3 ubiquitin ligases. Trends in Biochem Sci *34*, 562-570.

Jackson, S., and Xiong, Y. (2009b). Targeting protein ubiquitylation: DDB1 takes its RING off. Nat Cell Biol *4*, 379-381.

Jacquot, G., Le Rouzic, E., Maidou-Peindara, P., Maizy, M., Lefrere, J.J., Daneluzzi, V., Monteiro-Filho, C.M., Hong, D., Planelles, V., Morand-Joubert, L.*, et al.* (2009). Characterization of the molecular determinants of primary HIV-1 Vpr proteins: impact of the Q65R and R77Q substitutions on Vpr functions. PloS One *4*, e7514.

Jia, S., Kobayashi, R., and Grewal, S.I. (2005). Ubiquitin ligase component Cul4 associates with Clr4 histone methyltransferase to assemble heterochromatin. Nat Cell Biol *7*, 1007-1013.

Jiang, L., Rong, R., Sheikh, M.S., and Huang, Y. (2011). Cullin-4A{middle dot}DNA Damage-binding Protein 1 E3 Ligase Complex Targets Tumor Suppressor RASSF1A for Degradation during Mitosis. J Biol Chem *286*, 6971-6978.

Jin, J., Arias, E.E., Chen, J., Harper, J.W., and Walter, J.C. (2006). A family of diverse Cul4-Ddb1-interacting proteins includes Cdt2, which is required for S phase destruction of the replication factor Cdt1. Mol Cell *23*, 709-721.

Jones, J.M., Bhattacharyya, A., Simkus, C., Vallieres, B., Veenstra, T.D., and Zhou, M. (2011). The RAG1 V(D)J recombinase/ubiquitin ligase promotes ubiquitylation of acetylated, phosphorylated histone 3.3. Immunology Letters *136*, 156-62.

Jorgensen, S., Eskildsen, M., Fugger, K., Hansen, L., Larsen, M.S., Kousholt, A.N., Syljuasen, R.G., Trelle, M.B., Jensen, O.N., Helin, K.*, et al.* (2011). SET8 is degraded via PCNA-coupled CRL4(CDT2) ubiquitylation in S phase and after UV irradiation. J Cell Biol *192*, 43-54.

Jowett, J.B., Planelles, V., Poon, B., Shah, N.P., Chen, M.L., and Chen, I.S. (1995). The human immunodeficiency virus type 1 vpr gene arrests infected T cells in the G2 + M phase of the cell cycle. J Virol *69*, 6304-6313.

Jung, J.R., Kim, H., Jeun, S.S., Lee, J.Y., Koh, E.J., and Ji, C. (2005). The Phosphorylation status of merlin is important for regulating the Ras-ERK pathway. Mol Cells *20*, 196-200.

Kaempchen, K., Mielke, K., Utermark, T., Langmesser, S., and Hanemann, C.O. (2003). Upregulation of the Rac1/JNK signaling pathway in primary human schwannoma cells. Hum Mol Genet *12*, 1211-1221.

Kamura, T., Maenaka, K., Kotoshiba, S., Matsumoto, M., Kohda, D., Conaway, R.C., Conaway, J.W., and Nakayama, K.I. (2004). VHL-box and SOCS-box domains determine binding specificity for Cul2-Rbx1 and Cul5-Rbx2 modules of ubiquitin ligases. Genes Dev *18*, 3055-3065.

Kapetanaki, M.G., Guerrero-Santoro, J., Bisi, D.C., Hsieh, C.L., Rapic-Otrin, V., and Levine, A.S. (2006). The DDB1-CUL4ADDB2 ubiquitin ligase is deficient in xeroderma pigmentosum group E and targets histone H2A at UV-damaged DNA sites. Proc Natl Acad Sci U S A *103*, 2588-93.

Kawakami, T., Chiba, T., Suzuki, T., Iwai, K., Yamanaka, K., Minato, N., Suzuki, H., Shimbara, N., Hidaka, Y., Osaka, F.*, et al.* (2001). NEDD8 recruits E2-ubiquitin to SCF E3 ligase. EMBO J *20*, 4003-4012.

Kawamoto, H., and Katsura, Y. (2009). A new paradigm for hematopoietic cell lineages: revision of the classical concept of the myeloid-lymphoid dichotomy. Trends in Immunology *30*, 193-200.

Kim, J., Feng, H., and Kipreos, E.T. (2007). C. elegans CUL-4 prevents rereplication by promoting the nuclear export of CDC-6 via a CKI-1-dependent pathway. Curr Biol *17*, 966-972.

Kim, J., Guermah, M., McGinty, R.K., Lee, J.S., Tang, Z., Milne, T.A., Shilatifard, A., Muir, T.W., and Roeder, R.G. (2009). RAD6-Mediated transcription-coupled H2B ubiquitylation directly stimulates H3K4 methylation in human cells. Cell *137*, 459-471.

Kim, J., Hake, S.B., and Roeder, R.G. (2005). The human homolog of yeast BRE1 functions as a transcriptional coactivator through direct activator interactions. Mol Cell *20*, 759-770.

Kim, S.H., and Michael, W.M. (2008). Regulated proteolysis of DNA polymerase eta during the DNA-damage response in C. elegans. Mol Cell *32*, 757-766.

Kim, Y., Starostina, N.G., and Kipreos, E.T. (2008). The CRL4Cdt2 ubiquitin ligase targets the degradation of p21Cip1 to control replication licensing. Genes Dev *22*, 2507-2519.

Kipreos, E.T. (2005). Ubiquitin-mediated pathways in C. elegans. WormBook, 1-24.

Kipreos, E.T., Lander, L.E., Wing, J.P., He, W.-W., and Hedgecock, E.M. (1996). cul-1 is required for cell cycle exit in C.elegans and identifies a novel gene family. Cell *85*, 829-839.

Kissil, J.L., Wilker, E.W., Johnson, K.C., Eckman, M.S., Yaffe, M.B., and Jacks, T. (2003). Merlin, the product of the Nf2 tumor suppressor gene, is an inhibitor of the p21-activated kinase, Pak1. Mol Cell *12*, 841-849.

Kolas, N.K., Chapman, J.R., Nakada, S., Ylanko, J., Chahwan, R., Sweeney, F.D., Panier, S., Mendez, M., Wildenhain, J., Thomson, T.M.*, et al.* (2007). Orchestration of the DNA-damage response by the RNF8 ubiquitin ligase. Science *318*, 1637-1640.

Kopanja, D., Roy, N., Stoyanova, T., Hess, R.A., Bagchi, S., and Raychaudhuri, P. (2011). Cul4A is essential for spermatogenesis and male fertility. Developmental Biology *352,*278-87.

Kopanja, D., Stoyanova, T., Okur, M.N., Huang, E., Bagchi, S., and Raychaudhuri, P. (2009). Proliferation defects and genome instability in cells lacking Cul4A. Oncogene *28*, 2456-2465.

Kouzarides, T. (2007). Chromatin modifications and their function. Cell *128*, 693-705.

Kurz, T., Chou, Y.C., Willems, A.R., Meyer-Schaller, N., Hecht, M.L., Tyers, M., Peter, M., and Sicheri, F. (2008). Dcn1 functions as a scaffold-type E3 ligase for cullin neddylation. Mol Cell *29*, 23-35.

Kurz, T., Ozlu, N., Rudolf, F., O'Rourke, S.M., Luke, B., Hofmann, K., Hyman, A.A., Bowerman, B., and Peter, M. (2005). The conserved protein DCN-1/Dcn1p is required for cullin neddylation in C. elegans and S. cerevisiae. Nature *435*, 1257-1261.

Lai, M., Zimmerman, E.S., Planelles, V., and Chen, J. (2005). Activation of the ATR pathway by human immunodeficiency virus type 1 Vpr involves its direct binding to chromatin in vivo. J Virol *79*, 15443-15451.

Lallemand, D., Curto, M., Saotome, I., Giovannini, M., and McClatchey, A.I. (2003). NF2 deficiency promotes tumorigenesis and metastasis by destabilizing adherens junctions. Genes Dev *17*, 1090-1100.

Le Rouzic, E., Belaidouni, N., Estrabaud, E., Morel, M., Rain, J.C., Transy, C., and Margottin-Goguet, F. (2007). HIV1 Vpr arrests the cell cycle by recruiting DCAF1/VprBP, a receptor of the Cul4-DDB1 ubiquitin ligase. Cell Cycle *6*, 182-188.

Le Rouzic, E., and Benichou, S. (2005). The Vpr protein from HIV-1: distinct roles along the viral life cycle. Retrovirology *2*, 11.

Lee, J., and Zhou, P. (2007). DCAFs, the missing link of the CUL4-DDB1 ubiquitin ligase. Mol Cell *26*, 775-780.

Lee, J.H., Terzaghi, W., Gusmaroli, G., Charron, J.B., Yoon, H.J., Chen, H., He, Y.J., Xiong, Y., and Deng, X.W. (2008). Characterization of Arabidopsis and rice DWD proteins and their roles as substrate receptors for CUL4-RING E3 ubiquitin ligases. Plant Cell *20*, 152-167.

Lee, J.H., Yoon, H.J., Terzaghi, W., Martinez, C., Dai, M., Li, J., Byun, M.O., and Deng, X.W. (2010a). DWA1 and DWA2, two Arabidopsis DWD protein components of CUL4-based E3 ligases, act together as negative regulators in ABA signal transduction. Plant Cell *22*, 1716-1732.

Lee, K.P., Lee, J.H., Kim, T.S., Kim, T.H., Park, H.D., Byun, J.S., Kim, M.C., Jeong, W.I., Calvisi, D.F., Kim, J.M.*, et al.* (2010b). The Hippo-Salvador pathway restrains hepatic oval cell proliferation, liver size, and liver tumorigenesis. Proc Natl Acad Sci U S A *107*, 8248-8253.

Leung-Pineda, V., Huh, J., and Piwnica-Worms, H. (2009). DDB1 targets Chk1 to the Cul4 E3 ligase complex in normal cycling cells and in cells experiencing replication stress. Cancer Res *69*, 2630-2637.

Leupin, O., Bontron, S., Schaeffer, C., and Strubin, M. (2005). Hepatitis B virus X protein stimulates viral genome replication via a DDB1-dependent pathway distinct from that leading to cell death. J Virol *79*, 4238-4245.

Leupin, O., Bontron, S., and Strubin, M. (2003). Hepatitis B virus X protein and simian virus 5 V protein exhibit similar UV-DDB1 binding properties to mediate distinct activities. J Virol *77*, 6274-6283.

Li, B., Ruiz, J.C., and Chun, K.T. (2002). CUL-4A is critical for early embryonic development. Mol Cell Biol *22*, 4997-5005.

Li, T., Chen, X., Garbutt, K.C., Zhou, P., and Zheng, N. (2006). Structure of DDB1 in complex with a paramyxovirus V protein: viral hijack of a propeller cluster in ubiquitin ligase. Cell *124*, 105-117.

Li, B., Jia, N., Waning, D.L., Yang, F.C., Haneline, L.S., and Chun, K.T. (2007) Cul4A is required for hematopoietic stem-cell engraftment and self-renewal. Blood. *110*, 2704-2707.

Li, T., Robert, E.I., van Breugel, P.C., Strubin, M., and Zheng, N. (2010a). A promiscuous alpha-helical motif anchors viral hijackers and substrate receptors to the CUL4-DDB1 ubiquitin ligase machinery. Nat Struct Mol Biol *17*, 105-111.

Li, W., You, L., Cooper, J., Schiavon, G., Pepe-Caprio, A., Zhou, L., Ishii, R., Giovannini, M., Hanemann, C.O., Long, S.B.*, et al.* (2010b). Merlin/NF2 suppresses tumorigenesis by inhibiting the E3 ubiquitin ligase CRL4(DCAF1) in the nucleus. Cell *140*, 477-490.

Li, Y., Gazdoiu, S., Pan, Z.Q., and Fuchs, S.Y. (2004). Stability of homologue of Slimb F-box protein is regulated by availability of its substrate. J Biol Chem *279*, 11074-11080.

Liakopoulos, D., Doenges, G., Matuschewski, K., and Jentsch, S. (1998). A novel protein modification pathway related to the ubiquitin system. EMBO J *17*, 2208-2214.

Liang, X., Pickering, M.T., Cho, N.H., Chang, H., Volkert, M.R., Kowalik, T.F., and Jung, J.U. (2006). Deregulation of DNA damage signal transduction by herpesvirus latency-associated M2. J Virol *80*, 5862-5874.

Liu, C., Poitelea, M., Watson, A., Yoshida, S.H., Shimoda, C., Holmberg, C., Nielsen, O., and Carr, A.M. (2005). Transactivation of Schizosaccharomyces pombe cdt2+ stimulates a Pcu4-Ddb1-CSN ubiquitin ligase. EMBO J *24*, 3940-3951.

Liu, C., Powell, K.A., Mundt, K., Wu, L., Carr, A.M., and Caspari, T. (2003). Cop9/signalosome subunits and Pcu4 regulate ribonucleotide reductase by both checkpoint-dependent and -independent mechanisms. Genes Dev *17*, 1130-1140.

Liu, J., Furukawa, M., Matsumoto, T., and Xiong, Y. (2002). NEDD8 modification of CUL1 dissociates p120(CAND1), an inhibitor of CUL1-SKP1 binding and SCF ligases. Mol Cell *10*, 1511-1518.

Liu, L., Lee, S., Zhang, J., Peters, S.B., Hannah, J., Zhang, Y., Yin, Y., Koff, A., Ma, L., and Zhou, P. (2009). CUL4A abrogation augments DNA damage response and protection against skin carcinogenesis. Mol Cell *34*, 451-460.

Lovering, R., Hanson, I.M., Borden, K.L.B., Martin, S., O'Reilly, N.J., Evan, G.I., Rahman, D., Pappin, D.J.C., Trowsdale, J., and Freemont, P.S. (1993). Identification and preliminary characterization of a protein motif related to the zinc finger. Proc Natl Acad Sci USA *90*, 21112-22116.

Lu, C., and Mains, P.E. (2007). The C. elegans anaphase promoting complex and MBK-2/DYRK kinase act redundantly with CUL-3/MEL-26 ubiquitin ligase to degrade MEI-1 microtubule-severing activity after meiosis. Developmental Bbiology *302*, 438-447.

Lum, J.J., Bui T., Gruber, M., Gordan, J.D., DeBerardinis, R.J., Covello, K.L., Simon, M.C., and Thompson, C.B. (2007) The transcription factor HIF-1alpha plays a critical role in the growth factor-dependent regulation of both aerobic and anaerobic glycolysis. Genes Dev. *21*, 1037-49.

Maddika, S., and Chen, J. (2009). Protein kinase DYRK2 is a scaffold that facilitates assembly of an E3 ligase. Nat Cell Biol *11*, 409-419.

Mailand, N., Bekker-Jensen, S., Faustrup, H., Melander, F., Bartek, J., Lukas, C., and Lukas, J. (2007). RNF8 ubiquitylates histones at DNA double-strand breaks and promotes assembly of repair proteins. Cell *131*, 887-900.

Maillard, I., Chen, Y.X., Friedman, A., Yang, Y., Tubbs, A.T., Shestova, O., Pear, W.S., and Hua, X. (2009) Menin regulates the function of hematopoietic stem cells and lymphoid progenitors. Blood. *113*, 1661-9.

Martin-Lluesma, S., Schaeffer, C., Robert, E.I., van Breugel, P.C., Leupin, O., Hantz, O., and Strubin, M. (2008). Hepatitis B virus X protein affects S phase progression leading to chromosome segregation defects by binding to damaged DNA binding protein 1. Hepatology *48*, 1467-1476.

Mathias, N., Johnson, S.J., Winey, M., Adams, A.E.M., Goetsch, L., Pringle, J.R., Byers, B., and Gobel, M.G. (1996). Cdc53p acts in concert with cdc4p and cdc34p to control the G1-to-S phase transition and identifies a conserved family of proteins. Mol Cell Biol *16*, 6634-6643.

McCall, C.M., Miliani de Marval, P.L., Chastain, P.D., 2nd, Jackson, S.C., He, Y.J., Kotake, Y., Cook, J.G., and Xiong, Y. (2008). Human immunodeficiency virus type 1 Vpr-binding protein VprBP, a WD40 protein associated with the DDB1-CUL4 E3 ubiquitin ligase, is essential for DNA replication and embryonic development. Mol Cell Biol *28*, 5621-5633.

McClatchey, A.I., and Fehon, R.G. (2009). Merlin and the ERM proteins--regulators of receptor distribution and signaling at the cell cortex. Trends in Cell Biology *19*, 198-206.

McClatchey, A.I., Saotome, I., Mercer, K., Crowley, D., Gusella, J.F., Bronson, R.T., and Jacks, T. (1998). Mice heterozygous for a mutation at the Nf2 tumor suppressor locus develop a range of highly metastatic tumors. Genes Dev *12*, 1121-1133.

McClatchey, A.I., Saotome, I., Ramesh, V., Gusella, J.F., and Jacks, T. (1997). The Nf2 tumor suppressor gene product is essential for extraembryonic development immediately prior to gastrulation. Genes Dev *11*, 1253-1265.

McNally, F.J., and Thomas, S. (1998). Katanin is responsible for the M-phase microtubule-severing activity in Xenopus eggs. Molecular Biology of the Cell *9*, 1847-1861.

McNally, K., Audhya, A., Oegema, K., and McNally, F.J. (2006). Katanin controls mitotic and meiotic spindle length. J Cell Biol *175*, 881-891.

McNally, K.P., Bazirgan, O.A., and McNally, F.J. (2000). Two domains of p80 katanin regulate microtubule severing and spindle pole targeting by p60 katanin. Journal of Cell Science *113*, 1623-1633.

Minsky, N., Shema, E., Field, Y., Schuster, M., Segal, E., and Oren, M. (2008). Monoubiquitinated H2B is associated with the transcribed region of highly expressed genes in human cells. Nat Cell Biol *10*, 483-488.

Moldovan, G.L., Pfander, B., and Jentsch, S. (2007). PCNA, the maestro of the replication fork. Cell *129*, 665-679.

Morimoto, M., Nishida, T., Nagayama, Y., and Yasuda, H. (2003). Nedd8-modification of Cul1 is promoted by Roc1 as a Nedd8-E3 ligase and regulates its stability. Biochem Biophys Res Commun *301*, 392-398.

Morrison, H., Sherman, L.S., Legg, J., Banine, F., Isacke, C., Haipek, C.A., Gutmann, D.H., Ponta, H., and Herrlich, P. (2001). The NF2 tumor suppressor gene product, merlin, mediates contact inhibition of growth through interactions with CD44. Genes Dev *15*, 968-980.

Morrison, H., Sperka, T., Manent, J., Giovannini, M., Ponta, H., and Herrlich, P. (2007). Merlin/neurofibromatosis type 2 suppresses growth by inhibiting the activation of Ras and Rac. Cancer Res *67*, 520-527.

Nakagawa, T. and Xiong, Y. (2011) X-Linked Mental Retardation Gene Product CUL4B Targets Ubiquitylation of H3K4 Methyltransferase Core Component WDR5 and Regulates Neuronal Gene Expression. Mol Cell, in press

Nishitani, H., Shiomi, Y., Iida, H., Michishita, M., Takami, T., and Tsurimoto, T. (2008). CDK inhibitor p21 is degraded by a proliferating cell nuclear antigen-coupled Cul4-DDB1Cdt2 pathway during S phase and after UV irradiation. J Biol Chem *283*, 29045-29052.

Nishitani, H., Sugimoto, N., Roukos, V., Nakanishi, Y., Saijo, M., Obuse, C., Tsurimoto, T., Nakayama, K.I., Nakayama, K., Fujita, M*., et al.* (2006). Two E3 ubiquitin ligases, SCF-Skp2 and DDB1-Cul4, target human Cdt1 for proteolysis. EMBO J. *25*,1126-36.

Oda, H., Hubner, M.R., Beck, D.B., Vermeulen, M., Hurwitz, J., Spector, D.L., and Reinberg, D. (2010). Regulation of the histone H4 monomethylase PR-Set7 by CRL4(Cdt2)-mediated PCNA-dependent degradation during DNA damage. Mol Cell *40*, 364-376.

Ohtake, F., Baba, A., Takada, I., Okada, M., Iwasaki, K., Miki, H., Takahashi, S., Kouzmenko, A., Nohara, K., Chiba, T*., et al.* (2007). Dioxin receptor is a ligand-dependent E3 ubiquitin ligase. Nature *446*, 562-566.

Okada, T., Lopez-Lago, M., and Giancotti, F.G. (2005). Merlin/NF-2 mediates contact inhibition of growth by suppressing recruitment of Rac to the plasma membrane. J Cell Biol *171*, 361-371.

Olma, M.H., Roy, M., Le Bihan, T., Sumara, I., Maerki, S., Larsen, B., Quadroni, M., Peter, M., Tyers, M., and Pintard, L. (2009). An interaction network of the mammalian COP9 signalosome identifies Dda1 as a core subunit of multiple Cul4-based E3 ligases. Journal of Cell Science *122*, 1035-1044.

Osaka, F., Saeki, M., Katayama, S., Aida, N., Toh-E, A., Kominami, K., Toda, T., Suzuki, T., Chiba, T., Tanaka, K*., et al.* (2000). Covalent modifier NEDD8 is essential for SCF ubiquitin-ligase in fission yeast. EMBO J *19*, 3475-3484.

Panattoni, M., Sanvito, F., Basso, V., Doglioni, C., Casorati, G., Montini, E., Bender, J.R., Mondino, A., and Pardi, R. (2008). Targeted inactivation of the COP9 signalosome

impairs multiple stages of T cell development. The Journal of Experimental Medicine *205*, 465-477.

Parsons, L.M., Grzeschik, N.A., Allott, M.L., and Richardson, H.E. (2010). Lgl/aPKC and Crb regulate the Salvador/Warts/Hippo pathway. Fly *4*, 288-293.

Peschiaroli, A., Dorrello, N.V., Guardavaccaro, D., Venere, M., Halazonetis, T., Sherman, N.E., and Pagano, M. (2006). SCFbetaTrCP-mediated degradation of Claspin regulates recovery from the DNA replication checkpoint response. Mol Cell *23*, 319-329.

Pickart, C.M. (2001). Mechanisms Underlying Ubiquitination. Annu Rev Biochem *70*, 503-533.

Pintard, L., Kurz, T., Glaser, S., Willis, J.H., Peter, M., and Bowerman, B. (2003a). Neddylation and Deneddylation of CUL-3 Is Required to Target MEI-1/Katanin for Degradation at the Meiosis-to-Mitosis Transition in C. elegans. Curr Biol *13*, 911-921.

Pintard, L., Willis, J.H., Willems, A., Johnson, J.L., Srayko, M., Kurz, T., Glaser, S., Mains, P.E., Tyers, M., Bowerman, B.*, et al.* (2003b). The BTB protein MEL-26 is a substrate-specific adaptor of the CUL-3 ubiquitin-ligase. Nature *425*, 311-316.

Precious, B., Childs, K., Fitzpatrick-Swallow, V., Goodbourn, S., and Randall, R.E. (2005). Simian virus 5 V protein acts as an adaptor, linking DDB1 to STAT2, to facilitate the ubiquitination of STAT1. J Virol *79*, 13434-13441.

Rahman, A.H., Zhang, R., Blosser, C.D., Hou, B., Defranco, A.L., Maltzman, J.S., Wherry, E.J., and Turka, L.A. (2011). Antiviral memory CD8 T-cell differentiation, maintenance, and secondary expansion occur independently of MyD88. Blood *117*, 3123-3130.

Randow, F., and Lehner, P.J. (2009). Viral avoidance and exploitation of the ubiquitin system. Nat Cell Biol *11*, 527-534.

Rapic-Otrin, V., Navazza, V., Nardo, T., Botta, E., McLenigan, M., Bisi, D.C., Levine, A.S., and Stefanini, M. (2003). True XP group E patients have a defective UV-damaged DNA binding protein complex and mutations in DDB2 which reveal the functional domains of its p48 product. Hum Mol Genet *12*, 1507-1522.

Rodes, B., Toro, C., Paxinos, E., Poveda, E., Martinez-Padial, M., Benito, J.M., Jimenez, V., Wrin, T., Bassani, S., and Soriano, V. (2004). Differences in disease progression in a cohort of long-term non-progressors after more than 16 years of HIV-1 infection. AIDS *18*, 1109-1116.

Rogel, M.E., Wu, L.I., and Emerman, M. (1995). The human immunodeficiency virus type 1 vpr gene prevents cell proliferation during chronic infection. J Virol *69*, 882-888.

Ruzankina, Y., Pinzon-Guzman, C., Asare, A., Ong, T., Pontano, L., Cotsarelis, G., Zediak, V.P., Velez, M., Bhandoola, A., and Brown, E.J. (2007). Deletion of the developmentally essential gene ATR in adult mice leads to age-related phenotypes and stem cell loss. Cell Stem Cell *1*, 113-126.

Saha, A., and Deshaies, R.J. (2008). Multimodal activation of the ubiquitin ligase SCF by Nedd8 conjugation. Mol Cell *32*, 21-31.

Sakata, E., Yamaguchi, Y., Miyauchi, Y., Iwai, K., Chiba, T., Saeki, Y., Matsuda, N., Tanaka, K., and Kato, K. (2007). Direct interactions between NEDD8 and ubiquitin E2 conjugating enzymes upregulate cullin-based E3 ligase activity. Nat Struct Mol Biol *14*, 167-168.

Sansam, C.L., Shepard, J.L., Lai, K., Ianari, A., Danielian, P.S., Amsterdam, A., Hopkins, N., and Lees, J.A. (2006). DTL/CDT2 is essential for both CDT1 regulation and the early G2/M checkpoint. Genes Dev *20*, 3117-3129.

Saucedo, L.J., and Edgar, B.A. (2007). Filling out the Hippo pathway. Nat Rev Mol Cell Biol *8*, 613-621.

Schmidt, M.W., McQuary, P.R., Wee, S., Hofmann, K., and Wolf, D.A. (2009). F-box-directed CRL complex assembly and regulation by the CSN and CAND1. Mol Cell *35*, 586-597.

Schroeder, D.F., Gahrtz, M., Maxwell, B.B., Cook, R.K., Kan, J.M., Alonso, J.M., Ecker, J.R., and Chory, J. (2002). De-etiolated 1 and damaged DNA binding protein 1 interact to regulate Arabidopsis photomorphogenesis. Curr Biol *12*, 1462-1472.

Schrofelbauer, B., Hakata, Y., and Landau, N.R. (2007). HIV-1 Vpr function is mediated by interaction with the damage-specific DNA-binding protein DDB1. Proc Natl Acad Sci U S A *104*, 4130-4135.

Schrofelbauer, B., Yu, Q., Zeitlin, S.G., and Landau, N.R. (2005). Human immunodeficiency virus type 1 Vpr induces the degradation of the UNG and SMUG uracil-DNA glycosylases. J Virol *79*, 10978-10987.

Schwechheimer, C., and Isono, E. (2010). The COP9 signalosome and its role in plant development. European journal of cell biology *89*, 157-162.

Schwechheimer, C., Serino, G., Callis, J., Crosby, W.L., Lyapina, S., Deshaies, R.J., Gray, W.M., Estelle, M., and Deng, X.W. (2001). Interactions of the COP9 signalosome with the E3 ubiquitin ligase SCFTIRI in mediating auxin response. Science *292*, 1379-1382.

Scrima, A., Konickova, R., Czyzewski, B.K., Kawasaki, Y., Jeffrey, P.D., Groisman, R., Nakatani, Y., Iwai, S., Pavletich, N.P., and Thoma, N.H. (2008). Structural basis of UV DNA-damage recognition by the DDB1-DDB2 complex. Cell *135*, 1213-1223.

Senga, T., Sivaprasad, U., Zhu, W., Park, J.H., Arias, E.E., Walter, J.C., and Dutta, A. (2006). PCNA is a co-factor for Cdt1 degradation by CUL4/DDB1 mediated N-terminal ubiquitination. J Biol Chem.

Shaw, R.J., McClatchey, A.I., and Jacks, T. (1998). Regulation of the neurofibromatosis type 2 tumor suppressor protein, merlin, by adhesion and growth arrest stimuli. J Biol Chem *273*, 7757-7764.

Shibutani, S.T., de la Cruz, A.F., Tran, V., Turbyfill, W.J., 3rd, Reis, T., Edgar, B.A., and Duronio, R.J. (2008). Intrinsic negative cell cycle regulation provided by PIP box- and Cul4Cdt2-mediated destruction of E2f1 during S phase. Dev Cell *15*, 890-900.

Shiio, Y., and Eisenman, R.N. (2003). Histone sumoylation is associated with transcriptional repression. Proc Natl Acad Sci U S A *100*, 13225-13230.

Shimanouchi, K., Takata, K., Yamaguchi, M., Murakami, S., Ishikawa, G., Takeuchi, R., Kanai, Y., Ruike, T., Nakamura, R., Abe, Y.*, et al.* (2006). Drosophila damaged DNA binding protein 1 contributes to genome stability in somatic cells. J Biochem *139*, 51-58.

Sicinska, E., Aifantis, I., Le Cam, L., Swat, W., Borowski, C., Yu, Q., Ferrando, A.A., Levin, S.D., Geng, Y., von Boehmer, H.*, et al.* (2003). Requirement for cyclin D3 in lymphocyte development and T cell leukemias. Cancer Cell *4*, 451-461.

Soucy, T.A., Smith, P.G., Milhollen, M.A., Berger, A.J., Gavin, J.M., Adhikari, S., Brownell, J.E., Burke, K.E., Cardin, D.P., Critchley, S.*, et al.* (2009). An inhibitor of NEDD8-activating enzyme as a new approach to treat cancer. Nature *458*, 732-736.

Starr, T.K., Jameson, S.C., and Hogquist, K.A. (2003). Positive and negative selection of T cells. Annual review of immunology *21*, 139-176.

Sugasawa, K., Okuda, Y., Saijo, M., Nishi, R., Matsuda, N., Chu, G., Mori, T., Iwai, S., Tanaka, K., Tanaka, K.*, et al.* (2005). UV-induced ubiquitylation of XPC protein mediated by UV-DDB-ubiquitin ligase complex. Cell *121*, 387-400.

Suzuki, M., Mizutani-Koseki, Y., Fujimura, Y., Miyagishima, H., Kaneko, T., Takada, Y., Akasaka, T., Tanzawa, H., Takihara, Y., Nakano, M.*, et al.* (2002). Involvement of the Polycomb-group gene Ring1B in the specification of the anterior-posterior axis in mice. Development *129*, 4171-4183.

Takata, K., Yoshida, H., Yamaguchi, M., and Sakaguchi, K. (2004). Drosophila damaged DNA-binding protein 1 is an essential factor for development. Genetics *168*, 855-865.

Tamas, P., Macintyre, A., Finlay, D., Clarke, R., Feijoo-Carnero, C., Ashworth, A., and Cantrell, D. (2010). LKB1 is essential for the proliferation of T-cell progenitors and mature peripheral T cells. European journal of immunology *40*, 242-253.

Tamori, Y., Bialucha, C.U., Tian, A.G., Kajita, M., Huang, Y.C., Norman, M., Harrison, N., Poulton, J., Ivanovitch, K., Disch, L.*, et al.* (2010). Involvement of Lgl and Mahjong/VprBP in cell competition. PLoS biology *8*, e1000422.

Tan, L., Ehrlich, E., and Yu, X.F. (2007). DDB1 and Cul4A are required for human immunodeficiency virus type 1 Vpr-induced G2 arrest. J Virol *81*, 10822-10830.

Tan, M., Gallegos, J.R., Gu, Q., Huang, Y., Li, J., Jin, Y., Lu, H., and Sun, Y. (2006). SAG/ROC-SCF beta-TrCP E3 ubiquitin ligase promotes pro-caspase-3 degradation as a mechanism of apoptosis protection. Neoplasia (New York, NY *8*, 1042-1054.

Tan, P., Fuches, S.Y., Angus, A., Wu, K., Gomez, C., Ronai, Z., and Pan, Z.-Q. (1999). Recruitment of a ROC1-CUL1 ubiquitin ligase by Skp1 and HOS to catalyze the ubiquitination of IkBa. Mol Cell *3*, 527-533.

Tang, X., Orlicky, S., Lin, Z., Willems, A., Neculai, D., Ceccarelli, D., Mercurio, F., Shilton, B.H., Sicheri, F., and Tyers, M. (2007). Suprafacial orientation of the SCFCdc4 dimer accommodates multiple geometries for substrate ubiquitination. Cell *129*, 1165-1176.

Tarpey, P.S., Raymond, F.L., O'Meara, S., Edkins, S., Teague, J., Butler, A., Dicks, E., Stevens, C., Tofts, C., Avis, T.*, et al.* (2007). Mutations in CUL4B, which encodes a ubiquitin E3 ligase subunit, cause an X-linked mental retardation syndrome associated with aggressive outbursts, seizures, relative macrocephaly, central obesity, hypogonadism, pes cavus, and tremor. American journal of human genetics *80*, 345-352.

Terai, K., Abbas, T., Jazaeri, A.A., and Dutta, A. (2010). CRL4(Cdt2) E3 ubiquitin ligase monoubiquitinates PCNA to promote translesion DNA synthesis. Mol Cell *37*, 143-149.

Thiel, A.T., Blessington, P., Zou, T., Feather, D., Wu, X., Yan, J., Zhang, H., Liu, Z., Ernst, P., Koretzky, G.A., and Hua X. (2010) MLL-AF9-induced leukemogenesis requires coexpression of the wild-type Mll allele. Cancer Cell. *17*, 148-59.

Thon, G., Hansen, K.R., Altes, S.P., Sidhu, D., Singh, G., Verhein-Hansen, J., Bonaduce, M.J., and Klar, A.J. (2005). The Clr7 and Clr8 directionality factors and the Pcu4 cullin mediate heterochromatin formation in the fission yeast Schizosaccharomyces pombe. Genetics *171*, 1583-1595.

Tripathi, R., Kota, S.K., and Srinivas, U.K. (2007). Cullin4B/E3-ubiquitin ligase negatively regulates beta-catenin. Journal of biosciences *32*, 1133-1138.

Ulane, C.M., and Horvath, C.M. (2002). Paramyxoviruses SV5 and HPIV2 assemble STAT protein ubiquitin ligase complexes from cellular components. Virology *304*, 160-166.

Ulane, C.M., Kentsis, A., Cruz, C.D., Parisien, J.P., Schneider, K.L., and Horvath, C.M. (2005). Composition and assembly of STAT-targeting ubiquitin ligase complexes: paramyxovirus V protein carboxyl terminus is an oligomerization domain. J Virol *79*, 10180-10189.

Ulane, C.M., Rodriguez, J.J., Parisien, J.P., and Horvath, C.M. (2003). STAT3 ubiquitylation and degradation by mumps virus suppress cytokine and oncogene signaling. J Virol *77*, 6385-6393.

Vasseur, F., Le Campion, A., and Penit, C. (2001). Scheduled kinetics of cell proliferation and phenotypic changes during immature thymocyte generation. European journal of immunology *31*, 3038-3047.

Veis, D.J., Sorenson, C.M., Shutter, J.R., and Korsmeyer, S.J. (1993). Bcl-2-deficient mice demonstrate fulminant lymphoid apoptosis, polycystic kidneys, and hypopigmented hair. Cell *75*, 229-240.

Wang, H., Wang, L., Erdjument-Bromage, H., Vidal, M., Tempst, P., Jones, R.S., and Zhang, Y. (2004). Role of histone H2A ubiquitination in Polycomb silencing. Nature *431*, 873-878.

Wang, H., Zhai, L., Xu, J., Joo, H.Y., Jackson, S., Erdjument-Bromage, H., Tempst, P., Xiong, Y., and Zhang, Y. (2006). Histone H3 and H4 ubiquitylation by the CUL4-DDB-ROC1 ubiquitin ligase facilitates cellular response to DNA damage. Mol Cell *22*, 383-394.

Watanabe, N., Arai, H., Nishihara, Y., Taniguchi, M., Watanabe, N., Hunter, T., and Osada, H. (2004). M-phase kinases induce phospho-dependent ubiquitination of somatic Wee1 by SCFbeta-TrCP. Proc Natl Acad Sci U S A *101*, 4419-4424.

Welcker M, and Clurman B.E. (2008) FBW7 ubiquitin ligase: a tumour suppressor at the crossroads of cell division, growth and differentiation. Nat Rev Cancer. *8*, 83-93.

Wen, X., Duus, K.M., Friedrich, T.D., and de Noronha, C.M. (2007). The HIV1 protein Vpr acts to promote G2 cell cycle arrest by engaging a DDB1 and Cullin4A-containing ubiquitin ligase complex using VprBP/DCAF1 as an adaptor. J Biol Chem *282*, 27046-27057.

Wertz, I.E., O'Rourke, K.M., Zhang, Z., Dornan, D., Arnott, D., Deshaies, R.J., and Dixit, V.M. (2004). Human De-etiolated-1 regulates c-Jun by assembling a CUL4A ubiquitin ligase. Science *303*, 1371-1374.

Westbrook, T.F., Hu, G., Ang, X.L., Mulligan, P., Pavlova, N.N., Liang, A., Leng, Y., Maehr, R., Shi, Y., Harper, J.W*., et al.* (2008). SCFbeta-TRCP controls oncogenic transformation and neural differentiation through REST degradation. Nature *452*, 370-374.

Willems, A.R., Lanker, S., Patton, E.E., Craig, K.L., Nason, T.F., Mathias, N., Kobayashi, R., Wittenberg, C., and Tyers, M. (1996). Cdc53 targets phosphorylated G1 cyclins for degradation by the ubiquitin proteolytic pathway. Cell *86*, 453-463.

Wirbelauer, C., Sutterluty, H., Blondel, M., Gstaiger, M., Peter, M., Reymond, F., and Krek, W. (2000). The F-box protein Skp2 is a ubiquitylation target of a Cul1-based core ubiquitin ligase complex: evidence for a role of Cul1 in the suppression of Skp2 expression in quiescent fibroblasts. EMBO J *19*, 5362-5375.

Wu, J.T., Lin, H.C., Hu, Y.C., and Chien, C.T. (2005). Neddylation and deneddylation regulate Cul1 and Cul3 protein accumulation. Nat Cell Biol *7*, 1014-1020.

Wu, S., Huang, J., Dong, J., and Pan, D. (2003). hippo encodes a Ste-20 family protein kinase that restricts cell proliferation and promotes apoptosis in conjunction with salvador and warts. Cell *114*, 445-456.

Xu, L., Wei, Y., Reboul, J., Vaglio, P., Shin, T.H., Vidal, M., Elledge, S.J., and Harper, J.W. (2003). BTB proteins are substrate-specific adaptors in an SCF-like modular ubiquitin ligase containing CUL-3. Nature *425*, 316-321.

Yamaji, S., Zhang, M., Zhang, J., Endo, Y., Bibikova, E., Goff, S.P., and Cang, Y. (2010). Hepatocyte-specific deletion of DDB1 induces liver regeneration and tumorigenesis. Proc Natl Acad Sci U S A *107*, 22237-22242.

Yan, Q., Dutt, S., Xu, R., Graves, K., Juszczynski, P., Manis, J.P., and Shipp, M.A. (2009). BBAP monoubiquitylates histone H4 at lysine 91 and selectively modulates the DNA damage response. Mol Cell *36*, 110-120.

Yi, C., Troutman, S., Fera, D., Stemmer-Rachamimov, A., Avila, J.L., Christian, N., Luna Persson, N., Shimono, A., Speicher, D.W., Marmorstein, R.*, et al.* (2011). A Tight Junction-Associated Merlin-Angiomotin Complex Mediates Merlin's Regulation of Mitogenic Signaling and Tumor Suppressive Functions. Cancer Cell *19*, 527-540.

Zhang, N., Bai, H., David, K.K., Dong, J., Zheng, Y., Cai, J., Giovannini, M., Liu, P., Anders, R.A., and Pan, D. (2010). The Merlin/NF2 tumor suppressor functions through the YAP oncoprotein to regulate tissue homeostasis in mammals. Dev Cell *19*, 27-38.

Zhang, N., Hartig, H., Dzhagalov, I., Draper, D., and He, Y.W. (2005). The role of apoptosis in the development and function of T lymphocytes. Cell Research *15*, 749-769.

Zhang, S., Feng, Y., Narayan, O., and Zhao, L.J. (2001). Cytoplasmic retention of HIV-1 regulatory protein Vpr by protein-protein interaction with a novel human cytoplasmic protein VprBP. Gene *263*, 131-140.

Zhang, Y., Feng, S., Chen, F., Chen, H., Wang, J., McCall, C., Xiong, Y., and Deng, X.W. (2008). Arabidopsis DDB1-CUL4 ASSOCIATED FACTOR1 forms a nuclear E3 ubiquitin ligase with DDB1 and CUL4 that is involved in multiple plant developmental processes. Plant Cell *20*, 1437-1455.

Zhang, Y., Morrone, G., Zhang, J., Chen, X., Lu, X., Ma, L., Moore, M., and Zhou, P. (2003). CUL-4A stimulates ubiquitylation and degradation of the HOXA9 homeodomain protein. EMBO J *22*, 6057-6067.

Zhao, B., Lei, Q., and Guan, K.L. (2009). Mst out and HCC in. Cancer Cell *16*, 363-364.

Zhao, L.J., Mukherjee, S., and Narayan, O. (1994). Biochemical mechanism of HIV-I Vpr function. Specific interaction with a cellular protein. J Biol Chem *269*, 15577-15582.

Zhao, L.J., Zhang, S., and Chinnadurai, G. (2002). Sox9 transactivation and testicular expression of a novel human gene, KIAA0800. Journal of cellular biochemistry *86*, 277-289.

Zheng, J., Yang, X., Harrell, J.M., Ryzhikov, S., Shim, E.H., Lykke-Andersen, K., Wei, N., Sun, H., Kobayashi, R., and Zhang, H. (2002a). CAND1 binds to unneddylated CUL1 and regulates the formation of SCF ubiquitin E3 ligase complex. Mol Cell *10*, 1519-1526.

Zheng, N., Schulman, B.A., Song, L., Miller, J.J., Jeffrey, P.D., Wang, P., Chu, C., Koepp, D.M., Elledge, S.J., Pagano, M.*, et al.* (2002b). Structure of the Cul1-Rbx1-Skp1-F boxSkp2 SCF ubiquitin ligase complex. Nature *416*, 703-709.

Zhong, W., Feng, H., Santiago, F.E., and Kipreos, E.T. (2003). CUL-4 ubiquitin ligase maintains genome stability by restraining DNA-replication licensing. Nature *423*, 885-889.

Zhou, D., Conrad, C., Xia, F., Park, J.S., Payer, B., Yin, Y., Lauwers, G.Y., Thasler, W., Lee, J.T., Avruch, J.*, et al.* (2009). Mst1 and Mst2 maintain hepatocyte quiescence and suppress hepatocellular carcinoma development through inactivation of the Yap1 oncogene. Cancer Cell *16*, 425-438.

Zhou, P., and Howley, P.M. (1998). Ubiquitination and degradation of the substrate recognition subunits of SCF ubiquitin-protein ligases. Molecular Cell *2*, 571-580.

Zimmerman, E.S., Sherman, M.P., Blackett, J.L., Neidleman, J.A., Kreis, C., Mundt, P., Williams, S.A., Warmerdam, M., Kahn, J., Hecht, F.M.*, et al.* (2006). Human immunodeficiency virus type 1 Vpr induces DNA replication stress in vitro and in vivo. J Virol *80*, 10407-10418.

Zolezzi, F., Fuss, J., Uzawa, S., and Linn, S. (2002). Characterization of a Schizosaccharomyces pombe strain deleted for a sequence homologue of the human damaged DNA binding 1 (DDB1) gene. J Biol Chem *277*, 41183-41191.

Zou, Y., Liu, Q., Chen, B., Zhang, X., Guo, C., Zhou, H., Li, J., Gao, G., Guo, Y., Yan, C.*, et al.* (2007). Mutation in CUL4B, which encodes a member of cullin-RING ubiquitin ligase complex, causes X-linked mental retardation. American journal of human genetics *80*, 561-566.

Zou, Y., Mi, J., Cui, J., Lu, D., Zhang, X., Guo, C., Gao, G., Liu, Q., Chen, B., Shao, C.*, et al.* (2009). Characterization of nuclear localization signal in the N terminus of CUL4B and its essential role in cyclin E degradation and cell cycle progression. J Biol Chem *284*, 33320-33332.